PV CSP HYBRIDIZATION TO PRODUCE IRRIGATION WATER USING DESALINATION AND WASTEWATER TREATMENT

A THESIS SUBMITTED TO
THE GRADUATE SCHOOL OF NATURAL AND APPLIED SCIENCES
OF
MIDDLE EAST TECHNICAL UNIVERSITY

BY

EYLÜL GEDİK

IN PARTIAL FULFILLMENT OF THE REQUIREMENTS
FOR
THE DEGREE OF MASTER OF SCIENCE
IN
MECHANICAL ENGINEERING

JUNE 2023

Approval of the thesis:

PV CSP HYBRIDIZATION TO PRODUCE IRRIGATION WATER USING DESALINATION AND WASTEWATER TREATMENT

submitted by **EYLÜL GEDİK** in partial fulfillment of the requirements for the degree of **Master of Science** i**n Mechanical Engineering, Middle East Technical University** by,

Prof. Dr. Halil Kalıpçılar
Dean, Graduate School of **Natural and Applied Sciences** _____

Prof. Dr. Sahir Arıkan
Head of the Department, **Mechanical Engineering** _____

Prof. Dr. Derek Keith Baker
Supervisor, **Mechanical Engineering, METU** _____

Examining Committee Members:

Prof. Dr. Almıla Güvenç Yazıcıoğlu
Mechanical Engineering, METU _____

Prof. Dr. Derek Keith Baker
Mechanical Engineering, METU _____

Assoc. Prof. Dr. Onur Taylan
Mechanical Engineering, METU _____

Assoc. Prof. Dr. Sezer Özerinç
Mechanical Engineering, METU _____

Assist. Prof. Dr. Mehdi Mehrtash
Energy Systems Engineering, Atılım University _____

Date: 09.06.2023

I hereby declare that all information in this document has been obtained and presented in accordance with academic rules and ethical conduct. I also declare that, as required by these rules and conduct, I have fully cited and referenced all material and results that are not original to this work.

Name Last name : Eylül Gedik

Signature :

ABSTRACT

PV CSP HYBRIDIZATION TO PRODUCE IRRIGATION WATER USING DESALINATION AND WASTEWATER TREATMENT

Gedik, Eylül
Master of Science, Mechanical Engineering
Supervisor : Prof. Dr. Derek. K. Baker

June 2023, 140 pages

Wastewater reuse and reverse osmosis desalination have a large potential to meet the world's increasing need for irrigation water to produce food. Huge opportunities exist for solar systems to power these water systems for fertile but arid regions with large solar and seawater resources along with several challenges. Photovoltaics (PV) and concentrating solar power (CSP) hybridization is a potential solution to power water systems as PV provides cheap electricity whereas CSP system with thermal energy storage (TES) allows the dispatching of electricity and high capacity factors (CF). In this study, three solar systems are considered to power wastewater treatment plant (WWTP) and reverse osmosis (RO) systems to produce agricultural irrigation water: 1) PV-only, 2) CSP with TES and 3) PV and CSP hybridization with TES. Novel operating strategies for CSP and PV+CSP plants are proposed according to the water system requirements. Also, two different operating strategies of RO are analyzed: 1) nominal load operation and 2) variable load operation. These systems are assessed for Erdemli, Mersin, Türkiye. It is proven that PV and CSP hybridization to power the quaternary treatment stage of an urban WWTP and a RO plant operating at variable loads results in the highest CF of water systems with the lowest levelized cost of water (LCOW) when the

systems are hybridized with their stand-alone capacities. The hybridization of PV and CSP is studied also parametrically. The overall water system CF of 77.6% is reached with 90.3% CF of the WWTP plant resulting in LCOW of 1.03 € m^{-3}. Finally, the addition of the WWTP to the RO is found to decrease the LCOW and emission factor of the produced water by 9.6% and 6.9%, respectively.

Keywords: CSP, PV, Hybridization, RO, WWTP

ÖZ

DESALİNASYON VE ATIKSU ARITIMI İLE SULAMA SUYU ÜRETMEK İÇİN PV CSP HİBRİDİZASYONU

Gedik, Eylül
Yüksek Lisans, Makina Mühendisliği
Tez Yöneticisi: Prof. Dr. Derek K. Baker

Haziran 2023, 140 sayfa

Atık suyun yeniden kullanımı ve ters osmoz tuzdan arındırma, dünyanın gıda üretimi için artan sulama suyu ihtiyacını karşılamak için büyük bir potansiyele sahiptir. Büyük güneş ve deniz suyu kaynaklarına sahip verimli ancak kurak bölgeler için bu su sistemlerine güç sağlayacak güneş enerjisi sistemleri için büyük fırsatlar mevcut olmakla birlikte çeşitli zorluklar da bulunmaktadır. Fotovoltaik (PV) ve yoğunlaştırılmış güneş enerjisi (CSP) hibridizasyonu, PV ucuz elektrik sağlarken, termal enerji depolamalı (TED) CSP sistemi planlanabilen elektrik üretimine ve yüksek kapasite faktörlerine (KF) izin verdiği için su sistemlerine güç sağlamak için potansiyel bir çözümdür. Bu çalışmada, tarımsal sulama suyu üretmek için atık su arıtma tesisi (AAT) ve ters osmoz (TO) sistemlerine güç sağlamak üzere üç güneş enerjisi sistemi ele alınmıştır: 1) sadece PV, 2) TED ile CSP, ve 3) PV ve TED ile CSP hibridizasyonu. Su sistemi gereksinimlerine göre CSP ve PV+CSP tesisleri için yeni işletim stratejileri önerilmektedir. Ayrıca, RO'nun iki farklı işletim stratejisi analiz edilmiştir: 1) nominal yük işletimi ve 2) değişken yük işletimi. Bu sistemler Erdemli, Mersin, Türkiye için değerlendirilmiştir. Kentsel bir AAT'nin dördüncül arıtma aşamasına ve değişken yüklerde çalışan bir TO tesisine güç sağlamak için PV ve CSP hibridizasyonunun,

sistemler tek başına kapasiteleri ile hibridize edildiğinde en düşük seviyelendirilmiş su maliyeti (SSM) ile su sistemlerinin en yüksek KF ile sonuçlandığı kanıtlanmıştır. PV ve CSP'nin hibridizasyonu parametrik olarak da incelenmiştir. AAT tesisinin %90,3'lük KF'si ile %77,6'lık genel su sistemi KF'sine ulaşılmış ve bu da 1.03 € m^{-3} SSM ile sonuçlanmıştır. Son olarak, TO'ya AAT'nin eklenmesinin SSM'yi ve üretilen suyun emisyon faktörünü sırasıyla %9,6 ve %6,9 oranında azalttığı bulunmuştur.

Anahtar Kelimeler: CSP, PV, Hibridizasyon, TO, AAT

To all inhabitants of the planet Earth

ACKNOWLEDGMENTS

I would like to thank my supervisor and mentor, Prof. Dr. Derek Baker, there are no words in the world that can truly reflect his impact on me and the evolution of my career. I am so grateful for his endless support. I would like to acknowledge Dr. Diego-César Alarcón-Padilla and Dr. Isabel Oller for their valuable contributions to this work and beyond. I also wish to express my special thanks to Eduardo Zarza Moya. I genuinely owe everything "behind the scenes" of this thesis to these four amazing people.

Also, I would like to sincerely thank all PSA staff from the head of the units to Ph.D. students for their hospitality.

I would like to express my deepest gratitude to an amazing woman, my mom, Özden Aydınoğlu who has made everything I achieved so far possible. Also, I am grateful to have such a lovely and supportive sister, Yağmur Gedik. One thing is for sure, I wouldn't succeed if I was not surrounded with these powerful women.

I owe thanks to my Beste Derebaşı for her presence full of hope and unbelievably encouraging for the rest of us. I always admired and will admire her. I would like to thank Can Koç and Alperen Alparslan for their irreplaceable accompaniment throughout my journey. I would like to express my heartfelt thanks to my dear Carmen Serrano Lapuente, Fernando Aparicio Barcelo, and Guillaume Saliou for always believing in and supporting me even during the days of oppressive weather with no sunshine for me. I do appreciate my luck to get to know you all.

Finally, I would like to wholeheartedly thank all my colleagues around the world who do not recognize the country boundaries while working really hard to propose solutions to the global problems of our one and only world.

This work received funding from the European Union's Horizon 2020 research and innovation program SolarTwins project under Grant Agreement No 856619.

TABLE OF CONTENTS

LIST OF TABLES

TABLES

LIST OF FIGURES

FIGURES

LIST OF ABBREVIATIONS

ABBREVIATIONS

AOP	Advanced oxidation process
ARB&ARG	Antibiotic resistant bacteria and genes
BWRO	Brackish water reverse osmosis
CAPEX	Capital costs
CEC	Contaminants of emerging concern
CF	Capacity factor
CIEMAT	Centro de Investigaciones Energéticas, Medioambientales y Tecnológicas
CR	Central receiver
CSP	Concentrating solar power
DNI	Direct normal irradiation
EU	European Union
ERD	Energy recovery device
LCA	Life cycle assessment
LCOE	Levelized cost of electricity
LCOW	Levelized cost of water
MED	Multi effect distillation
NREL	National Renewable Energy Laboratory
OPEX	Operation and maintenance costs

PSA	Plataforma Solar de Almería
PV	Photovoltaics
RE	Renewable energy
RO	Reverse osmosis
SAM	System Advisor Model
SDG	Sustainable Development Goals
SEC	Specific energy consumption
SOW	Safe operating window
SWRO	Seawater reverse osmosis
TES	Thermal energy storage
UF	Utilization factor
UN	United Nations
UV	Ultraviolet
WWTP	Wastewater treatment plant
PV+CSP	The hybridization of PV with CSP
RO+WWTP	The water system with both RO and WWTP

LIST OF SYMBOLS

SYMBOLS

$A_{receiver}$	Receiver area, m^2
$A_{ref,receiver}$	Reference area of the receiver, m^2
$c_{p,HTF}$	Specific heat capacity of the heat transfer fluid, kJ kg^{-1} $°C^{-1}$
Cap_W	Installed daily capacity of the water system, m^3 day^{-1}
Cap_E	Installed hourly capacity of the energy system, kWh
$CAPEX$	Capital costs, €
$CAPEX_E$	Capital costs of the specified energy system, €
$CAPEX_W$	Capital costs of the specified water system, €
$CAPEX_{receiver}$	Capital costs of the receiver, USD
$CAPEX_{tower}$	Capital costs of the solar tower, USD
CF	Capacity factor, -
$Cost_{fix,tower}$	Fixed tower costs, USD
$Cost_{ref,receiver}$	Reference cost of the receiver, USD
E_{ann}	Annual electricity production of the energy system, kWh
$E_{ann,CSP,ut}$	Annually utilized energy to produce water supplied by CSP system, kWh
$E_{ann,PV,ut}$	Annually utilized energy to produce water supplied by PV system, kWh

$E_{ann,ut}$	Annually electricity production of the specified energy system, kWh
EF	Efficiency factor of the turbine, -
$F_{CO_2,CSP}$	Emission factor of CSP system, $gCO_{2,eq}$ kWh^{-1}
$F_{CO_2,PV}$	Emission factor of PV system, $gCO_{2,eq}$ kWh^{-1}
$F_{CO_2,W}$	Emission factor of the produced water, $gCO_{2,eq}$ m^{-3}
F_{UE}	Utilized electricity fraction, -
$h_{heliostat}$	Heliostat height, m
$h_{receiver}$	Receiver height, m
h_{tower}	Tower height, m
LF	Load factor of the turbine, -
$LCOE$	Levelized cost of electricity, € kWh^{-1}
$LCOE$	Levelized cost of water, € m^{-3}
$m_{HTF,HT}$	Mass of the heat transfer fluid in the hot tank, kg
$m_{HTF,CT}$	Mass of the heat transfer fluid in the cold tank, kg
$m_{HTF,HT,beg}$	Mass of the heat transfer fluid in the hot tank at the beginning of the hour, kg
$m_{HTF,HT,end}$	Mass of the heat transfer fluid in the hot tank at the end of the hour, kg
n	Lifetime of the specified system, years
$OPEX$	Operation and maintenance costs, €
$OPEX_E$	Operation and maintenance costs of the specified energy system, €

$OPEX_W$	Operation and maintenance costs of the specified water system, €
$OPEX_{elec,RO}$	Electrical energy operating costs of RO, €
$OPEX_{elec,WWTP}$	Electrical energy operating costs of UV/H_2O_2, €
P_{CSP}	Electricity output of CSP plant, kWh
P_{th}	Thermal energy that is converted to electricity by power block, kWh_{th}
$Q_{Av,TES}$	Thermal energy that is available to the thermal energy system to be stored, kWh_{th}
Q_{feed}	Feed flow rate, $m^3\ day^{-1}$
Q_{HTF}	Thermal energy that can be transferred to heat transfer fluid, kWh_{th}
$Q_{permeate}$	Permeate flow rate, $m^3\ day^{-1}$
RR	Recovery rate, -
r	Interest rate, -
$sc_{receiver}$	Receiver cost scaling exponent, -
sc_{tower}	Tower cost scaling exponent, -
SEC_{RO}	Specific energy consumption of RO, kWh m^{-3}
SEC_{WWTP}	Specific energy consumption of UV/H_2O_2, kWh m^{-3}
SOC	State of charge, -
SOC_{HT}	State of charge of the hot tank, -
t	Year, years
T_{hot}	Temperature of the heat transfer fluid at the hot tank, °C

T_{cold}	Temperature of the heat transfer fluid at the cold tank, °C
$Train_{ope,ann,RO}$	Total number of trains operated annually, -
$Train_{RO,no}$	Train number of the RO system, -
UF	Utilization factor, -
V_{HTF}	Total volume of the heat transfer fluid, m^3
$V_{W,ann,RO}$	Annual water volume produced by RO, m^3
$V_{W,ann,WWTP}$	Annual water volume treated by UV/H_2O_2, m^3
$V_{W,ann,tot}$	Annually produced total water volume, m^3
$V_{W,ann}$	Annual water production of the specified water system, m^3
η_{gross_net}	Gross to net efficiency of the turbine, -
η_{th}	Thermal efficiency of the turbine, -
ρ_{HTF}	Density of the heat transfer fluid, kg m^{-3}

CHAPTER 1

INTRODUCTION

1.1 Motivation

Food security has become a global challenge due to the increasing population and decreasing resources. Water is central to food production. Even though water is abundant on earth, only 2.5% of it is freshwater. Glaciers and permanent snow cover comprise 68.7% of this freshwater, leaving less than 1% of the water resources available for human use. Furthermore, only 0.3% of the freshwater resources are surface water, whereas fresh groundwater has a share of 29.9% in the total amount of freshwater [1].

Lately, agriculture accounts for 69% of the world's water withdrawals [2]. For Türkiye, this ratio is even higher with 74% [3]. By 2050, agriculture is estimated to produce 60% more food globally, resulting in further stress on the freshwater resources [4].

UN Sustainable Development Goals (SDG) set priorities for global action. UN SDG Goal 2 targets ending hunger, ensuring food security, and promoting sustainable agriculture [5]. Expanding water activities such as desalination and wastewater treatment is aimed at Goal 6 to manage the availability and sustainability of water. Goals 7 and 13 of the Sustainable Development Goals target to promote the sustainable energy supply and reduce the effects of climate change. Similarly, the main objective of the Paris Agreement is to limit the global average temperature increase to 2 ℃, preferably 1.5 ℃, compared with the pre-industry levels to decrease the impacts of climate change [6]. Considering the Sustainable Development Goals 2, 6, 7, and 13 and Paris Agreement together with

the “Leave No One Behind” principle, it is required to adopt low greenhouse gas emission strategies while securing food and water supply for everyone.

Reuse of the treated wastewater and desalination can be addressed to support water and food security. Treated wastewater is reported to have the potential to meet 15% of the agricultural water demand besides being a good nutrient source for crops [2]. Seawater can serve as an additional water source through desalination and provide large volumes of water. Combining the treated wastewater's nutritional content with the large volumes of desalinated water results in a considerable amount of high-quality irrigation water.

However, desalination and wastewater treatment processes can be highly energy intensive based on the technology adopted. In accordance with SDG 7 and Paris Agreement, powering those with renewable energy sources is crucial. The co-location of arid but fertile lands with good solar resources near urban settlements and seawater resources creates a vast potential to produce agricultural irrigation water with sustainable solar resources. However, intermittent operation is not desired for water treatment plants, membrane desalination, and wastewater treatment, due to the higher operation and maintenance costs and the performance decline. Also, low capacity factors of the water systems can lead high unit costs of water due to high capital costs of those. Therefore, non-continuous energy supply and low capacity factors become significant concerns while the water treatment systems are powered with renewable energy resources.

Considering the upfront cost and levelized cost of electricity (LCOE) decrease associated with photovoltaics (PV) technologies worldwide, and Türkiye’s large and mature market regarding PV, solar PV is a feasible option to produce electricity [7]. However, PV systems are mostly coupled with batteries which are not economical storage systems. Even though concentrating solar power (CSP) systems have higher LCOE, with thermal energy storage (TES), they deliver economically competitive dispatchable electricity when the solar resources are not sufficient and reach higher capacity factors. Therefore, the hybridization of PV and

CSP can result in a relatively continuous energy supply and high capacity factors with reasonable electricity prices.

Türkiye is one of the ten countries with the largest agricultural production, and almost 25% of the population is employed in the agriculture sector [8]. However, Türkiye is a semi-arid region with 1350 m^3 $capita^{-1}$ of annual water availability, and it is expected that by 2030, these resources will decrease to 1000 m^3 $capita^{-1}$ with the increasing population [9]. Considering the urgent need for sustainable food production globally and the key role of Türkiye as a supplier, Türkiye needs to secure its food and water production with sustainable resources.

1.2 System Descriptions

1.2.1 Water Treatment Systems

In this study, two water treatment systems are considered: UV/H_2O_2 as the quaternary treatment of an urban wastewater treatment plant and a reverse osmosis desalination system.

1.2.1.1 Wastewater Treatment and Advanced Oxidation: UV/H_2O_2

Wastewater treatment refers to the restoration of the water used and contaminated by human activity to the level of quality desired [10]. The treatment can be achieved by physical, chemical, or biological processes.

Different resources classify the wastewater treatment stages differently; however, treatment stages can be conventionally described as [11]

- Preliminary Treatment: The coarse constituents are removed to prevent maintenance or operational problems with the equipment, system, or operation.

- Primary Treatment: The suspended solids and organic matter are separated from the wastewater. The separation can be enhanced by the addition of chemicals or filtration.
- Secondary Treatment: In addition to the suspended solids and biodegradable organic matter, also, the removal of the nutrients, nitrogen, phosphorus, or both can be performed.
- Tertiary Treatment: The residual suspended solids are separated from the secondary effluent. Disinfection and nutrient removal are generally included in tertiary treatment.
- Advanced Treatment: The remaining dissolved and suspended solids are removed when the previous steps are insufficient to meet the required quality criteria for water reuse.

The wastewater can be categorized based on its source. Municipal wastewater is generated by a community's domestic, industrial, or commercial activities [12]. Urban wastewater also includes rainwater outflows or, more generally, urban runoffs [13].

Urban wastewater treatment is standardized in Europe by Council Directive 91/271/EEC [14]. In 2022, EC tabled a proposal to update the directive to adapt to the current requirements and challenges. In this proposal [15], the EU re-defined the wastewater treatment stages as

- Secondary Treatment: the step where the urban wastewater is treated by biological treatment and a secondary settlement or a similar process
- Tertiary Treatment: the process where the removal of the nitrogen and phosphorus is performed
- Quaternary Treatment: the stage where a broad spectrum of micro-pollutants is removed from the urban wastewater

to clarify and converge on the terminology [16].

Contaminants of emerging concern (CEC) is a term used to refer to microplastics and micropollutants. Microplastics are small solid particles of plastics. Micropollutants are tiny parts of daily products such as pharmaceuticals, industrial chemicals, cosmetics, and pesticides [17].

Conventional WWTPs are not effective in removing CECs [18], [19], and their discharge to the environment creates serious health concerns; particularly when the effluent is used for agricultural irrigation [20]. Also, the antibiotic resistant bacteria and genes (ARB&ARG) existing in wastewater requires special attention. Therefore, more advanced treatment technologies should be applied to remove CECs and ARB&ARGs from the wastewater and meet the criteria for wastewater reuse for agricultural irrigation.

Advanced oxidation processes (AOPs) can be employed as the quaternary treatment stage of urban wastewater plants. AOPs generate hydroxyl radicals that are highly reactive and nonselective to degrade the organic contaminants and recalcitrant chemicals [21], [22]. The UV/ H_2O_2 process is a typical AOP. In the presence of UV light, the hydrogen peroxide's photolysis produces hydroxyl radicals which abate a wide range of CECs and ARB&ARGs [20].

Also, it is crucial to emphasize that the energy consumption of the UV/H_2O_2 treatment is solely in form of electricity.

1.2.1.2 Desalination and Reverse Osmosis

Desalination is the process of producing fresh water from saline water by removing the dissolved salts. Conventional desalination methods can be classified into two categories: thermal methods and membrane methods [23]. In thermal processes, heat is introduced to the saline water to separate salts and water, primarily by evaporation. On the other hand, in membrane methods, separation occurs mainly through a membrane. Multistage flashing and multi effect distillation (MED) are

well-known examples of thermal processes, whereas reverse osmosis (RO) and electrodialysis are the most common membrane methods.

Currently, RO constitutes 65% of the global online desalination capacity as it is a relatively simple and mature process [24]. Among the other desalination methods, RO has one of the lowest specific energy consumption (SEC). Its energy consumption is solely in form of electricity and in the range of 2.5-4.0 kWh m^{-3} [25], [26].

Osmosis is the natural transportation of water molecules from a low concentration solution to high concentration solution through a semipermeable membrane. The solute molecules are rejected during osmosis, whereas water molecules are allowed to pass until the osmotic equilibrium is achieved. When an external pressure higher than the osmotic pressure difference is applied on the high concentration side, the water molecules are forced to move from the high concentration to the low concentration side [27]. This process is known as reverse osmosis. The osmosis, osmotic equilibrium, and reverse osmosis are schematically represented in Fig. 1.1.

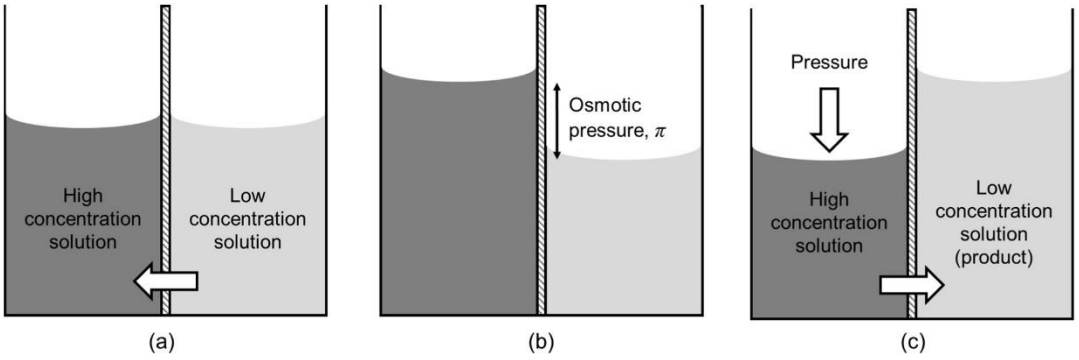

Figure 1.1. Schematic representation of a) osmosis, b) osmotic equilibrium, and c) reverse osmosis [27].

Depending on the quality of the water to be desalinated, the RO processes can be divided into two subgroups: brackish water reverse osmosis (BWRO) where the salinity of the source water is between 500 mg l^{-1} and 10 000 mg l^{-1}, and seawater

reverse osmosis (SWRO) where 35 000 mg l^{-1} is the approximate level of the salinity [27], [28].

Three streams are associated with seawater RO desalination: feed, permeate, and concentrate. Feed is the seawater which is the input of the system with high salt concentration. Permeate is the stream allowed by the membrane with low salt concentration, and it is desalinated water. Finally, concentrate is the highly concentrated stream that includes the salts rejected by the membrane, and it is called brine.

1.2.2 Solar Energy Systems

Solar energy is utilized to power the water treatment systems using two different technologies: photovoltaics (PV) and concentrating solar power (CSP). The type of concentrating solar power studied here is the central receiver (CR) with thermal energy storage (TES).

1.2.2.1 Photovoltaics

PV technology generates electricity from semiconductor materials when they are irradiated by photons [29]. This phenomenon is called the photovoltaic effect.

PV systems mainly include modules, inverters, converters, and, optionally, storage systems. Modules are the components where the solar radiation is converted to direct current through the photovoltaic effect. Currently, crystalline silicon is the most common module material with two types, monocrystalline and multicrystalline [30]. The solar-to-electricity efficiency of monocrystalline cells is around 15-20%, whereas multicrystalline cells have lower efficiencies but are more economical [31]. The modules are connected in series to form strings, and strings are mounted in parallel to form PV arrays [32]. Tracking systems can be added to PV arrays to increase the electricity output. Based on the degree of freedom,

tracking systems can be analyzed in two subgroups, one-axis tracking and dual-axis tracking. Dual-axis tracking systems can produce more electricity than fixed and single-axis tracking PV systems with increased demand for maintenance and complexity in design and control [30]. Inverters convert the direct current produced via PV modules into alternating current to maintain the compatibility of the generated power with AC-powered equipment and grid. Converters change the input voltage to a desired value to regulate and boost the system output [33]. Finally, storage systems can be added to PV systems to match the delivery of the PV system with the demand, as solar radiation is variable. Even pumped hydro storage is an option as the storage system, usually battery systems are coupled with PV installations with a variety of options such as lead-acid, Pb-Sb, Li-ion, NiMH, NiCd, Zn-air, etc. [34].

1.2.2.2 Concentrating Solar Power and Central Receiver Systems

Concentrating solar power systems utilize concentrated solar radiation to generate heat, electricity, or fuels by the addition of other technologies. CSP systems can use only the direct beam component of solar radiation, unlike PV technologies where diffused irradiation can also be used. The term concentrating solar power (CSP) herein specifically refers to electricity generation.

The CSP plants are basically constituted of four main components: solar collector, receiver, power block and optionally but mostly, thermal energy storage system [35]. In conventional CSP technologies, the direct beam solar irradiation is concentrated and reflected to the receiver by the collector field, then transferred to a heat transfer medium in the form of thermal energy. The gained thermal energy is used either to operate a power block to produce electricity or to be stored in thermal energy storage system to be utilized later [36].

The main technologies of CSP are shown in Fig. 1.2; linear focus systems: a) linear Fresnel collectors, b) parabolic trough collectors, and point focus systems: c)

central receivers, and d) parabolic dish collectors, ordered by increasing concentration ratio where concentration ratio is defined as the ratio of aperture area to the absorber area [37].

Central receiver systems have considerable potential and advantage in electricity production as they can reach higher temperatures compared to linear focus systems resulting in more efficient steam cycles or gas turbines with higher exergies [36].

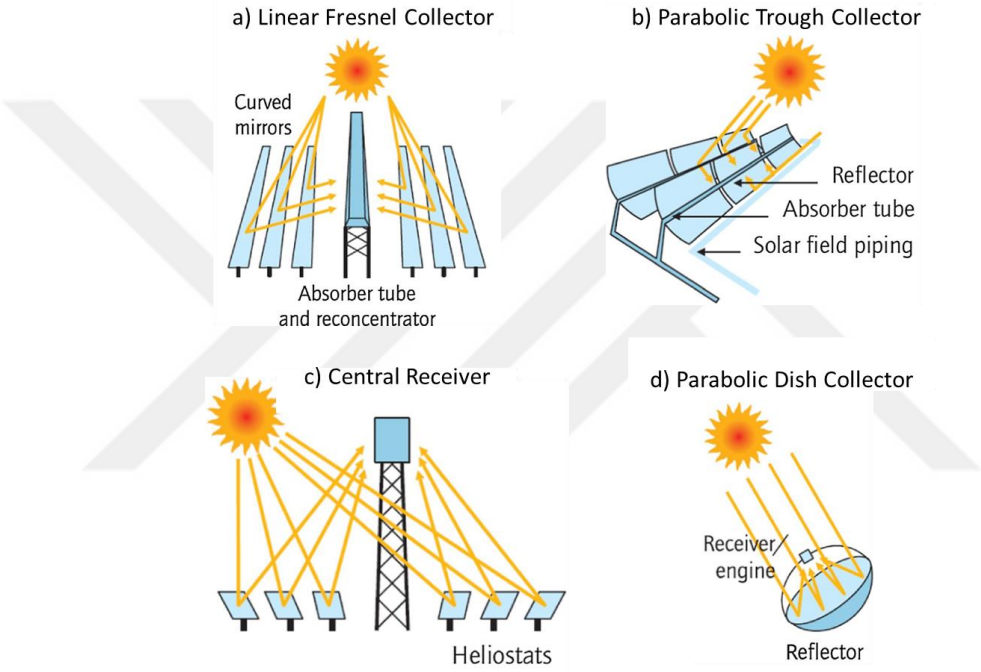

Figure 1.2. Currently available CSP technologies (Adapted from [38]).

Central receiver systems are based on a large array of heliostats that concentrates the solar radiation onto a receiver located at the top of a high tower [39]. The concentration ratios associated with the central receiver systems can reach up to 1000 [37]. The highly concentrated solar radiation is absorbed by the receiver, converted into thermal energy, and transferred to a heat transfer medium. The heat transfer/storage media can be in the form of either liquid (e.g., molten salts) [40], gas (e.g., air) [41], or solid (e.g., ceramic particles) [42].

TES system decreases the temporal mismatch between the energy demand and supply, and improve dispatchable electricity generation. One of the most convenient TES configurations, also adapted in this study, is a two-tank storage system where molten salt is the heat transfer/storage fluid. Typically, a Rankine cycle is coupled with molten salt TES as the power cycle of the CSP plant. The operating principle of this configuration is straightforward. First, the cold molten salt is sent to the receiver, heated, and pumped to the hot molten salt storage tank. The hot molten salt is fed to the power block and transfers heat to the water by a heat exchanger, and steam is produced to operate the turbine. The cooled molten salt returns to the cold storage tank, is pumped to the receiver and heated once again.

CHAPTER 2

LITERATURE REVIEW

2.1 Literature Review of PV CSP Hybridization

The hybrid PV and CSP plants are classified into two groups: a) compact and b) non-compact systems. The two technologies are integrated into a single plant in compact systems. On the other hand, in non-compact systems, the PV and CSP plants are physically distinct, and their operation is independent from each other. Non-compact systems are attributed to have high flexibilities in terms of integration and operational strategies, as the hybridization is done by means of electricity dispatching strategies. Also, compared to stand-alone PV and CSP technologies, significantly higher capacity factors are obtained with non-compact hybridization [43]. The hybridized PV and CSP scheme used in this study is "non-compact"; therefore, the literature review is focused on this type. An example of a non-compactly hybridized PV CSP system is presented in Fig. 2.1.

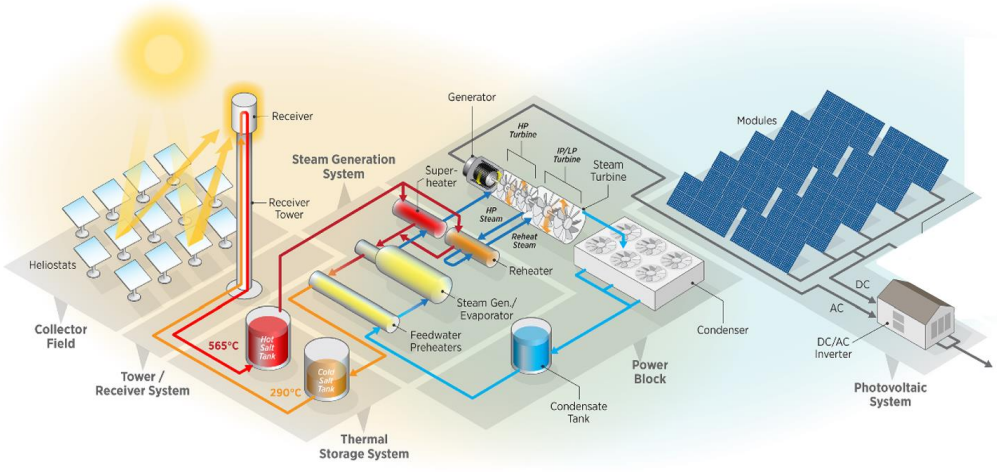

Figure 2.1. Non-compact CSP PV hybridization (Adapted from [44]).

The PV and CSP non-compact hybridization has gained attention in recent years; there are several ongoing commercial projects. Atacama I/ Cerro Dominador, Chile is an operational plant consisting of 110 MW CSP and 100 MW PV with a 17.5 hour capacity molten salt thermal storage system [45]. Noor Energy I, Dubai, is implementing a project, 700 MW CSP and 250 MW PV capacity, with 15 hours of the thermal storage system. This solar complex aims to reach 24 hours of electricity supply [46]. Lately, China announced more than 25 CSP+PV projects to be built until 2024 [47].

In addition to the commercial plants described above, there are several modeling and dispatching approaches for PV CSP hybridization in the literature.

Green et al. [48] studied a PV-CSP system for Atacama and suggested a dispatching strategy where CSP responds to PV production with multiple priority levels. They found that capacity factors even higher than 90% are achievable.

Starke et al. [49] conducted a techno-economical study where they analyzed two hybrid PV CSP plants with TES for Atacama, with parabolic trough collectors or central receiver, both combined with PV by putting a constraint on the capacity factor for the supply of baseload energy to the grid. They concluded that by hybridization, the CSP plants could achieve capacity factors higher than 80% with a 30-40% percent reduction in solar field size and a 1.5-7% decrease in LCOE depending on the CSP type.

Pan [50] studied a similar case for South Africa; a central receiver with TES was added to PV systems to provide base load to the grid, and capacity factors up to 90% were reached with lowered LCOE.

Zhai et al. [51] analyzed two different PV-CSP systems, PV+ Battery+CSP+TES and PV+CSP+TES, where the battery storage of PV was replaced with TES. Also, they compared two different dispatch strategies for the hybridized PV CSP plant, conventional, where the electricity outputs of the two systems do not interfere with each other, and constant-output strategy, where two systems operate synergistically

to deliver a constant output. The results showed that solar energy can be utilized better with a PV+CSP+TES system with lowered LCOE than a PV+Battery+CSP+TES configuration in a constant output strategy.

Moser et al. [52] also analyzed a hybrid PV CSP plant compared to a standalone CSP and PV+battery scheme for Northern Chile to meet the baseload demand. They found that at low renewables share of up to 40%, PV without battery results best economically; between 40-70% solar share, PV+battery is the cheapest option and, for more ambitious solar shares, i.e.,>70%, CSP+PV delivers the lowest LCOE.

A new integration scheme where PV and CSP were combined with a mutual thermal energy storage system was introduced by Giaconia et al. [53]. They showed that their scheme with a 24 hour storage capacity was able to meet 67% and 90% of the power demand of a typical Mediterranean region where the load varies hourly, daily, and also seasonally, and an industrial district in the sub-Saharan region with constant power demand, respectively. They compared the LCOE of the hybridized scheme with the PV scenario, and only 0.057 and 0.041 € kWh^{-1} increase was observed in LCOE.

As the viability of PV+CSP was verified, the research trends have been directed to the optimization of the hybrid plant.

Petrollese and Cocco [54] conducted an optimization study for a hybrid PV CSP scheme where minimizing LCOE was the objective function of the study. The system was assessed for two locations, Ottana, Italy (low DNI) and Quarzazate, Morocco (high DNI), with different load durations and capacity factor requirements. It was demonstrated that hybridization is cost-effective independent of location or targeted capacity factor when power generation is required for the whole day.

Starke et al. [55] suggested a multi-objective optimization procedure based on their previous study to design and size hybrid CSP and PV system where LCOE, total

investment cost, and capacity factor were set as the objective functions. The capacity factor was found to achieve 85%, and the LCOE was observed to be lower than isolated CSP plants.

Bravo and Friedrich [56] presented a two-stage optimization method with multiple objectives for a hybridized PV CSP power plant where operational information was supplied to the design process. It was proven that the dispatchable generation can be increased, and the LCOE can be reduced simultaneously.

2.2 Literature Review of Renewable Powered Desalination

Renewable powered RO desalination has been widely studied in the literature for different scales: for islands [57] where energy and water supply are costly, for rural areas [58], and for cities [59].

Wang et al. [60] investigated possible hybridized energy schemes with PV, wind turbines, CSP with TES, and cogenerating MED and batteries to supply 100% RE based electricity and water obtained from the RO of an island. They focused on minimizing the overall costs of the hybridized energy scheme instead of seeking the lowest CSP cost. The scheme with WT, CSP, MED, RO, and batteries resulted in the lowest cost and achieved 100% RE share.

Casimiro et al. [61] conducted an analysis to compare the annual performance of a CSP+RO plant with a CSP+MED system for the co-generation of electricity and freshwater for Trapani, West Sicily, Italy. They concluded that RO is more favorable for Trapani considering higher capacity factors of both the energy and water system.

Laissaou et al. [62] conducted a techno-economic study to compare two RO plants powered by stand-alone PV and CSP systems for Tenes, Algeria, to explore the impact of variable load operation of the desalination plant. They found that the variable load operation is more suitable for RO plant to compete with power

fluctuations. Also, they concluded that CSP results better both in terms of economic and technical aspects compared to PV.

The electricity and freshwater co-generation systems have been studied with PV+CSP as the power supply and MED as the thermal desalination method.

Valenzuela et al. [63] studied a PV+CSP+MED cogeneration plant for Atacama Desert, Chile. They concluded that the sizes of the PV and CSP power systems should be determined depending on whether freshwater or electricity production is prioritized.

Similarly, Mata-Torres et al. [64] conducted a thermoeconomic analysis of a PV+CSP+MED system located in Northern Chile. They reached the same conclusion as Valenzuela et al. [63], as water production reduces with increased PV capacity while a net increase in electricity generation is observed.

Also, as the base of this current study, the hybridization of PV with CSP for RO desalination for the Canary Islands was investigated by Silvestre [65]. It was demonstrated that PV+CSP powered RO can result in lower LCOW than grid powered RO considering the island's isolated location. Also, the parametric study showed that capacity factors even higher than 90% were achievable.

As this study focuses on solar powered RO desalination, the operational characteristic of the plant should also be addressed. Conventional RO plants are operated continuously; however, when renewable energy systems power the desalination plants, fluctuations in power and intermittent operation are inevitable. Though RO is a mature and well-studied process, the variable load and non-continuous operation still need to be investigated.

The variation of power provided by RES due to the availability of resources raised the studies of operational strategies of RO. The Safe Operating Window (SOW) concept was first proposed by Feron to handle both the intermittency and the power fluctuations of a wind-powered RO plant [66]. Broadly, SOW sets the limits of the RO operation based on membrane specifications and operational requirements.

Pohl et al. [67] identified four operational strategies within SOW, i. constant feed pressure, ii. constant permeate recovery, iii. constant feed flow, and iv. constant concentrate flow, to be used for a SWRO system with fluctuating power supply. They concluded that a constant recovery rate is the optimum strategy as it provides fairly good permeate quality, low pressure variations, and a broad load range with low SEC.

Similarly, Richards et al. [68] conducted a study to determine the SOW and investigate operational strategies for a RE powered BWRO system. They validated that the constant recovery rate is the best strategy based on the same criteria as Pohl et al. [67].

Ruiz-Garcia and Nuez [69] investigated the boron rejection of a single stage SWRO under variable operating conditions. They demonstrated that boron rejection should also be considered as a factor for determining SOW.

Besides the operational strategies, analyzing the effect of the non-continuous or instable RO operation on the membrane is also significant, as any deterioration or fouling of the membrane causes deviations from the designed operation. Scaling and biofouling are the most dominant mechanisms responsible from performance decline in the case of RO. Scale results from the precipitation of dissolved metal salts in the seawater on the membrane [70]. The severity of scaling depends on the feed water composition and recovery rate. As a substantial amount of the water content of feedwater is utilized as permeate, the concentration of the salts reaches the solubility limits, and the precipitated salts start to accumulate on the surface of the membrane as scale. By using antiscalants, the chemicals which can maintain the salt in the solution even if the limit of solubility is outreached, the scaling control is available. On the other hand, biofouling is described as the growth of bacteria on the surface of the membrane surface [70]. Biofouling is enhanced when the fluid is stagnant near the membrane surface, which is the case for shutdowns of RO. Periodic treatment of membranes and disinfection of the water can control the biofouling.

Several studies in the literature inspected the impact of intermittent or fluctuating power supply on the membrane and, associatively, on the process. Richards et al. [71] examined the effects of alternating solar radiation on a solar powered BWRO system performance experimentally. They first experimented with constant solar irradiance at different levels as the reference case. They compared the periodic fluctuations of i) magnitude, ii) frequency, and iii) on-time period with the base scenario. They mainly concluded that above a certain threshold of solar radiation, the system can produce high quality permeate independent of the fluctuations. They also found that the shutdowns can result in a natural backwash which disrupts the concentration polarization layer.

Gormaly and Bilton [72] experimentally investigated the short-term membrane fouling behavior of a PV+battery powered RO system by quantifying the variations in the membrane permeability under intermittent operation, antiscalants addition, and rinsing. They improved their study by testing real groundwater with extended shutdowns and validating their lab-scale results with a pilot-scale system to assess the compatibility of two results obtained with two different membrane sizes and configurations [73]. Both studies highlighted the need to rinse the membrane for intermittent operation with antiscalant additions, as the antiscalants can serve as a nutrient source for bacterial growth during the shutdown periods.

Besides the short term assessment of membrane performance, the long term intermittent operation of RO was also examined. Ruiz-Garcia and Nuez [74] analyzed a full-scale BWRO plant constantly operating 9 hours per day over 14 years with antiscalants and rinsing. They found that the SEC value of the plant increased by around 20%, with a 50% decrease in membrane permeability in 14 years with only one chemical cleaning. They claimed that intermittent operation is feasible in the long term, and with proper and frequent chemical cleanings, the performance of the BWRO can be improved.

2.3 Literature Review of Advanced Oxidation Processes

The literature mainly focuses on the investigation of the level of degradation of CEC and ARB&ARGs instead of the energy source of the AOP processes. Several sources compare the UV/H_2O_2 process with other AOPs with different conditions, contaminants, and purposes [75]–[80].

As the main objective of this study is the investigation of the system-level modeling of a WWTP quaternary stage with RE resources, not the contaminant degradation assessment, no more studies are presented here, and the relevant studies are referred in the following chapters of this study.

2.4 Objective and Scope

Before defining the objective and scope of this study, the findings from the literature are summarized, and the associated research gaps are addressed.

As presented in Section 2.1, PV CSP hybridization was studied well in literature, and its viability and feasibility for electricity production were proved in several publications. Accordingly, its commercialization started and is progressing with increasing attention.

Renewable energy resources, particularly solar resources, were widely investigated in literature to supply energy to the desalination systems as described in Section 2.2. Accordingly, the potential problems regarding the non-continuous operation of RO systems associated with renewable energy resources were examined in different aspects. Based on the literature, it is concluded that fluctuating energy supply does not have a significant additional adverse effect on the membrane in either short or long term if the process is designed deliberately. Also, it was shown that the adverse effects of RO intermittent operation can be reduced with adequate measures. However, it should be noted that the cleaning or rinsing of the RO, a fundamental requirement for intermittent operation, is an additional step and labor

to the process. The frequent shut-off/start-up instances with short off periods are undesirable as they add operational complexity to the RO. Therefore, the operational strategy of the RE powered RO systems should be adaptable to variable energy supply, and target to minimize the frequent stop/start instances and enhance the continuous operation of the desalination plant.

In conclusion, even though many published studies and commercial projects hybridize PV and CSP for electricity production, the modeling and operation of hybridized energy systems for water treatment systems are different from those as the operational limits and requirements of water systems possess new restrictions on the energy system. As mentioned in Section 2.2, Silvestre [65] proposed PV+CSP hybridization to power a RO desalination plant. Even though only the nominal load operation of the RO plant was considered and the strategy of the PV+CSP hybridization was fairly simple in his study, the results are already quite promising. It is expected that with the variable load operation of the RO plant and a more sophisticated control scheme of the PV+CSP plant, the LCOW can be further decreased, and the operation of the RO plant can be improved with increased CF and continuous operation of trains.

Also, solar-powered of WWTPs/ WWTP treatment stages needs to be more widely investigated in the literature. Even though the combination of treated wastewater and desalination has a vast potential to meet the need for the irrigation water also in alliance with SDGs of the EU, there is no published work that combines seawater desalination and wastewater treatment for agricultural irrigation water production.

Hence, this study aims to model, simulate and assess a stand-alone water system comprised of UV/H_2O_2 quaternary treatment of a WWTP and a RO plant, which can operate at variable loads, powered by non-compactly hybridized PV and CSP system to produce water for agricultural irrigation.

CHAPTER 3

METHODOLOGY

3.1 Overview of the Systems

In this study, 3 different energy system scenarios are analyzed:

1. PV-only without storage
2. CSP with TES
3. Non-compactly hybridized PV and CSP with TES.

Please note that the hybridization of PV with CSP is represented by “PV+CSP” in this thesis. Also, in the following sections and chapters, CSP and PV+CSP always includes the TES.

As the water system scenarios, 2 different systems are considered:

1. RO-only
2. RO and UV/H_2O_2 quaternary treatment of a WWTP

Please note that the water system comprising of both RO and UV/H_2O_2 quaternary treatment of a WWTP is represented by “RO+WWTP” in this thesis.

The overview of the overall system with hybridized energy scenario and combined water scheme is presented in Figure 3.1.

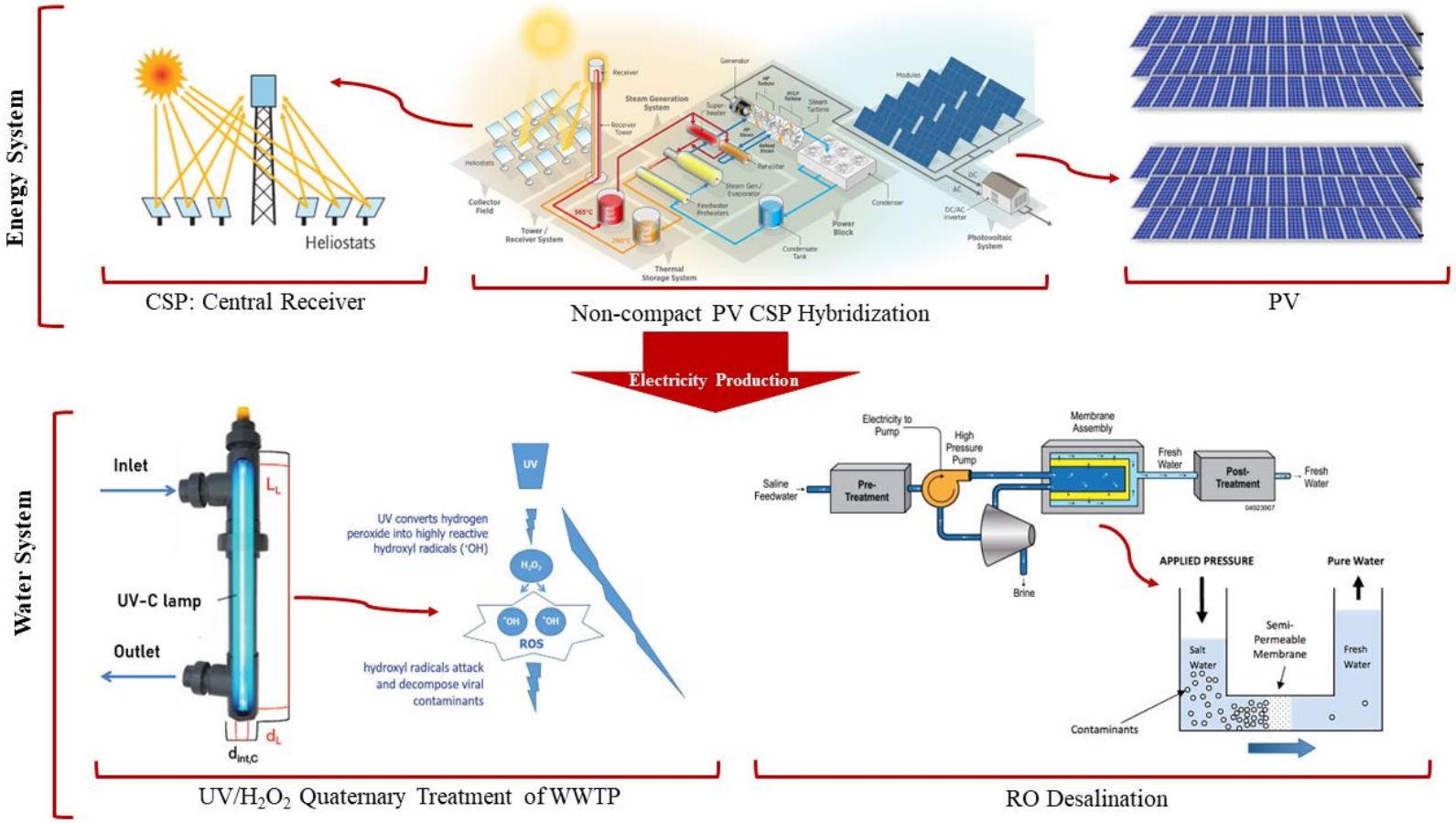

Figure 3.1. Overview of the systems (Created by combining the adaptations from [38], [44], [173], [120], [174], [175], [176]) .

3.2 Technical Analysis

In this section, the technical model definitions, simulation details, assumptions, operating strategies, inputs and key performance indicators of the water and energy systems are presented.

3.2.1 Modeling and Simulations

This section aims to provide the details of the modeling and simulation of the systems studied.

3.2.1.1 Water Systems

Two different complementary water systems are analyzed in this study: UV/H_2O_2 quaternary treatment of a WWTP as the prioritized water source and RO desalination plant as the complementary one.

Please note that the water system comprising of both RO and WWTP is represented by “RO+WWTP” in this thesis.

3.2.1.1.1 Wastewater Treatment System

In this work, the wastewater treatment plant is not modeled. The stages before the quaternary treatment of the wastewater plant are considered previously constructed and operated with a grid connection for discharging the treated water to the Mediterranean Sea without any reuse. For the reuse purpose, the quaternary treatment part, UV/H_2O_2 treatment, is added and connected to the solar systems. When there is not enough energy from solar systems, the quaternary treatment of the wastewater is not operated, and the treated water from the conventional plant is discharged to the Mediterranean Sea. On the other hand, when solar systems

produce electricity, the effluent of the conventional wastewater treatment plant is treated with UV/H_2O_2 process to be used for agricultural irrigation purposes.

The following assumptions are made for the wastewater treatment system:

1. The hourly, daily and seasonal fluctuations of the wastewater supply are neglected, and the supply is assumed to be constant throughout the year.
2. The quaternary treatment is operated only at the design load.
3. The specific energy consumption of the wastewater treatment plant is taken as constant.

In the following sections of this thesis, WWTP stands for the quaternary treatment of wastewater treatment, UV/H_2O_2 treatment unless otherwise stated.

3.2.1.1.2 Reverse Osmosis System

The reverse osmosis process is simulated using Toray DS2 [81] in this study. TORAY DS2 is a free software released by TORAY to design and manage RO membrane systems for different operational conditions [82].

The simulations are conducted to find the specific energy consumption (SEC) of the process at the design load and partial loads; and ensure that the permeate quality meets the irrigation water requirements. It should be emphasized that SEC is one of the most significant parameter related to water systems. It is the measure of the energy intensity of the plant. SEC is defined as the energy requirement per m^3 of freshwater obtained, and it is in form of electricity for RO systems.

The RO configuration is determined as multi train, single stage, single pass with no feed bypass. The definitions regarding RO configurations are explained as follows:

- Train: In this study, the train is defined as the sub-unit of the reverse osmosis system. In more detail, it is the group of pressure vessels that are controlled together. Each train of the RO plant can be shut down or started independently.

- Stage: In a single stage system, the seawater enters the RO and leaves it either as desalinated water or brine. On the other hand, in a two-stage system, the brine of the first stage serves as the feed of the second stage. The additional stages increase the recovery rate as brine is further concentrated; however, it also results in higher energy consumption.
- Pass: In single pass systems, the seawater is fed to the RO system, and separation occurs. If high quality water is required as the product, i.e., drinking water, single pass may not be sufficient. In that case, the permeate of the first pass is fed to the second pass to be further desalinated.
- Feed Bypass: Feed bypass corresponds to blending of the feed water with the permeate. This can be applied to meet the permeate quality requirements when the permeate is too demineralized. It is a common configuration to produce irrigation water from brackish water, which has lower salt concentrations than seawater.

The schematical representation of the reverse osmosis configuration proposed in this study is given in Figure 3.2.

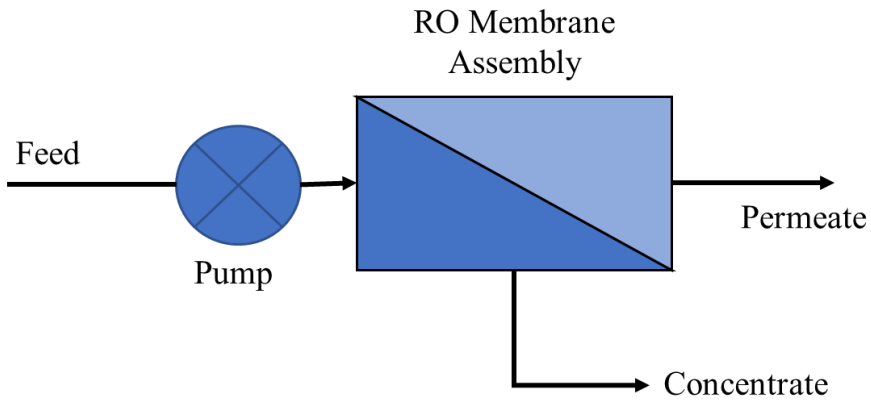

Figure 3.2. Schematical representation of the RO configuration with single stage, single pass with no feed bypass.

With the employed RO configuration, two different operational modes are studied:

1. Nominal Load Operation where each train is operated only at nominal load or turned off in a binary manner.
2. Variable Load Operation where the trains are allowed to operate between any load between their minimum safe load and nominal load.

For the variable load operation, the operational strategy is selected as constant recovery as suggested by Pohl et al. [67] and Richards et al. [68], and the reverse osmosis system is simulated accordingly.

The recovery rate, *RR*, is the ratio of the permeate flow rate, $Q_{permeate}$, to the feed flow rate, Q_{feed} , as shown in Eqn. 3.1.

$$RR\ (\%) = \frac{Q_{permeate}}{Q_{feed}} * 100 \tag{3.1}$$

The procedure of the RO simulation is described as follows:

Step 1: The feedwater data is entered. The water type, temperature, pH, and concentrations of the cations and anions present in the seawater are defined.

Step 2: The system configuration is selected. The number of stages, passes, etc., are determined at this step.

Step 3: The nominal permeate flow rate is defined. This value corresponds to the design flow rate of each train.

Step 4: The recovery rate is defined.

Step 5: From the product library, the membrane is selected according to the system requirements.

Step 6: The number of pressure vessels and elements for each pressure vessel is decided based on the recovery rate, the desired permeate flow rate, and the selected membrane type. Also, the efficiencies of the pumps and energy recovery device are defined.

Step 7: The system is run, and the operation report is published. The report contains the ion concentrations of the permeate and concentrate, the warnings, errors, and cautions regarding the operation, and most importantly, the SEC of the process.

For nominal load operation, the procedure is stopped at Step 7.

For variable operation, with the same

- seawater data,
- system configuration
- membrane type

and by keeping

- the recovery rate
- the number of pressure vessels and elements

as constant, these additional steps are followed:

Step 8: The permeate flow rate is decreased by 5% increments of the design flow.

Step 9: The simulation is run and the report of the operation is published. The permeate quality and specific energy consumption are found.

For variable load operation, the simulations are continued by decreasing the permeate flow rate until the system reaches its safe operational limits. The minimum load of the reverse osmosis plant is determined based on the membrane specifications, limitations, and operational requirements.

Then, the SEC values obtained for each permeate flow rate are fitted to an equation to estimate the specific energy consumption of the plant at any load between the minimum safe load and the design load.

The following assumptions are followed for the reverse osmosis system:

1. The performance decrease of the system due to aging of the membranes, fouling, scaling etc., is neglected.
2. The RO is assumed to constitute 71% of the total energy consumption of the desalination plant [25], [83]. The simulated SECs for RO are divided by 71% to calculate the SEC of the overall desalination plant.

3.2.1.2 Energy Systems

It is of significance to recall that the energy requirement of water systems is exclusively in the form of electricity. Therefore, the energy systems of this study aim to supply solely electricity.

The energy systems analyzed in this study are simulated to different extents through System Advisor Model (SAM) [84], and the outputs are further processed with MATLAB [85]. SAM is a free software released by National Renewable Energy Laboratory (NREL) to model several types of RE systems and conduct techno-economic analysis of those [86].

Three scenarios are considered: a) PV-only, b) CSP with TES, and c) PV+CSP with TES, all isolated from grid.

According to EU, RE powered off-grid desalination systems are crucial for isolated regions due to the associated high costs, and limited accessibility or availability regarding the connection of desalination systems to the electricity grid [87]. It should be emphasized once again that the RO is an energy intensive process, and it is claimed in [88] that the reliance and dependence of this installation on the existing infrastructure is the main challenge for implementation of this technology in remote areas. Hence, several studies in literature have focused on the stand-alone desalination systems powered by RE systems for isolated regions [89]–[92]. Furthermore, UV/H_2O_2 method can and should also be included in the discussion, as its electricity requirement is also significant.

Even though, the discussions and studies of off-grid energy systems are mainly focused on isolated regions, it is noteworthy to state that the integration and deep penetration of renewable energy systems to pre-existing grids is not free of problems even in mainland. It is often concerned whether the current grids could accommodate the considerable variable electricity supplies from renewable energy resources [93]. The integration and penetration of these renewable energy resources with variable nature to the grid initiates several challenges, such as system stability, voltage control, need for demand and supply forecasting and management [94].

It is clear that at high capacities, water systems create a significant additional demand and require huge solar installations which could affect the grid greatly. Therefore, investigation of the off-grid water treatment systems is essential for isolated regions, and also for mainland with grid reliability issues. Hence, in this study, the energy systems used to power water systems, RO desalination and UV/H_2O_2 wastewater treatment are taken as isolated from grid.

Also, please note that the hybridization of PV with CSP is represented by "PV+CSP" in this thesis.

3.2.1.2.1 PV Plant

The PV system is simulated through SAM, and the hourly electricity generation of the PV plant is exported directly to MATLAB.

Perez Model is used in the SAM PV simulations as it accounts for circumsolar solar diffusion and horizon brightening in addition to the isotropic diffuse radiation [95]. Perez Model uses empirically derived coefficients. Compared to the isotropic sky and HDKR model available in SAM, it is more complex, detailed, and computationally intensive [96].

The assumptions made for the modeling of the PV plant can be listed as follows:

1. The PV plant is assumed to have no parasitic losses when there is no electricity generation.
2. The lifetime of the PV plant is taken as 25 years. The PV panels are reported with 25-30 year lifetimes in [97] and [98].
3. The degradation rate is assumed as zero even though the degradation rate is reported as around 0.5% $year^{-1}$ [99], [100].

3.2.1.2.2 CSP Plant

A central receiver (CR) CSP system is simulated through SAM with a thermal energy storage consisting of two storage tanks. In this study, the terms central receiver and power tower are used interchangeably.

As will be explained in Section 3.2.2.2, in this study, the CSP plant is not operated with respect to the control scheme of SAM. SAM aims to provide the maximum possible hourly electricity output as default. However, in this study, the CSP system operation is regulated based on the water system requirements and operating strategies. Therefore, to be able to manipulate the CSP plant's hourly electricity production according to the requirements of this study, the solar collector field and the power tower are separated from the power block and thermal energy storage system. The solar field and power tower are simulated through SAM, and hourly results for the thermal energy that can be transferred to heat transfer fluid, Q_{HTF}, in the receiver are taken as the output from SAM and exported to MATLAB for the electricity production and thermal energy storage system calculations.

As the control scheme proposed by SAM is not used, a slightly different approach is employed in the simulations. SAM, by default, defocuses the heliostat field when the storage is full. However, as the result of the operating strategy proposed by this work, the desired hourly electricity production of the CSP plant is different from SAM simulations. Hence, due to the discrepancy between the hourly electricity

production of this study and SAM's default control scheme, the hourly state of charge of the TES is also different between two approaches. Therefore, to eliminate the risk of defocusing of the heliostat field due to SAM's operating strategy, the storage system is oversized to 36 hours for the SAM simulations of the CSP system. By oversizing the storage system, it is ensured that the receiver can achieve maximum radiation that can be reflected by the heliostat field instead of having reduced incident irradiation due to the storage system limitations resulted from SAM's control scheme which does not reflect the operational characteristics of the CSP system studied here. Then, the thermal energy available to the heat transfer fluid, Q_{HTF}, is found as the output of the SAM simulations. After finding the maximum energy that can be gained by the molten salts, the actual thermal storage system capacity is defined in MATLAB. Depending on the state of charge of the thermal energy storage system, the excessive energy that can not be used in either power block or TES is discarded by the MATLAB model, indicating the defocusing of heliostats.

Thermal to electricity conversion of the CSP turbine is represented by Eqn. 3.2

$$P_{CSP} = P_{th} * EF * \eta_{th} * \eta_{gross\_net} \tag{3.2}$$

where $P_{CSP,}$ P_{th}, η_{th} and η_{gross_net} is defined as the electricity output of CSP plant, thermal energy that is converted to electricity by power block, thermal efficiency and gross to net efficiency of the turbine, respectively. Here, the CSP electricity output is constrained to be between the minimum load and nominal load of the turbine.

The thermal efficiency, η_{th} was calculated by PSA with Engineering Equation Solver and found to be 41.78% [65]. The thermal efficiency of the Rankine Cycle is reported as 42% for GemaSolar PowerPlant in Sevilla [101], [102] for CR system with a similar power block capacity. Therefore, the thermal efficiency value used in this study can be concluded to be in good agreement with the reported thermal efficiency values of similar turbine capacities.

The efficiency factor, *EF*, of the turbine serves as a correction factor of the thermal efficiency for partial load operations of the turbine based on the load factor. The load factor, *LF*, is defined as the ratio of electricity output at a partial load to the nominal electricity output of the turbine. Subsequently, *EF* is defined as the ratio of thermal efficiency at a partial load to thermal efficiency at nominal load. The efficiency factor is expressed as a function of load factor according to the study conducted by PSA [65] and presented in Eqn. 3.3 as a function of the load factor.

$$EF = -0.4615LF^3 + 0.8333LF^2 - 0.2291LF + 0.8572 \quad (3.3)$$

The energy available to the thermal energy system, $Q_{Av,TES}$, is determined by Eqn. 3.4.

$$Q_{Av,TES} = Q_{HTF} - \frac{P_{CSP}}{EF*\eta_{th}*\eta_{gross\_net}} \quad (3.4)$$

State of charge, *SOC*, is defined as the level of charge of the tank relative to its capacity. As an example, the definition of the state of charge of the hot tank, SOC_{HT}, is presented by Eqn. 3.5

$$SOC_{HT} = \frac{m_{HTF,HT}}{\rho_{HTF}*V_{HTF}} \quad (3.5)$$

where $m_{HTF,HT}$, ρ_{HTF} and V_{HTF} corresponds to the mass of the heat transfer fluid present in the hot tank, heat transfer fluid density and total heat transfer fluid volume, respectively. Accordingly, the mass of the heat transfer fluid inside the cold tank, $m_{HTF,CT}$, can be found by Eqn. 3.6.

$$m_{HTF,CT} = (\rho_{HTF} * V_{HTF}) - m_{HTF,HT} \quad (3.6)$$

The details of charging of the TES is provided in Figure 3.3, where the relevant equations and the strategy are also shown.

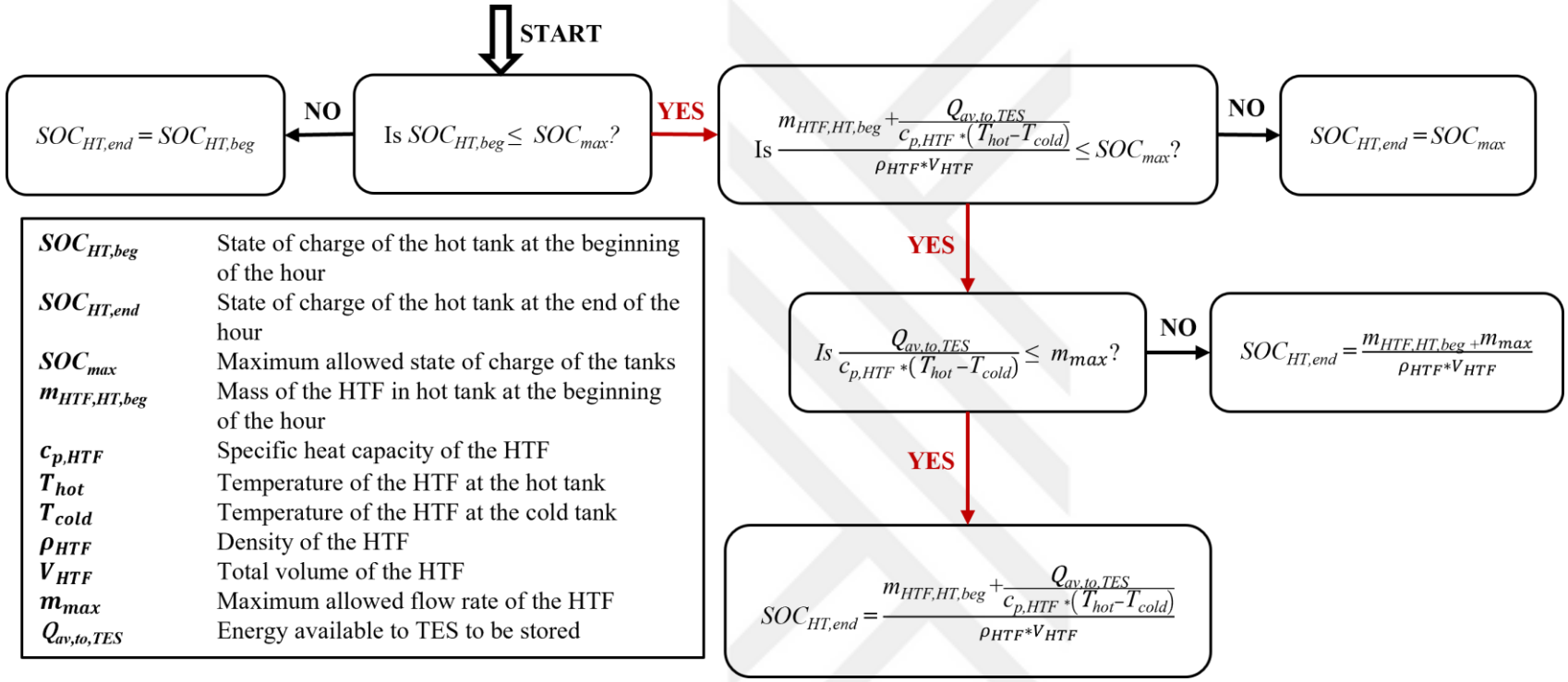

Figure 3.3. The operating strategy for the charging of the TES.

The electricity generation of CSP plant with discharging of the TES when Q_{HTF} is not sufficient is covered by Eqn. 3.7

$$P_{CSP} = \frac{Q_{HTF}+(m_{HTF,HT,beg}-m_{HTF,HT,end})*c_{p,HTF}*(T_{hot}-T_{cold})/3600}{EF*\eta_{th}*\eta_{gross\_net}} \quad (3.7)$$

where $m_{HTF,HT,beg}$, $m_{HTF,HT,end}$, $c_{p,HTF}$, T_{hot} and T_{cold} corresponds to the mass of the heat transfer fluid in the hot tank at the beginning of the hour, the mass of the heat transfer fluid in the hot tank at the end of the hour, the specific heat capacity of the heat transfer fluid, temperature of the heat transfer fluid at the hot tank and temperature of the heat transfer fluid at the cold tank, respectively.

The assumptions for the modeling of the CSP plant are listed as follows:

1. The specific heat capacity of the molten salt is taken as constant.
2. The TES is assumed to be adiabatic. The TES efficiency is reported as 98.5% in [103]; therefore, the adiabatic assumption is reasonable.
3. The piping system and heat exchangers are assumed to have no heat losses.
4. The turbine is not modeled or simulated as transient. Even though this is a major simplification, the CSP power block is operated by forecasting the number of consecutive hours when there are no solar resources and distributing the energy stored in TES among those hours to maintain the continuous operation of the turbine and RO trains as will be explained in Section 3.2.2.2 in detail. Therefore, the ramping rate and decrease in energy production are assumed to be minimal.

3.2.1.2.3 PV+CSP Plant

As the PV and CSP systems are hybridized non-compactly, the modeling and simulation approach is the same, regardless of whether the systems are alone or hybridized. The PV and CSP systems are modeled separately as explained in Sections 3.2.1.2.1 and 3.2.1.2.2, but operated synergetically as will be explained in Section 3.2.2.2 extensively.

3.2.2 Operating Strategies

In this section, the operational strategies of the water and energy systems are presented.

3.2.2.1 Water Systems

The specific energy consumption, SEC, of the quaternary treatment of the WWTP is lower than the specific energy consumption of the RO plant. Also, wastewater production is inevitable, where water withdrawal from the sea for desalination is optional. Therefore, the WWTP operation is always prioritized over the RO plant operation.

3.2.2.1.1 Wastewater Quaternary Treatment Operating Strategy

The UV/H_2O_2 system is operated at only nominal load with predetermined unit capacities. The unit corresponds to the group of UV lamps that are controlled together. Each unit of the quaternary treatment can be shut down or started independently.

By the nominal load operation of the UV/H_2O_2 system, each unit is operated only at nominal load or turned off in a binary manner depending on the available energy.

The operating strategy of the quaternary treatment of WWTP is shown in Figure 3.4. The number of operated WWTP units and energy available to RO after the WWTP operation is found by following the presented strategy.

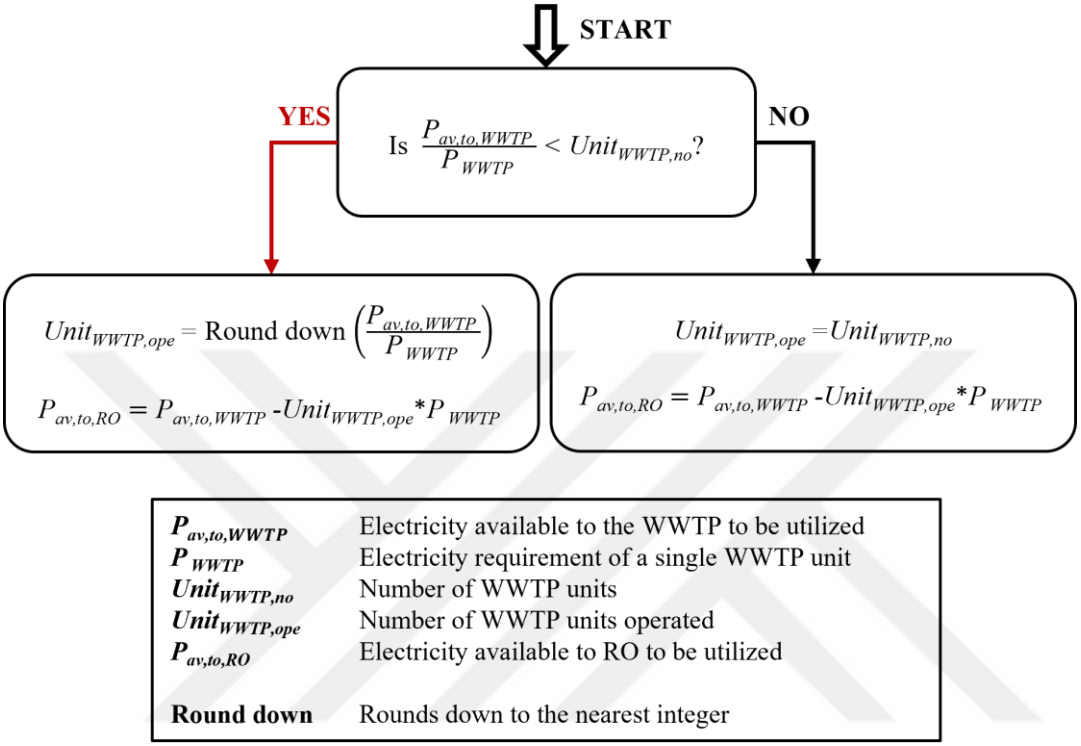

Figure 3.4. The operating strategy of the quaternary treatment of WWTP.

3.2.2.1.2 Reverse Osmosis Desalination Operating Strategy

As mentioned previously, two different RO operating strategies are proposed: nominal load operation and variable load operation.

By nominal load operation, each RO train is operated only at nominal load or turned off in a binary manner. As a reminder, train is defined as the sub-unit of the reverse osmosis system. In more detail, it is the group of pressure vessels that are controlled together. Each train of the RO plant can be shut down or started independently.

The nominal operating strategy of the reverse osmosis desalination system is presented in Figure 3.5.

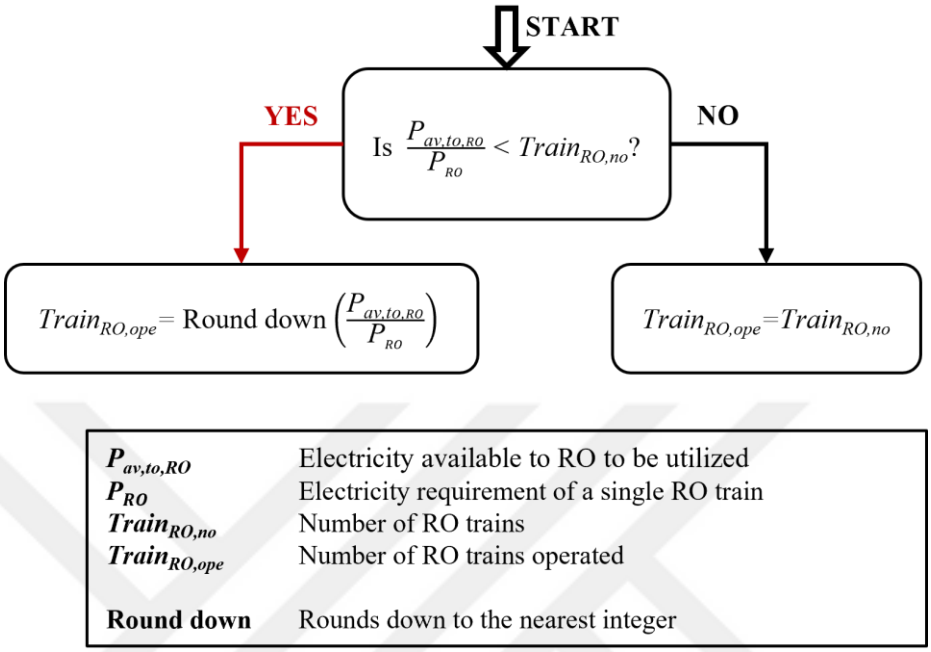

Figure 3.5. The operating strategy of RO plant for nominal load operation.

On the other hand, with variable load operation, the trains are allowed to operate between any load between their minimum safe load and nominal load. The variable load operating strategy of the reverse osmosis desalination system is given in Figure 3.6. Variable load RO operation is expected to lead to better utilization of the electricity by the RO plant as the energy threshold for train operation is decreased. Also, with the variable load operation strategy proposed here, the maximum number of RO trains is operated at lower loads, which is the same for all trains, instead of operating fewer trains at nominal load. This way, the number of start-stop instances is targeted to be minimized. Also, considering that SEC decreases as the permeate flow rate decreases for constant recovery ratio [67], this strategy results in reduced specific energy consumption.

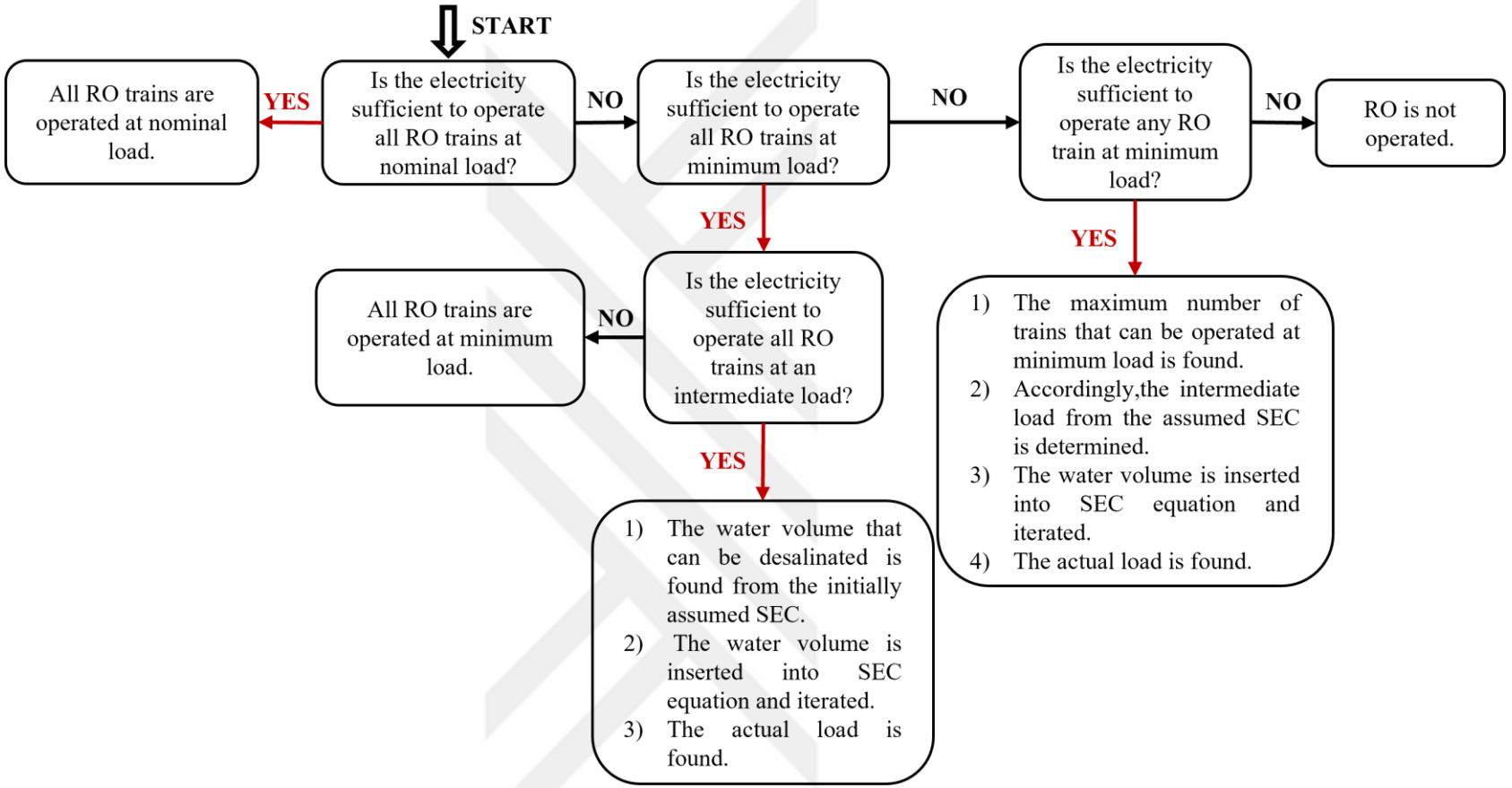

Figure 3.6. The operating strategy of RO plant for variable load operation.

3.2.2.2 Energy Systems

All the energy systems presented in this study are isolated from the grid, and their electricity production is used only by the water systems.

3.2.2.2.1 PV Plant Operating Strategy

As the PV system considered here is not coupled with any storage system, the electricity produced by the PV is directly used by the water systems.

In the case of excess electricity, when the water systems cannot utilize all the electricity produced, the PV curtailment or dissipation of the excess electricity is required. It should be noted that excess electricity generation is inevitable when RO is operated with nominal load operating strategy due to strict energy requirement of trains even though the PV system is undersized.

3.2.2.2.2 CSP Plant Operating Strategy

Regarding the operation of the CSP plant, two different strategies are studied.

1. Base Strategy: The nominal turbine output is targeted at all hours. The base strategy for CSP operation is shown in Fig. 3.7. In this strategy, the CSP plant is operated independently from the water systems requirements without any interaction or feedback, only by aiming to produce maximum hourly electricity output.
2. Proposed Strategy: The proposed strategy aims to operate the CSP plant in coordination with the water systems. The requirements and restrictions of the water systems are included in the CSP plant operating strategy to improve the performance of energy and water systems. Figure 3.8 presents the proposed strategy for CSP operation.

In this strategy, when the thermal energy that can be transferred to heat transfer fluid in the receiver, Q_{HTF}, is zero, and the TES is not fully discharged, the number of consecutive hours in which Q_{HTF} is zero is forecasted and the energy stored in the TES is distributed among these hours to have the continuous operation of the CSP turbine and RO system with certain restrictions. In other words, the continuous operation of the turbine at partial loads for more extended periods is preferred instead of the nominal load operation for a limited duration. This way, the operating hours of the CSP turbine and water systems are targeted to be increased and the shut-downs of both CSP turbine and RO trains are aimed to be eliminated or at least minimized. It should be noted that in addition to RO trains, the frequent start-ups, shut-downs, and steep load gradients of CSP turbine are also undesirable as they cause high thermal stresses which result in reduced lifetime of the turbine [104], [105].

Also, the excess electricity generation of the CSP system is aimed to be prevented with this strategy as the CSP system studied here is isolated from the grid, i.e., the excess energy cannot be injected into the grid and needs to be dissipated. Besides the waste of enormous practical value of already produced but unused electricity for a grid-isolated scenario, this situation also increases the LCOE of the CSP system which is already comparatively higher. Hence, the minimum load of the turbine is re-addressed by setting the minimum electricity requirement of the water system which is just equal to or above than the minimum turbine load as the new minimum load of the turbine. The determination of the minimum electricity requirement of the system and the minimum turbine load is provided in Fig. 3.9 and 3.10 for nominal load RO operation and variable load RO operation, respectively. In addition to the re-setting of the minimum turbine load, the CSP generation between the minimum and nominal turbine load is also determined such that water systems can completely utilize all the electricity produced by CSP. The determination of intermediate CSP turbine loads is presented in Fig. 3.11 and 3.12 for nominal and variable RO operation, respectively.

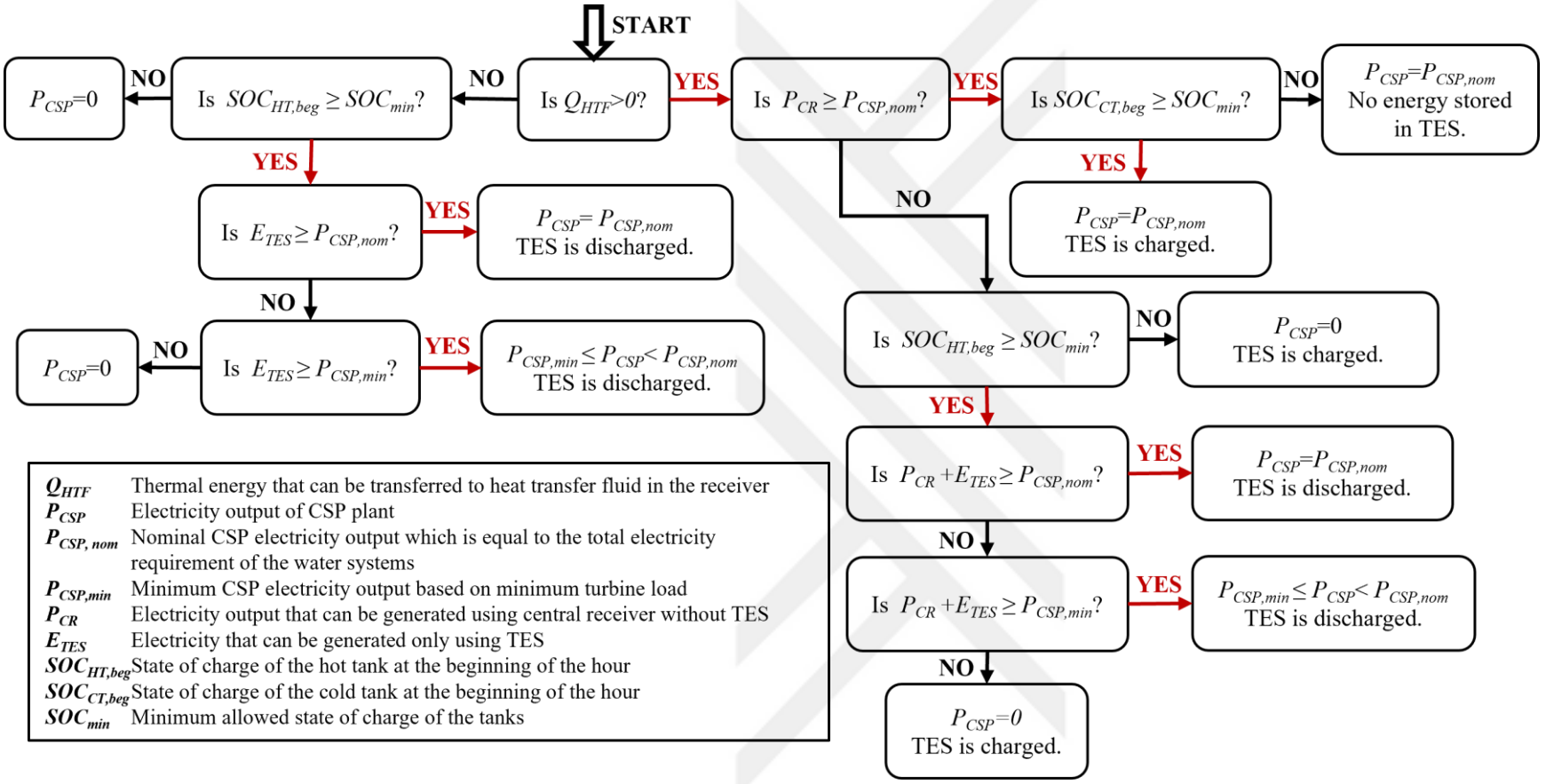

Figure 3.7. Base operating strategy of CSP plant.

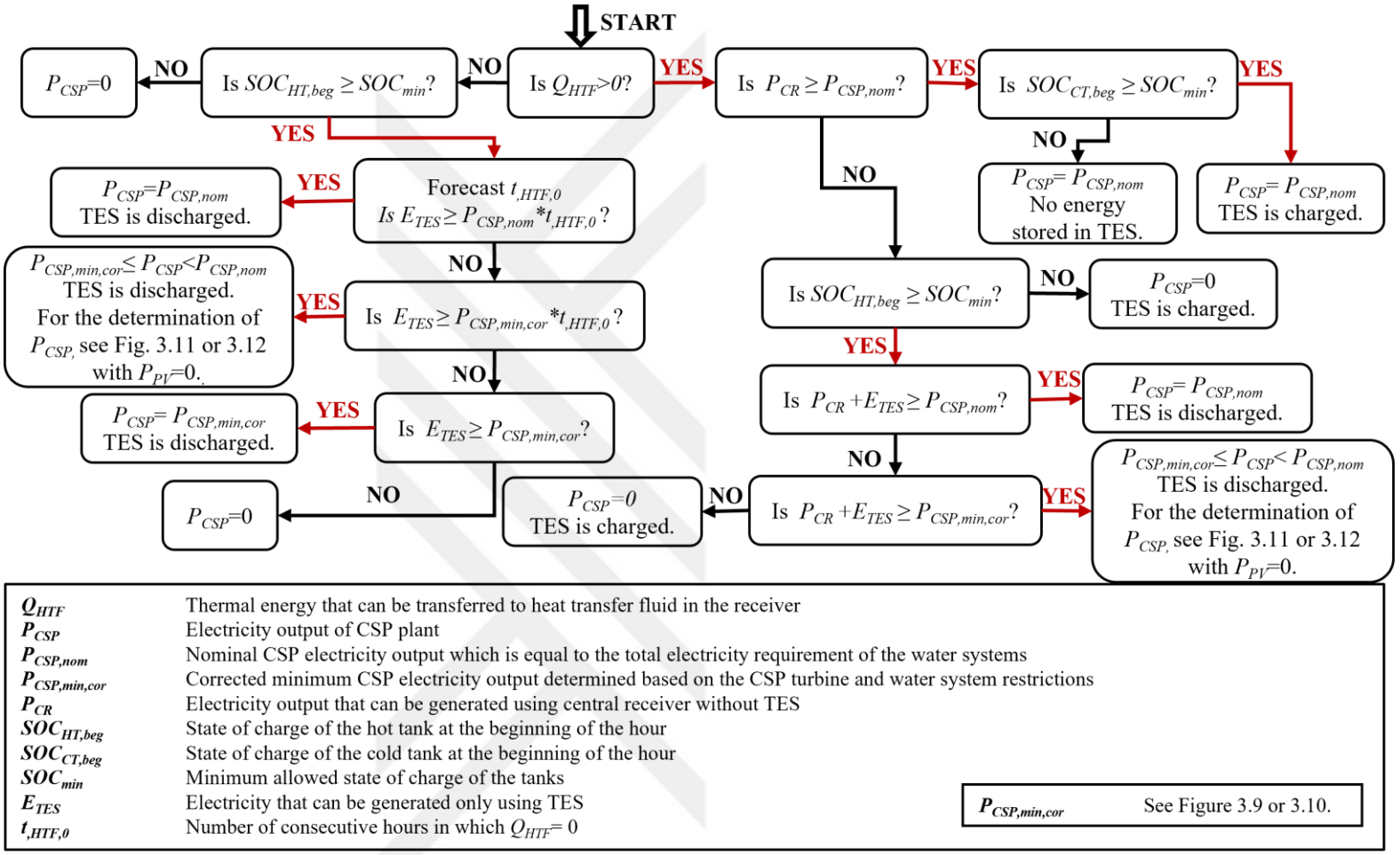

Figure 3.8. Proposed operating strategy of CSP plant.

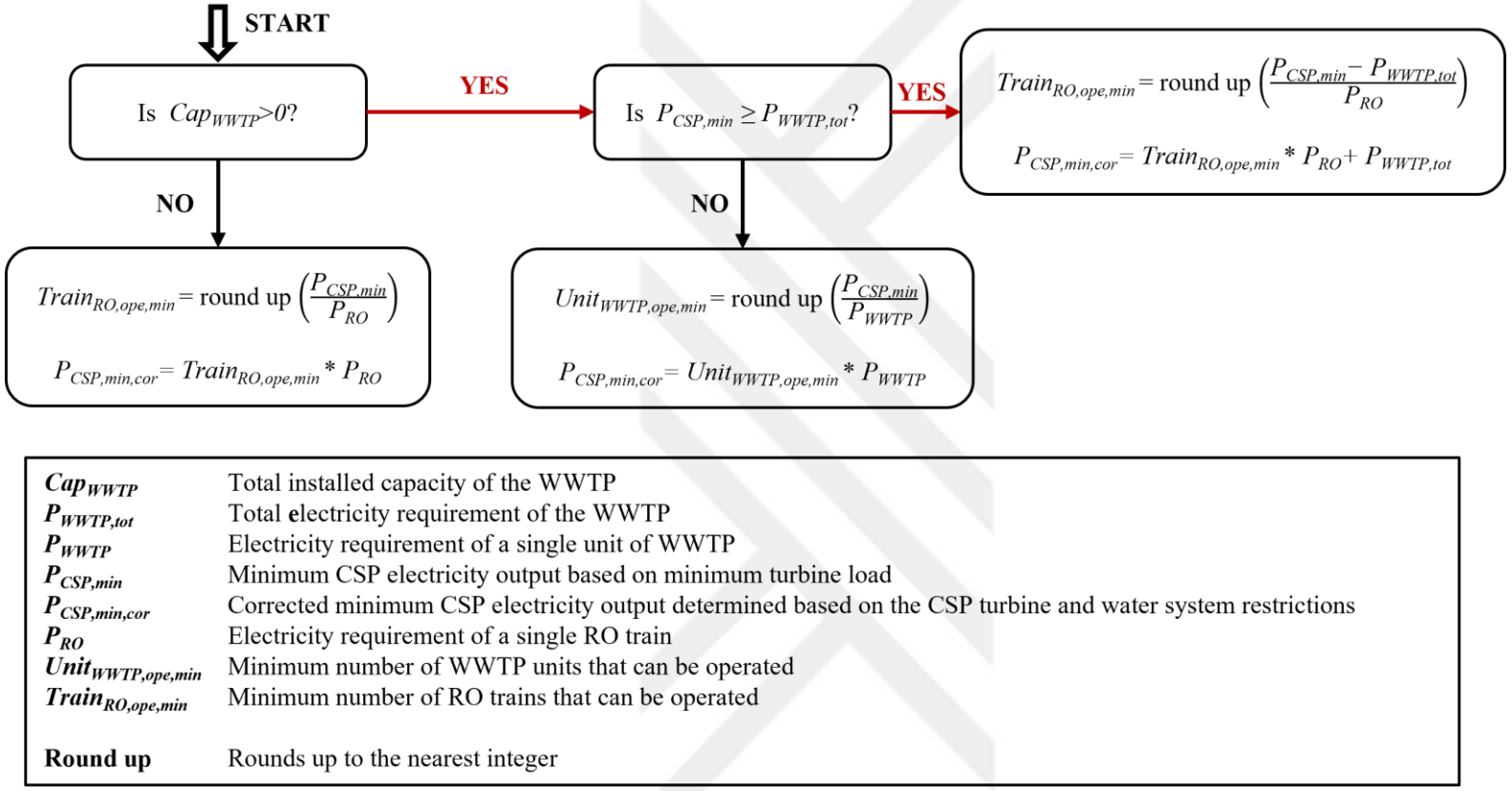

Cap_{WWTP}	Total installed capacity of the WWTP
$P_{WWTP,tot}$	Total electricity requirement of the WWTP
P_{WWTP}	Electricity requirement of a single unit of WWTP
$P_{CSP,min}$	Minimum CSP electricity output based on minimum turbine load
$P_{CSP,min,cor}$	Corrected minimum CSP electricity output determined based on the CSP turbine and water system restrictions
P_{RO}	Electricity requirement of a single RO train
$Unit_{WWTP,ope,min}$	Minimum number of WWTP units that can be operated
$Train_{RO,ope,min}$	Minimum number of RO trains that can be operated
Round up	Rounds up to the nearest integer

Figure 3.9. The corrected minimum load of the CSP plant of the proposed CSP operating strategy for the nominal load operation of RO.

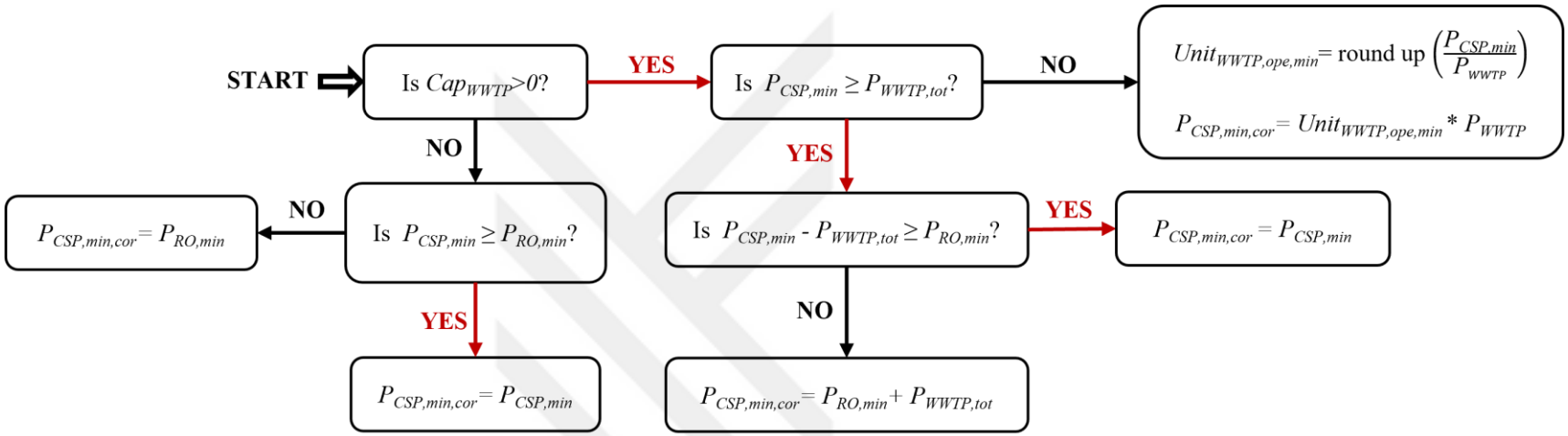

Cap_{WWTP}	Total installed capacity of the WWTP
$P_{WWTP,tot}$	Total electricity requirement of the WWTP
P_{WWTP}	Electricity requirement of a single unit of WWTP
$P_{CSP,min}$	Minimum CSP electricity output based on minimum turbine load
$P_{CSP,min,cor}$	Corrected minimum CSP electricity output determined based on the CSP turbine and water system restrictions
$P_{RO,min}$	Minimum electricity requirement of a single RO train based on the allowable load range
$Unit_{WWTP,ope,min}$	Minimum number of WWTP units that can be operated
Round up	Rounds up to the nearest integer

Figure 3.10. The corrected minimum load of the CSP plant of the proposed CSP operating strategy for the variable load operation of RO.

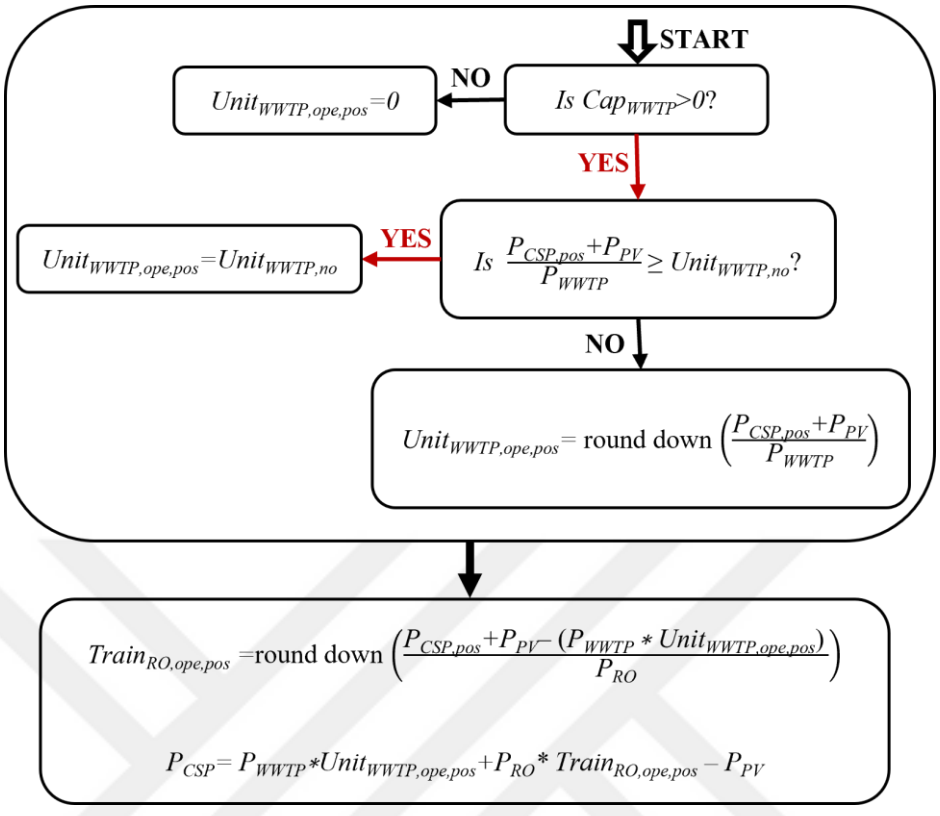

Cap_{WWTP}	Total installed capacity of the WWTP
$Unit_{WWTP,ope,pos}$	Number of units that can be possibly operated by the electricity provided
$Unit_{WWTP,no}$	Number of WWTP units
P_{PV}	Electricity output of PV plant
$P_{CSP,pos}$	Electricity that can possibly be provided by CSP system using receiver and TES
P_{WWTP}	Electricity requirement of a single unit of WWTP
P_{RO}	Electricity requirement of a single RO train
$Train_{RO,ope,pos}$	Number of RO trains that can be operated with the available electricity
P_{CSP}	Electricity output of CSP plant
Round down	Rounds down to the nearest integer

Figure 3.11. The determination of CSP output at intermediate loads of turbine for the proposed CSP operating strategy for the nominal load operation of RO.

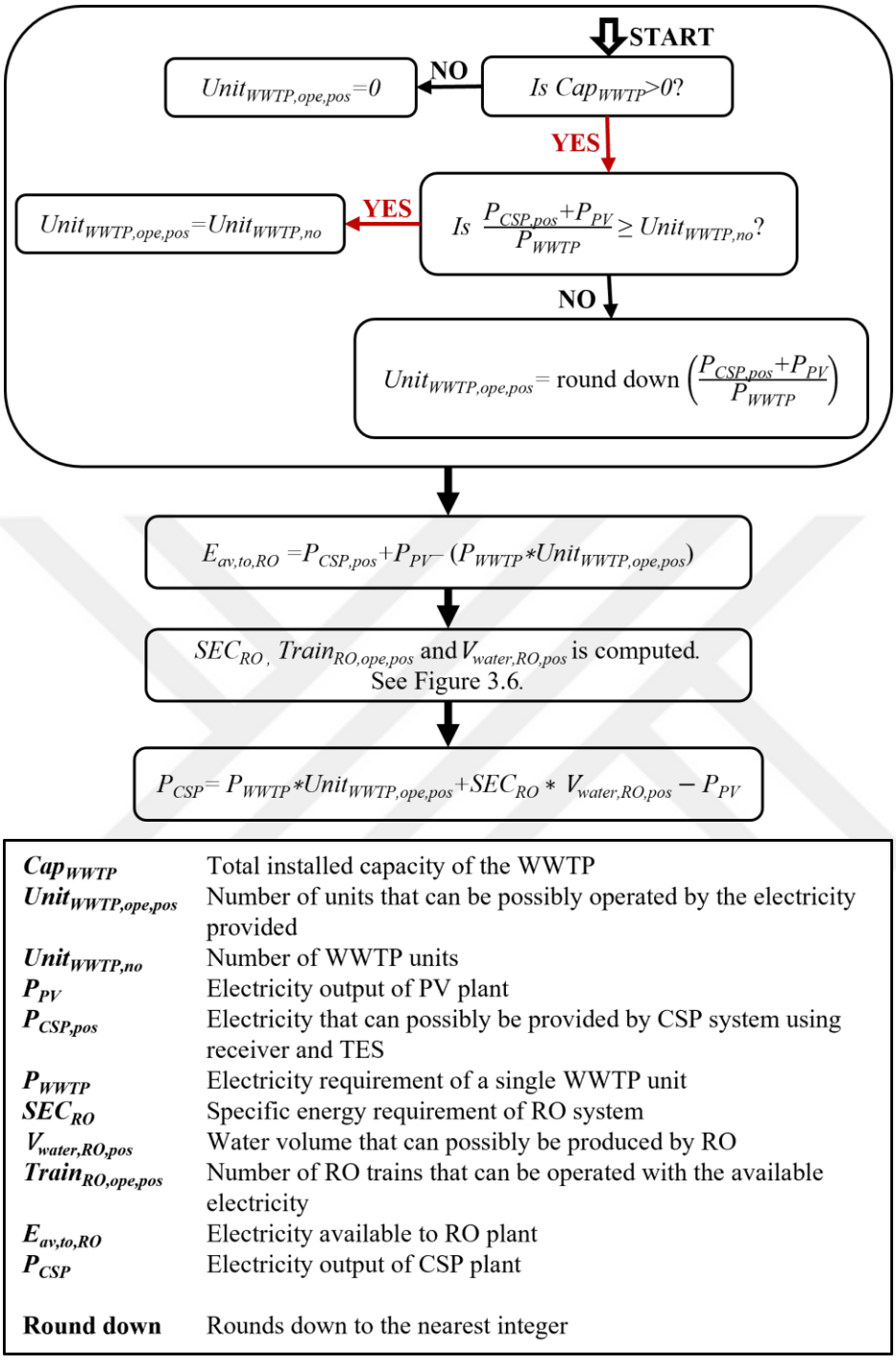

Figure 3.12. The determination of CSP output at intermediate loads of turbine for the proposed CSP operating strategy for the variable load operation of RO.

All in all, with the proposed CSP operating strategy, the minimum load of the turbine and electricity produced by the CSP system is tailored according to the water system requirements and limitations in addition to the CSP system restrictions.

3.2.2.2.3 PV+CSP Plant Operational Strategy

While operating the PV+CSP system, PV is always prioritized to power the water systems when there is solar radiation. During those hours, the CSP system serves as the complementary energy system to supply electricity. CSP firstly supports the PV system when the PV electricity generation is not sufficient to operate the water systems in the pre-defined operational ranges, and secondly stores energy in TES to power the water systems in the absence of solar resources. This strategy targets to take advantage of the cheaper PV electricity whenever possible, expand the operation time of water systems and decrease the impacts of the variable solar resources on the RO plant by the CSP plant. The operating strategy of the PV+CSP system is provided in Fig. 3.13 and 3.14 for $Q_{HTF}>0$ and $Q_{HTF}=0$, respectively.

As in the case of the CSP-alone plant, again, the CSP plant of PV+CSP is operated in coordination with the water systems. However, with the hybridization, the hourly produced PV electricity imposes an additional constraint in the operational strategy of the CSP system. The minimum load of the turbine for PV+CSP scheme is re-defined and its determination is presented in Fig. 3.15 and 3.16 for nominal and variable RO operation, respectively. It should be noted that with PV CSP hybridization, the value of the corrected minimum turbine load varies hourly as the electricity demanded from CSP changes hourly depending on the supply of the PV system whereas the corrected minimum turbine load is a single value applicable to all hours in the CSP scenario. Also, the method provided in Fig. 3.11 and 3.12 is used to decide on the CSP electricity at intermediate loads for nominal and variable RO operation, respectively.

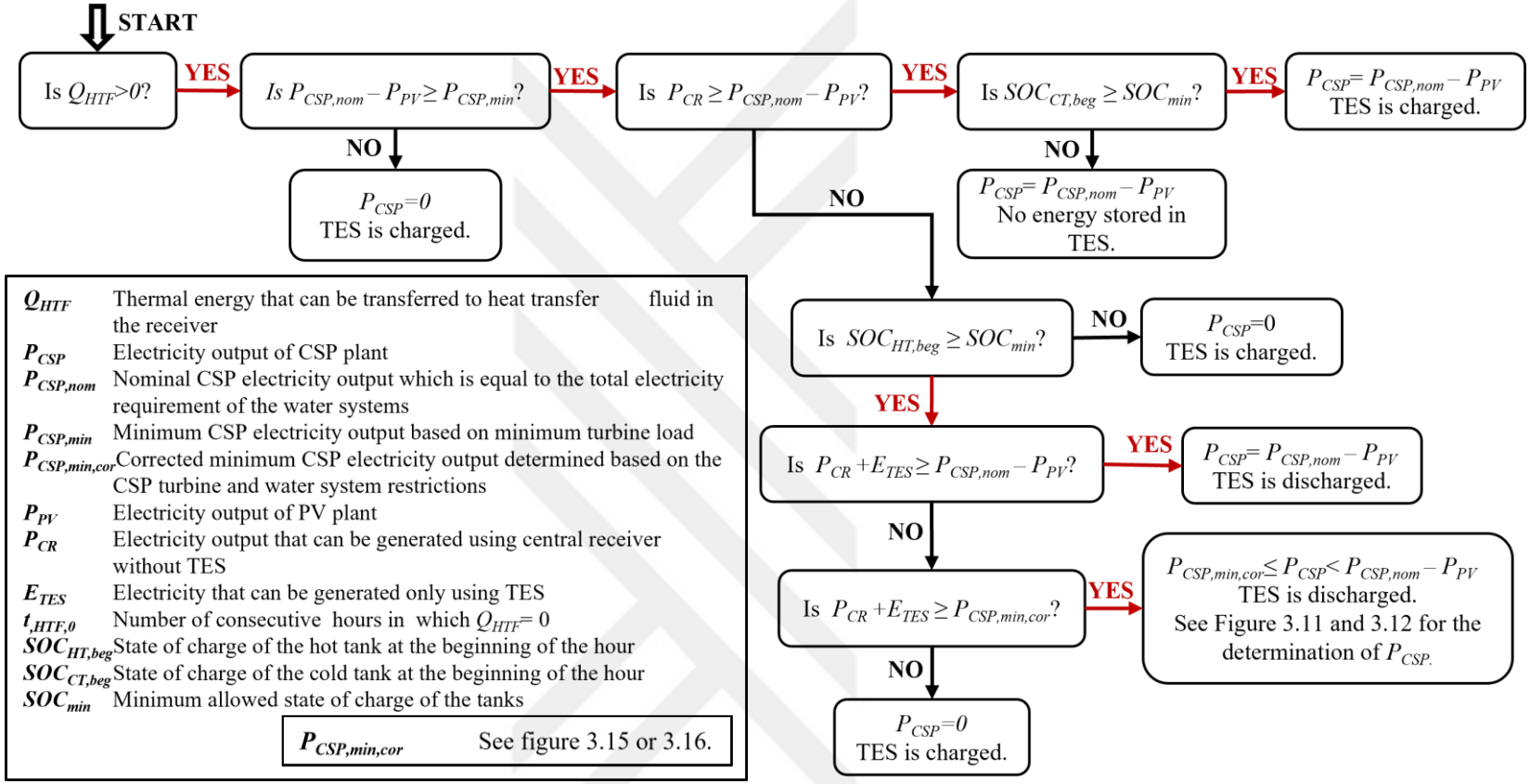

Figure 3.13. The proposed PV+CSP operating strategy for when $Q_{HTF}>0$.

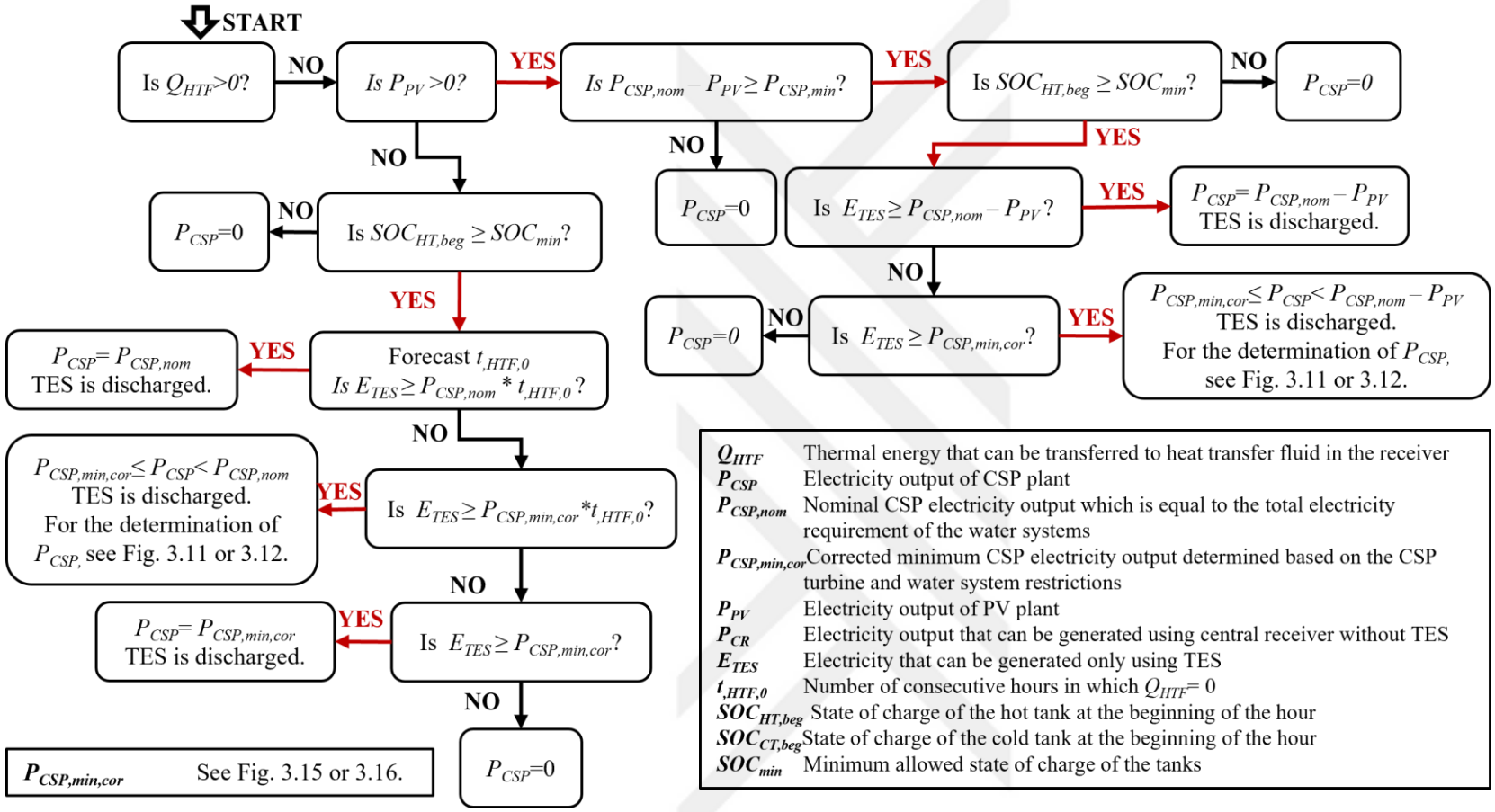

Figure 3.14. The proposed PV+CSP operating strategy for when $Q_{HTF}=0$.

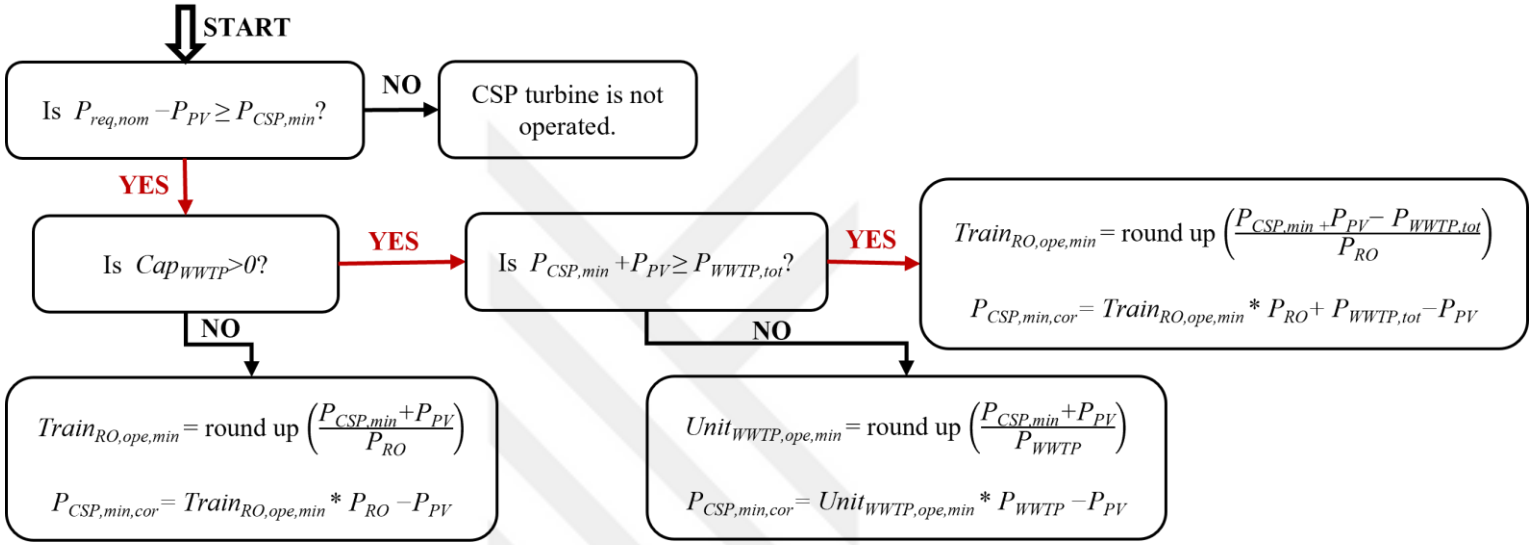

Cap_{WWTP}	Total installed capacity of the WWTP
$P_{WWTP,tot}$	Total electricity requirement of the WWTP
P_{WWTP}	Electricity requirement of a single unit of WWTP
P_{PV}	Electricity output of PV plant
P_{CSP}	Electricity output of CSP plant
$P_{CSP,min}$	Minimum CSP electricity output based on minimum turbine load
$P_{CSP,min,cor}$	Corrected minimum CSP electricity output determined based on the CSP turbine and water system restrictions
P_{RO}	Electricity requirement of a single RO train
$Unit_{WWTP,ope,min}$	Minimum number of WWTP units that can be operated
$Train_{RO,ope,min}$	Minimum number of RO trains that can be operated
Round up	Rounds up to the nearest integer

Figure 3.15. The corrected minimum load of the CSP plant of the proposed PV+CSP operating strategy for the nominal load operation of RO.

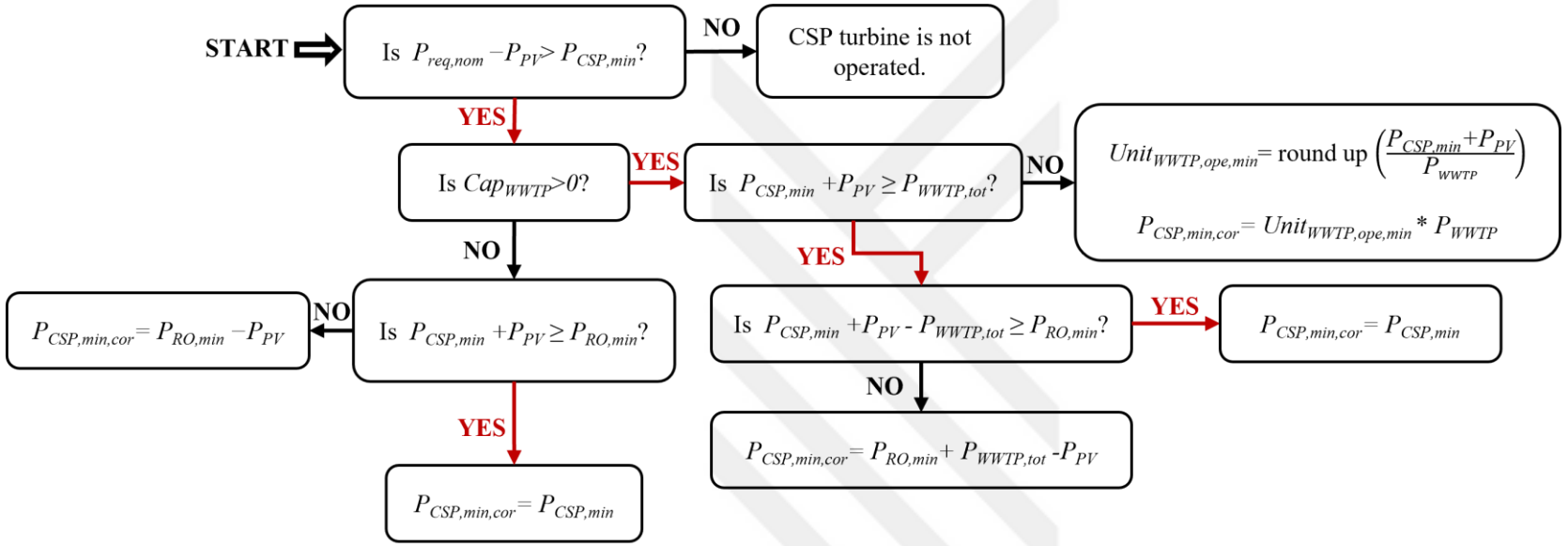

Cap_{WWTP}	Total installed capacity of the WWTP
$P_{WWTP,tot}$	Electricity requirement of the whole WWTP
P_{WWTP}	Electricity requirement of a single unit of WWTP
P_{PV}	Electricity output of PV plant
$P_{CSP,min}$	Minimum allowable electrical power output of CSP plant based on CSP plant requirements
$P_{CSP,min,cor}$	Corrected minimum CSP electricity output determined based on the CSP turbine and water system restrictions
$P_{RO,min}$	Minimum electricity requirement of a single RO train based on the allowable load range
$Unit_{WWTP,ope,min}$	Minimum number of WWTP units that can be operated
Round up	Rounds up to the nearest integer

Figure 3.16. The corrected minimum load of the CSP plant of the proposed PV+CSP operating strategy for the variable load operation of RO.

3.2.3 Key Performance Indicators

This section provides the key performance indicators used to evaluate the technical performance of the systems.

3.2.3.1 Specific Energy Consumption

The specific energy consumption, *SEC*, is the most significant parameter related to water systems. It is the measure of the energy intensity of the plant. SEC is defined as the energy requirement per m^3 of freshwater obtained. It is worth emphasizing once more that in case of UV/H_2O_2 and RO, the energy requirement is purely electricity.

3.2.3.2 Capacity Factor

The capacity factor, *CF*, is the ratio of the actual production of a system over the production that would be achieved if the system was operated at nominal capacity throughout the year.

The capacity factor, CF, of the energy systems is found by Eqn. 3.8

$$CF = \frac{E_{ann}}{Cap_E * 8760} \tag{3.8}$$

where E_{ann} and Cap_E corresponds to annual electricity production and installed hourly capacity of the energy system, respectively. Also, 8760 is the number of hours in a typical year.

Similarly, capacity factor, CF, of water systems is computed through Eqn. 3.9

$$CF = \frac{V_{W,ann}}{Cap_W * 365} \tag{3.9}$$

where $V_{W,ann}$ and Cap_W corresponds to annual water production and installed daily capacity of the water system, respectively. 365 is the number of days in a typical year.

3.2.3.3 Utilization Factor

The utilization factor, *UF*, is the ratio of the sum of hours each train is operated to the product of number of trains and the total number of hours over the year. It is only applicable where the variable load operation is employed for RO as utilization factor is precisely equal to the capacity factor for nominal load operation.

The utilization factor, UF, is found by Eqn. 3.10

$$UF = \frac{Train_{ope,ann,RO}}{Train_{RO,no} * 8760} \tag{3.10}$$

where $Train_{ope,ann,RO}$ and $Train_{RO,no}$ are the total number of trains operated annually and the train number of the RO system, respectively.

While CF is an indicator of the overall system performance, UF provides an understanding of how the sub-components of the system are operated. Considering the RO system where the continuous operation of trains is desired, with a variable load RO strategy, several trains can be operated at partial loads instead of fewer trains operating at nominal load. Even though CF is almost the same for both scenarios, the UF of the former case is higher.

3.2.3.4 Utilized Electricity Fraction

The utilized electricity fraction, F_{UE}, represents the fraction of the utilized annual electricity by water systems over the total annual electricity production. It is a non-dimensional measure of the excess electricity production of the energy systems.

The utilized electricity fraction, F_{UE}, is calculated through Eqn. 3.11

$$F_{UE} = \frac{E_{ann,ut}}{E_{ann}} \quad (3.11)$$

where $E_{ann,ut}$ and E_{ann} stands for the annual utilized and total electricity production, respectively.

3.2.3.5 Emission Factor

The emission factor of the produced water is evaluated to assess the environmental impact of water production. The emissions considered here are only restricted to CO_2 emissions of the electricity production with different energy systems to operate the water systems.

Life cycle assessment (LCA) is defined as a technique to analyze the environmental effects of a product's or system's life by considering all its stages, starting from the extraction of the raw materials until the disposal phase [106]. It is also referred to as cradle-to-grave analysis. Even though renewable energy technologies are associated with zero carbon emissions, a certain amount of CO_2 is emitted throughout their life cycles, such as during the manufacturing and mantling processes. By accounting for all stages of their life, LCA provides an inclusive method to quantify the impacts of the systems in question on the environment.

As the end product of this study is water, the emissions are converted from $gCO_{2,eq}\ kWh^{-1}$ to $gCO_{2,eq}\ m^{-3}$ of produced water. The emission factor of produced water, $F_{CO_2,W}$, is calculated by Eqn. 3.12

$$F_{CO_2,W} = \frac{E_{ann,CSP,ut} * F_{CO_2,CSP} + E_{ann,PV,ut} * F_{CO_2,PV}}{V_{W,ann,tot}} \quad (3.12)$$

where $E_{ann,CSP,ut}$, $E_{ann,PV,ut}$, $F_{CO_2,CSP}$, $F_{CO_2,PV}$, and $V_{W,ann,tot}$ correspond to annual utilized energy to produce water supplied by CSP system, annual utilized energy to produce water supplied by PV system, the emission factor of CSP system, the emission factor of PV system, and annual produced total water volume, respectively.

3.2.4 Inputs

3.2.4.1 The Location

Two main criteria are targeted to be fulfilled during the determination of the location for which the proposed system is run:

1. It should have large solar resources to be utilized by the solar energy systems.
2. It should be at a coastal region to have easy access to the seawater for the RO system.

Fig. 3.17 shows the daily and annual DNI of Türkiye. As marked in Fig. 3.17 with the black frame, Mersin is one of the most promising coastal region in Türkiye considering the solar resources.

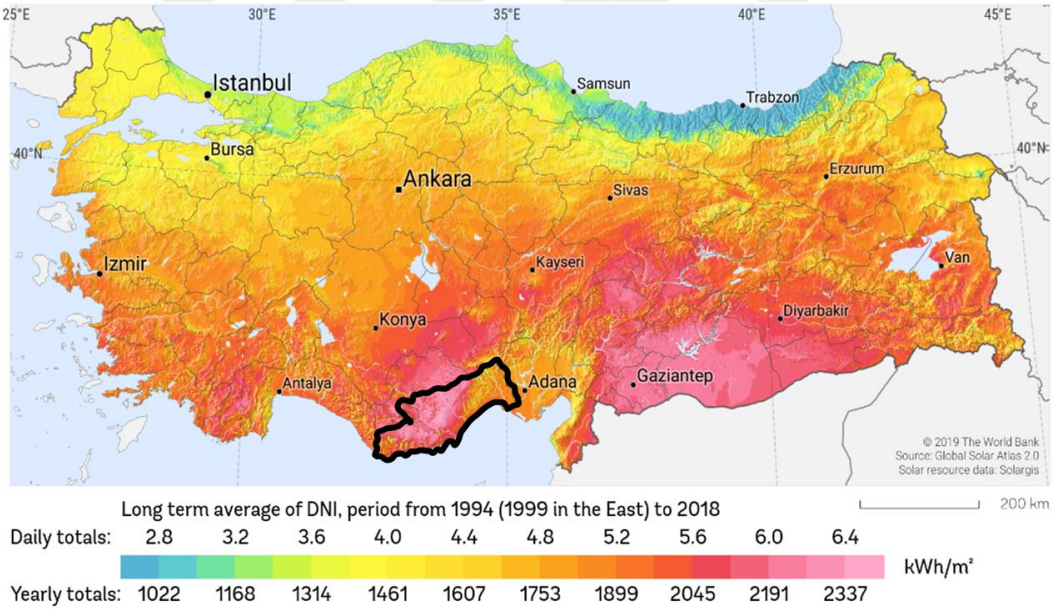

Figure 3.17. The daily and annual DNI of Türkiye in which Mersin is shown with the black frame [107].

Also, regarding vegetative production, Mersin is ranked as the 4th top city in Türkiye with a good diversity of crops [108]. In terms of tomato production, which

can be considered as a suitable candidate to be irrigated by the produced water, in greenhouses, Mersin is reported as the 3rd top region in Türkiye, Erdemli being one of the leading districts [109].

Therefore, the model is run for Erdemli, Mersin, Türkiye. The hourly meteorological data is obtained from Meteonorm 7.2 [110] and used as the input of SAM. The latitude, longitude, and annual DNI of Erdemli, Mersin, Türkiye are provided in Table 3.1.

Table 3.1 Lattitude, longitude, and annual DNI of Erdemli, Mersin, Türkiye [110].

Parameter	Value	Unit
Lattitude	36.68	°
Longitude	34.31	°
Annual DNI	1635	kWh m^{-2}

3.2.4.2 Water Requirement for Irrigation and Supply Scheme

Irrigation constitutes 77% of Türkiye's water consumption, with 44 billion m^3 per year. It is reported that 6.96 million hectares are irrigated in Türkiye in 2022 [111]. Simply, the agricultural irrigation water requirement of agricultural land is calculated as 6 321.84 m^3 ha^{-1}. This value is in the range of actual water demanded and water supplied for Türkiye per hectare, according to [112].

Even though 87 764.4 hectares of Erdemli's surface area is suitable for agriculture, only 20 300.6 hectares of it is irrigated, while 46.6% of it is not used at all [113]. Using the average agricultural irrigation water consumption of Türkiye per hectare, 6 321.84 m^3 ha^{-1}, and the irrigated land in Erdemli, the annual water consumption is calculated as 128.34 million m^3 $year^{-1}$ which corresponds to 351 608.57 m^3 day^{-1} if the water demand is targeted to be met by daily water production.

When the crop types are analyzed, it is seen that approximately 50% of the lands are cultivated for citrus with a huge share of lemons. Boron removal is challenging in reverse osmosis desalination, and citrus types, lemon in particular, are boron sensitive crops [114]. Therefore, by excluding the water demand of citrus, the daily production of water systems is determined to be 180 000 m^3 day^{-1}.

As there is no complete available data regarding Erdemli, Mersin's urban wastewater production, San Javier Wastewater Treatment Plant from Murcia, Spain is used as a sample plant. The plant is designed and operated to discharge the treated water to the Mediterranean Sea or to be used in agricultural irrigation. The sludge of the plant is also used for agriculture. Therefore, the profile of the mentioned WWTP is very suitable to the objective of this study. According to the San Javier Wastewater Treatment Plant data, the average daily treated flow is 7 410 m^3 day^{-1} for the population of 40 822. Erdemli's population is 147 512, according to Turkish Statistical Institute [115]. By upscaling the wastewater generation of San Javier for Erdemli based on the number of inhabitants of San Javier and Mersin, the urban wastewater production of Erdemli is found as 26 776 m^3 day^{-1}. This value complies with the estimations of wastewater amount of Erdemli for 2020 and 2030 with 23 695 and 28 363 m^3 day^{-1}, respectively [116]. This value is also in compliance with the estimation of the Turkish Statistical Institution regarding average wastewater production per capita per day, 189 liters, resulting in 27 880 m^3 day^{-1} for Erdemli's population [117].

All in all, the wastewater treatment plant of Erdemli is assumed to treat 30 000 m^3 day^{-1}. As the daily production of water systems is determined to be 180 000 m^3 day^{-1}, the RO plant is sized to produce 150 000 m^3 day^{-1}.

The nominal water supply targeted through different systems is represented in Table 3.2.

Table 3.2 Targeted water supply through different systems.

Category	Value	Unit
Total Water Supply	180 000	m^3 day^{-1}
Treated Wastewater	30 000	m^3 day^{-1}
Desalinated Water	150 000	m^3 day^{-1}

Even though the approach above excludes many parameters, such as

- irrigation methods
- characteristics of different crop types and soil
- cultivation periods and durations of different crop types
- seasonal or daily fluctuations in the water requirement
- hourly, daily or seasonal fluctuations in wastewater generation

still, it is sufficient and representative enough for this study as

- the water systems are undersized compared to water requirements, and the water production can always be supported by additional units or plants depending on the demand
- water storage can be employed to compensate for the water demand fluctuations.

Also, even if the systems were oversized, they would serve as an initiative and resource for the irrigation of unused or non-irrigated lands suitable for agriculture.

3.2.4.3 Wastewater Treatment System Inputs

In summary, the quaternary treatment technology for this work is decided as UV/H_2O_2 and its capacity is determined as 30 000 m^3 day^{-1} as described previously.

As the modeling and simulation of the quaternary treatment of the wastewater plant is beyond the scope of this study, experimental data provided by CIEMAT-PSA is

used regarding the UV and H_2O_2 doses required to achieve sufficient treatment of the urban wastewater. Table 3.3 presents the technical inputs of the of UV/H_2O_2 treatment.

Table 3.3 Technical inputs of UV/H_2O_2.

Category	Value	Unit	Comment
Unit size	2 000	m^3 day^{-1}	Assumed
Number of units	15	-	Assumed
UV dose	1.59	kJ l^{-1}	Provided by PSA
H_2O_2 dose	25	mg l^{-1}	Provided by PSA

The UV dose is converted from kJ l^{-1} to kWh m^{-3}, and found as 0.44 kWh m^{-3}. It is stated in [118] that only 30% of the electricity can be converted to UV radiation. However, the experiments showed lower values regarding the efficiency [119], [120]. Therefore, UV efficiency is taken slightly lower than 30%, as 25% in this study.

The UV lamps for UV/H_2O_2 treatment are major contributors to electricity consumption. The peripheral device electricity consumption is assumed as 10% of UV lamp consumption [121]. Some studies [122] do not account for pump power at all, whereas others [101], [102] show that the pump power is much lower than the UV lamp consumption, especially for long illumination time which is the case also for this study. However, as a conservative approach, the pump power is assumed as 10% of the UV lamp consumption in this study.

The breakdown of the UV/H_2O_2 energy consumption is presented in Table 3.4.

Baresel et al. [123] predicted 20% less energy consumption for full-scale plants in comparison to pilot plants. Therefore, the auxiliary electricity consumptions of the UV/H_2O_2, besides the primary consumptions provided in Table 3.4, are assumed to be compensated by the larger scale of the plant.

Table 3.4 Breakdown of the UV/H_2O_2 energy consumption.

Category	Value	Symbol	Unit
UV Lamp	1.77	E_{UV}	kWh m^{-3}
Peripheral Electrical Devices	0.18	$0.1E_{UV}$	kWh m^{-3}
Pump Power	0.18	$0.1E_{UV}$	kWh m^{-3}
Total	2.12	1.2 E_{UV}	kWh m^{-3}

3.2.4.4 Reverse Osmosis System Inputs

The Mediterranean seawater composition introduced to Toray DS2 is presented in Table 3.5 and Table 3.6.

The range of the average flux of the system should be determined based on the feedwater quality. As the fouling tendency of the membrane increases due to the feedwater composition, the system limitations become stricter. In seawater reverse osmosis systems, the high fluxes of the permeate create a high risk of fouling. The fouling causes more frequent need for cleaning, reduced capacity, increased feed pressure requirement and reduced membrane life [124]. On the other hand, the low brine flux causes the concentration polarization [125]. Concentration polarization increases the osmotic pressure, subsequently, the pressure requirement of the process; reduces the flux and selectivity of the membrane leading to the performance decrease of the process [126]. Therefore, to ensure the desired performance of the process and increase the membrane life, the design flux range of 12-17 LMH provided in the datasheet [81] of the membrane is followed when the variable load strategy is employed.

Table 3.5 The cations in Mediterranean seawater composition [81], [127].

Cations	Value (mg l^{-1})
Calcium	415
Magnesium	1302
Sodium	11 544
Potassium	388
Barium	0.01
Strontium	6.3
Ammonium	0
Iron	0

Table 3.6 The anions in Mediterranean seawater composition [81], [127].

Anions	Value (mg l^{-1})
Bicarbonate	146
Chloride	20 500
Sulphate	2790
Nitrate	0
Fluoride	0
Silica	5
Boron	5

The typical recovery rate for seawater reverse osmosis plants is at most 35-50% [70]. As the salt concentration of the brine increases throughout the process due to the membrane separation of the water, it imposes a high osmotic pressure and, subsequently, becomes a restriction regarding the maximum practical recovery rate.

The RO system is composed of several pressure vessels connected in parallel. These vessels typically house 6-8 membrane modules connected in series (referred as element in Table 3.5) [128]. The recovery rate is proportional to the number of

modules as the concentrate of one module becomes the feed of the other module and is further concentrated.

The highest energy consumption in reverse osmosis is due to the high pressurization requirement of the feedwater to overcome the osmotic pressure and provide the desired flow rate of the permeate. Energy recovery devices (ERD) are commonly utilized in seawater reverse osmosis plants to recover the pressure of the brine. The utilization of this pressure significantly reduces the specific energy consumption of the plant [129]. Isobaric energy recovery devices enable the decoupling of the pumps and ERD resulting in flexibility in design and operation [130]. Zein et al. [131] also used an isobaric energy recovery device while assessing the variable load operation of a reverse osmosis plant powered by solar energy. The efficiency of isobaric energy devices is reported to reach 97% in [130], [132] and implemented as 97% in [133]. Toray DS2 [81] also reports it as 96%; hence, it is taken as 96% in this study. Finally, the pump efficiencies are assumed as 80% as the default value recommended in Toray DS2 [81] and implemented in [134].

The technical inputs of the RO system are provided in Table 3.7.

Table 3.7 The technical inputs of the RO system.

Parameter	150 Trains	15 Trains
Feedwater flow rate (m^3 day^{-1})	1 750 – 2 500	17 500 – 25 000
Permeate flow rate (m^3 day^{-1})	700 - 1 000	7 000 - 10 000
Recovery	40%	40%
Element Type	TM820M-400	TM820M-400
Number of pressure vessels	11	110
Number of elements in each vessel	6	6
Pump Efficiency	80%	80%
ERD Efficiency	96%	96%

3.2.4.5 Energy Requirement of the Water Systems

Even though the results of the SEC of the RO plant are presented in Section 4.1 in detail, to justify the sizing of the energy systems, the design SEC of RO is presented in Table 3.8 together with the SEC of the UV/H_2O_2 treatment.

Table 3.8 The specific energy consumption of UV/H_2O_2 treatment and RO plant at design load.

System	SEC (kWh m^{-3})
UV/H_2O_2	2.12
RO	3.24

The energy requirements of two different water supply scenarios with a total capacity of 180 000 m^3 day^{-1} is shown in Table 3.9.

Table 3.9 The energy requirement of two different water supply scenarios with a total capacity of 180 000 m^3 day^{-1}.

Water System	Required Energy (MWh)
RO only	24.3
RO+WWTP	22.9

It is essential to keep in mind that the water supply from WWTP is the water treated by UV/H_2O_2. The details of the energy system design and the relevant inputs are provided in Sections 3.2.4.6, 3.2.4.7 and 3.2.4.8 only for RO+WWTP system as this combined water scheme is the main focus of this study. The energy system inputs of RO only scenario can be found in Appendix A.

3.2.4.6 PV System Inputs

The surface azimuth angle determines the east-west orientation of the PV array. In SAM, facing north, east, south, and west is represented by 0, 90, 180, and 270 degrees, respectively [84].

Tilt or slope is the angle between the horizontal and the surface of the PV module. 0 and 90 degrees correspond to the horizontal and vertical orientation, respectively [135]. As a rule of thumb, the latitude of the location in question can be defined as the optimal array tilt angle for simplicity, even though the actual tilt angle varies depending on the project requirements [84].

The technical details of the PV system are provided in Table 3.10.

Table 3.10 The technical inputs of the PV system.

Parameter	Value	Unit
Module type	SunPower SPR-E20-440-COM	-
Inverter type	SunPower: SPR-24000m-3-H	-
DC to AC Ratio	1.1	-
Capacity	27.5	MWdc
Tracking	1 Axis (tilted N-S axis)	-
Tilt angle	Latitude	°
Surface azimuth angle	180	°

3.2.4.7 CSP System Inputs

Design Point DNI is the DNI value at which the system generates the rated power. A higher design point DNI value indicates that fewer heliostats are required. The low design point DNI values can cause excess energy especially for systems without TES, whereas high design point DNI can lead to low capacity factors [136].

Solar Multiple, SM, is the ratio of thermal power that can be generated by the solar field to the thermal power requirement of the power block at the design point [137]. The solar multiple should be close to 1 in plants without a storage system.

It should be noted that SAM optimizes the tower height and heliostat field based on the initial value entered as the tower height, as SAM finds the local optimum. The initial guess for the tower height is entered as 160 m by taking the Gemasolar CSP plant with 19.9 MWe production capacity and the tower height of 140 m as the reference [138].

Finally, the minimum state of charge is defined to avoid deep discharging of the molten salt thermal storage tanks as suggested by Silvestre [65].

The technical inputs of the central receiver CSP system are presented in Table 3.11.

Table 3.11 The technical inputs of the central receiver CSP system for WWTP with 30 000 m^3 day^{-1} and RO plant with 150 000 m^3 day^{-1} capacity.

Parameter	Value	Unit
DNI design point	800	W m^{-2}
Solar multiple	3	-
Design turbine gross output	25.5	MWe
Turbine gross to net efficiency	90%	-
Turbine operating range	30%-100%	-
HTF fluid	60% $NaNO_3$, 40% KNO_3	-
Hot tank fluid temperature	575	℃
Cold tank fluid temperature	290	℃
Storage size	12	h
Initially charged volume of hot tank	30%	-
Minimum state of charge	2%	-
Maximum flow rate to the receiver	518.3	kg s^{-1}

Also, the specific heat capacity of the HTF fluid is taken as 1.5174 kJ kg^{-1} $°C^{-1}$ at the average HTF temperature [40].

3.2.4.8 PV+CSP System Inputs

As the first approach, the systems are hybridized using the individual inputs of PV and CSP systems provided in Tables 3.10 and 3.11.

3.2.4.9 Emission Factor Inputs

Table 3.12 represents the CO_2 emission factors of the solar energy systems based on their life cycle assessments (LCA). Even though it is not clarified in [139] whether the emission factor of the grid for Türkiye is based on LCA, the reported value remains within the range of the presented CO_2 emission factors in [140] calculated based on LCA for coal and natural gas which constitutes the majority of the resources used for electricity generation in Türkiye [141].

Table 3.12 The CO_2 emissions of different energy systems.

Energy System	Emission Factor ($gCO_{2eq}\,kWh^{-1}$)	Reference
PV	85.33	[142]
CSP (Central Receiver)	85.67	[142]
Grid	724.40	[139]

3.3 Economic Analysis

In this section, the details of the economic analysis conducted for water and energy systems are provided. The relevant modeling approach, assumptions and inputs are also shown.

3.3.1 Modeling, Simulations and Key Performance Indicators

Levelized cost of electricity (LCOE) is a measure to evaluate the costs of electricity production considering its lifetime and compare different electricity generation technologies. The lifetime costs can be classified as

- Capital Costs (CAPEX): Capital costs are the upfront expenditures to build a power plant.
- Operation and Maintenance Costs (OPEX): Operation and maintenance costs are the costs that occur to operate a power plant. These costs can also be further categorized as fixed and variable costs.
    - Fixed Operation and Maintenance Costs: Fixed costs are independent of the electricity generation of the plant. They are generally given based on per installed capacity.
    - Variable Operation and Maintenance Costs: Variable costs are directly related to the electricity production of the plant. They are defined as per kWh electricity production of the plant.
- Disposition Costs: Disposition costs incur when the systems reach the end of their lifetime. The disposition costs for solar systems are neglected as the scrap value of the materials and the equipment mostly compensate for the disposition costs [143].

It is worth emphasizing that LCOE is not an absolute measure to guide investment decisions; instead, it is a simple relative criterion to compare different systems.

The LCOE is governed by Eqn. 3.13

$$LCOE = \frac{CAPEX_E + \sum_{t=1}^{n} \frac{OPEX_{E_t}}{(1+r)^t}}{\sum_{t=1}^{n} \frac{E_{ann,ut_t}}{(1+r)^t}} \tag{3.13}$$

where r, n, t, $CAPEX_E$, $OPEX_{E_t}$ and E_{ann,ut_t} are the discount rate, the lifetime of the specified system, year, capital costs of the specified energy system, annual operation and maintenance costs of the specified energy system in year t and,

annually utilized electricity production of the specified energy system in year *t*, respectively.

It should be noted that the LCOE in this study is evaluated based on the utilized portion of the total electricity production of the energy systems.

As the final objective of this analysis is to estimate the water production costs, not electricity costs, another measure is required. Similar to LCOE, to compare the unit cost of water production produced by different water systems and powered by different energy systems, the levelized cost of water (LCOW) is evaluated.

The associated costs of the water systems are limited to CAPEX and OPEX. The disposition costs are again assumed to be zero, as many studies don't account for the disposition costs of the water systems [120], [134], [144]–[147].

The LCOW is found by Eqn. 3.14

$$LCOW = \frac{CAPEX_W + \sum_{t=1}^{n} \frac{OPEX_{W_t}}{(1+r)^t}}{\sum_{t=1}^{n} \frac{V_{W,ann_t}}{(1+r)^t}} \quad (3.14)$$

where $CAPEX_W$, $OPEX_{W_t}$ and $V_{W,ann,t}$ stands for capital costs of the specified water system, operation and maintenance costs of the specified energy system in year *t*, and the annual water production of the specified water system in year *t*, respectively.

The OPEX associated with the water systems strongly depends on the LCOE as the electrical consumption is one of the significant contributors regarding the operating costs of the reverse osmosis and quaternary wastewater treatment system. Therefore, the effect of the LCOE is reflected through the LCOW.

As a further comment, carbon pricing is a powerful and widely adopted strategy in Europe to help countries reduce their carbon dioxide emissions and support their green transition [148]. Unfortunately, Türkiye has no direct carbon pricing now, but the price of carbon is embedded in the cost of the fuels implicitly as taxes [149]. Even though carbon pricing should be included in the LCOE and LCOW

model when European countries are assessed, currently, it does not apply to Türkiye.

The following assumptions are followed:

- The discount rate is taken as the interest rate, and it is assumed as constant.
- The degradation rate of the systems and the reductions in their production are neglected. Electricity and water production are assumed to be constant throughout the lifetime of the systems.
- The lifetime of all systems is taken as the same.

3.3.2 Inputs

The cost inputs are provided in their original currencies in the relevant sections and converted to € using the conversion factor shown in Table 3.13. Table 3.13 presents the general economic inputs of all systems.

Table 3.13 General economic inputs used for all systems.

Category	Value	Unit
Interest rate [150]	8.5	%
Lifetime	25	years
USD to Euro conversion factor	0.9	-

3.3.2.1 PV System Inputs

The economic inputs of the PV system are presented in Table 3.14. It should be noted that the O&M costs of the PV system are fixed costs by installed capacity.

Table 3.14 PV system capital and operation and maintenance costs [151].

Category	Value	Unit
Capital Costs		
Module	0.33	USD W_{DC}^{-1}
Inverter	0.04	USD W_{DC}^{-1}
Structural Components	0.15	USD W_{DC}^{-1}
Electrical Components	0.12	USD W_{DC}^{-1}
EPC Overhead	0.08	USD W_{DC}^{-1}
Installation, Labor and Equipment	0.13	USD W_{DC}^{-1}
Sales Tax	0.04	USD W_{DC}^{-1}
Permitting Fee	0.02	USD W_{DC}^{-1}
Developer Profit	0.07	USD W_{DC}^{-1}
Contingency	3	% of the CAPEX
O&M Costs		
O&M Expenses	16	USD $(kW\text{-}year)^{-1}$

3.3.2.2 CSP System Input

The economic inputs of the CSP system are provided in Table 3.15.

Land costs are estimated as 10 000 USD $acre^{-1}$ as the default value of SAM and not corrected for Türkiye as the land costs vary tremendously depending on the soil quality, location and purpose of use, and there is no relevant data available in the literature in this regard. Also, it is found in [152] that the land costs are almost negligible considering the other costs of the central receiver CSP system. Therefore, it is concluded that the correction of land costs for Türkiye is not necessary for this study.

Table 3.15 CSP system capital and operation and maintenance costs [153].

Category	Value	Unit
Capital Costs		
Site improvements	16	USD m^{-2}
Heliostat field	140	USD m^{-2}
Tower Cost	See Equation 3.15.	
Receiver Cost	See Equation 3.16.	
Thermal Energy Storage	22	USD $kWht^{-1}$
Power Cycle	1 040	USD kWe^{-1}
Balance of plant	290	USD kWe^{-1}
Contingency	7	%
EPC & Owners Cost	13	%
Sales Tax	5	%
Land Cost	10 000	USD $acre^{-1}$
O&M Costs		
O&M Fixed Cost	66	USD $(kW\text{-}year)^{-1}$
O&M Variable Cost	3.5	USD MWh^{-1}

The CAPEX of the tower, $CAPEX_{tower}$, and receiver, $CAPEX_{receiver}$, is governed by the Eqns. 3.15 and 3.16 according to [84],

$$CAPEX_{tower} = Cost_{fix,tower} * \exp\left(sc_{tower} * \left(h_{tower} - \frac{h_{receiver}}{2} + \frac{h_{heliostat}}{2}\right)\right) \quad (3.15)$$

$$CAPEX_{receiver} = Cost_{ref,receiver} * \left(\frac{A_{receiver}}{A_{ref,receiver}}\right)^{sc_{receiver}} \quad (3.16)$$

where h_{tower}, $h_{receiver}$ and $h_{heliostat}$ corresponds to the heights of tower, receiver and heliostat, respectively, and $A_{receiver}$ is the area of the receiver. The values of the remaining parameters which appear in Eqns. 3.15 and 3.16 are shown in Table 3.16.

Table 3.16 Inputs for Eqns. 3.15 and 3.16 [84].

Category	Explanation	Value	Unit
Eqn 3.11			
$Cost_{fix,tower}$	Fixed tower costs	3 000 000	USD m^{-2}
sc_{tower}	Tower cost scaling exponent	0.0113	-
Eqn 3.12			
$A_{ref,receiver}$	Receiver reference area	1571	m^2
$Cost_{ref,receiver}$	Receiver reference cost	103 000 000	USD
$sc_{receiver}$	Receiver cost scaling exponent	0.7	-

3.3.2.3 RO System Inputs

The RO system is sized as 150 000 m^3 day^{-1} as an addition to the WWTP capacity of 30 000 m^3 day^{-1} as provided in Table 3.2. The same economic inputs of RO are also used for only desalination scenario with 180 000 m^3 day^{-1}.

The RO system economic inputs are provided in Table 3.2

Table 3.17 RO system economic inputs [154].

Category	Value	Unit	Comments
CAPEX	1 119	USD $(m^3\,day^{-1})^{-1}$	P.I.C.
Fixed OPEX			
Parts	10.95	USD $(m^3\,day^{-1})^{-1}$	P.I.C.
Labour	20.82	USD $(m^3\,day^{-1})^{-1}$	P.I.C.
Membranes	10.95	USD $(m^3\,day^{-1})^{-1}$	P.I.C.
Variable OPEX			
Chemicals	0.07	USD m^{-3}	P.W.P.
Electrical Energy		See Equation 3.17.	

The RO OPEXs' are classified as variable or fixed here to better understand the effect of the capacity factor on the water economics. Please note that the parts, labor, and membrane costs are taken as fixed OPEX, based on installed capacity, in this study to account for the extra costs which may occur due to variable load operation.

Electrical energy operating costs of RO, $OPEX_{elec,RO}$, is governed by Eqn. 3.17

$$OPEX_{elec,RO} = SEC_{RO} * LCOE * V_{W,ann,RO} \quad (3.17)$$

where SEC_{RO}, $LCOE$ and $V_{W,ann,RO}$ are the specific energy consumption of RO, levelized cost of electricity and annual water volume produced by RO, respectively.

3.3.2.4 UV/H_2O_2 System Inputs

The CAPEX of the WWTP depends on the characteristics of the wastewater to be treated, the purpose, process and equipment specifications such as the contaminants present in the water, UV transmittance of the water, volume of the UV unit, the residence time, the desired flow rate of the treated water, used chemicals, etc. Therefore, the CAPEX of the UV/H_2O_2 process is unique to each case and requires careful design and assessment. It is not possible to find a complete dataset regarding CAPEX of full-scale UV/H_2O_2 treatment that is generically valid. So, the CAPEX is estimated using the cost breakdown presented by [155] where all the other costs are calculated based on the AOP reactor cost. The UV reactor cost is found by upscaling the value indicated by [119] which uses a similar UV dose and illumination time for the process. Also, it should be noted that, the CAPEX found here is in the same order of the magnitude but higher than the values reported in [123], [156] for commercial plants whose details are not clarified.

The UV/H_2O_2 system economic inputs are presented in Table 3.18.

Table 3.18 UV/H_2O_2 system economic inputs (P.I.C: per installed capacity as m^3 day^{-1}, P.W.P: per m^3 water production)

Category	Value	Unit	Comment	Reference
CAPEX	8.21	Million USD	Total	[119], [155]
Fixed OPEX				
Labor	0.33	€ $(m^3\,day^{-1})^{-1}$	P.I.C.	[120]
Variable OPEX				
H_2O_2	0.0375	€ m^{-3}	P.W.P.	PSA
Replacement of parts	0.008	USD $(m^3\,day^{-1})^{-1}$	P.I.C.	[157]
Electrical Energy	See Equation 3.18.			

Electrical energy operating costs of UV/H_2O_2, $OPEX_{elec,WWTP}$, is governed by Eqn. 3.18

$$OPEX_{elec,WWTP} = SEC_{WWTP} * LCOE * V_{W,ann,WWTP} \quad (3.18)$$

where SEC_{WWTP}, $LCOE$ and $V_{W,ann,WWTP}$ are the specific energy consumption of UV/H_2O_2, levelized cost of electricity and annual water volume produced by UV/H_2O_2, respectively.

CHAPTER 4

RESULTS

In this section, WWTP refers to the UV/H_2O_2 quaternary treatment stage.

4.1 RO Plant Specific Energy Consumption

The RO plant is simulated for permeate flow rates between 70% to 100% of the design flow rate in 5% increments. The SEC of the RO system is found to vary between 2.04 kWh m^{-3} and 2.30 kWh m^{-3} which corresponds to the minimum load and design load, respectively. However, to include the other systems' energy consumption and evaluate the overall energy consumption of the complete RO plant, the found SECs are corrected, as explained in Section 3.2.1.1.2. The variation of the operational parameters in the load range is presented in Figure 4.1.a and Figure 4.1.b for 1 000 m^3 day^{-1} and 10 000 m^3 day^{-1} train capacities, respectively.

The SEC is observed to decrease by 11.2% for the 70% load operation compared to the design load as a direct result of 11.3% reduction in feed pressure requirement as presented in Fig. 4.1.

The quality of the produced water by desalination is suitable to be used in agricultural irrigation in Türkiye according to [158].

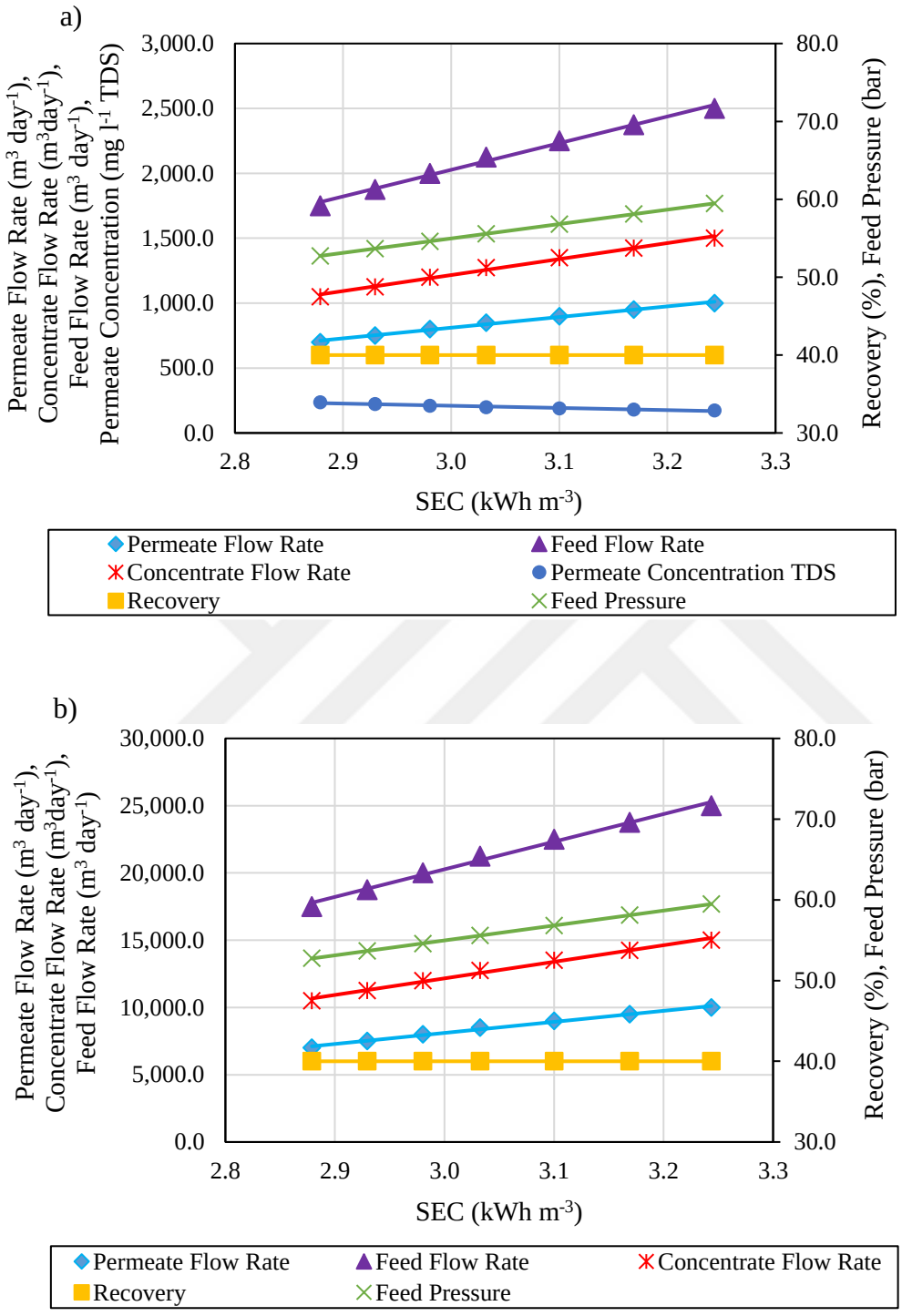

Figure 4.1. Variation of the operational parameters of the RO with constant permeate recovery rate of 40% for a) 1 000 m^3 day^{-1} b) 10 000 m^3 day^{-1} train capacity.

The simulated permeate flow rates and the corresponding overall energy consumptions are fitted to a polynomial function to be used in the model for the variable operation of the RO plant and presented in Fig. 4.2 (a) and (b) for 1 000 m^3 day^{-1} and 10 000 m^3 day^{-1} train capacities, respectively.

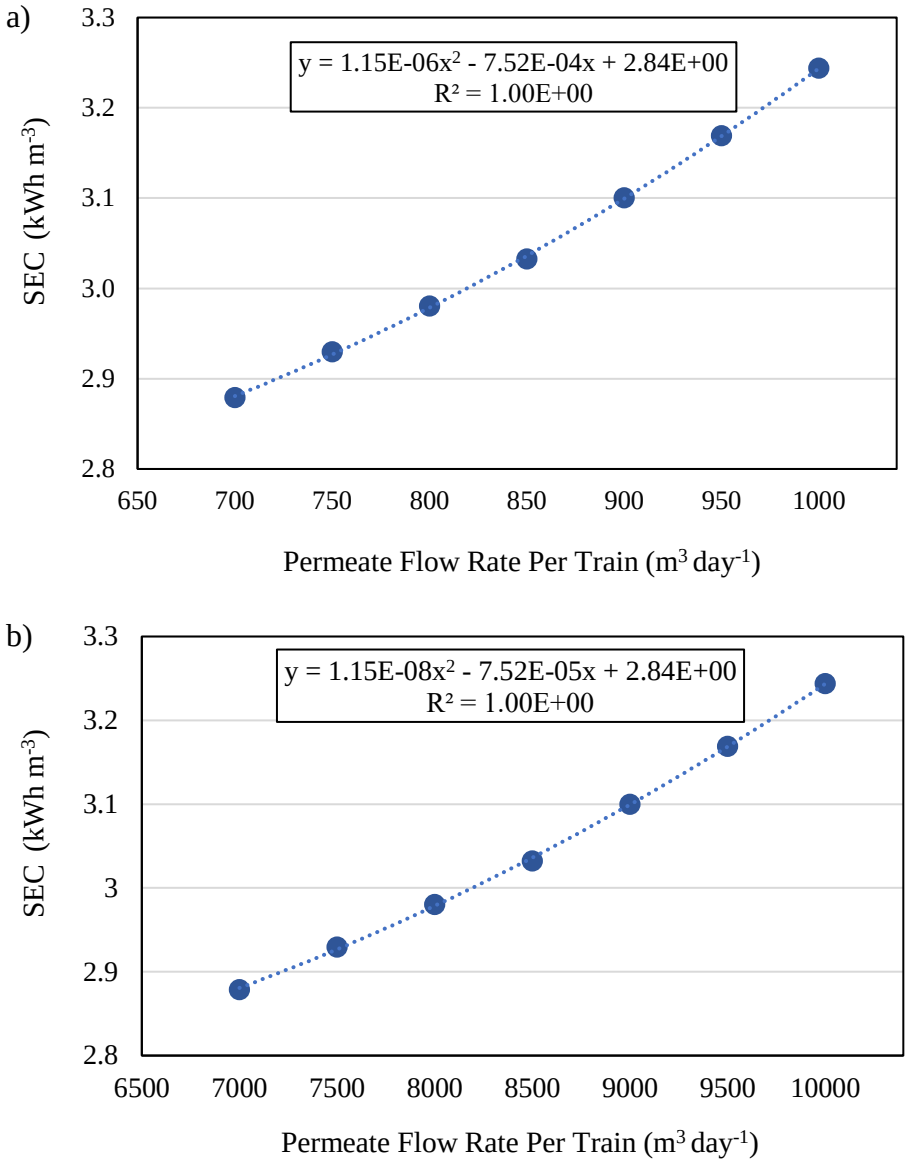

Figure 4.2. The overall SEC of the RO plant in the determined operational range with a) 1 000 m^3 day^{-1} and b) 10 000 m^3 day^{-1} train capacities.

4.2 Validation

The earliest version of the models for PV, CSP, PV+CSP and RO-nominal load operation was validated by Silvestre's study [65] for Canarian Islands, reported and submitted to EC in SolarTwins Deliverable: D3.1 [159].

The previous version of the models and operating strategies, without WWTP addition, was presented in SolarPACES 2022, and the study was accepted as full paper [160].

Finally, here, the turbine electricity generation model of this study is compared with SAM's. The capacity factor of the CSP plant found by SAM with its default electricity production strategy and the capacity factor computed for the base CSP strategy analyzed in this study are compared in Table 4.1 for RO+WWTP.

Table 4.1 Validation of the CSP electricity generation model used in this study with SAM.

Source	Capacity Factor (%)	Error (%)
SAM simulation	49.5	2.9
This study	48.1	

Even though the proposed electricity generation model in this thesis is relatively simple compared to SAM's, the annual performance characteristics are in good compliance with a 2.9% error. The model used in this study excludes the start-up and ramping rates and associated additional inefficiencies of the turbine; however, on the other hand, the SAM model results in higher gross to net efficiencies than the estimated gross to net efficiency defined as the input. It can be concluded that the reduced outputs of the turbine due to the transient states are compensated by the higher hourly gross to net efficiencies than the estimated one; hence, the electricity generation model proposed in this study is able to represent the annual performance of the system.

4.3 RO+WWTP Powered by PV

The PV system is run for the combined water systems of reverse osmosis and UV/H_2O_2 treatment, referred as WWTP in this section.

The PV energy system performance is first analyzed through the utilized electricity fraction, $F_{UE,}$ and LCOE. The CF of the PV plant is found to be 22.2%. However, as the PV system is isolated from the grid and the sub-units of the water system, i.e., trains for RO and units for WWTP, have thresholds to start operating, all of the PV generation may not be used by the water systems. As explained in Section 3.3.1, the LCOE is determined based on the utilized electricity instead of the total electricity production, i.e., LCOE depends on F_{UE}. The relation between the fraction of the utilized electricity and the LCOE of PV is provided in Fig. 4.3 for nominal and variable RO operation. The WWTP operating strategy is always the same; therefore, it does not affect F_{UE} or LCOE. As shown in Fig. 4.3, The F_{UE} is the lowest with the nominal load operation of RO plant with 15 trains as the threshold electricity requirement of each train to operate is the highest; therefore, 4.8% of the electricity production of PV cannot be used. As a result, the highest LCOE is observed in this scenario. The higher modularization of the RO plant enables higher utilization of the PV energy as the overall energy requirement of the RO plant is more discretized by the higher number of trains; therefore, 4.5% increase in F_{UE} is observed with a 4.2% decrease in LCOE for 150 trains nominal load scenario compared to 15 trains one. Switching to variable load operation increases the utilization of the generated PV electricity as expected by lowering the start-up and operating energy requirement; as a result, F_{UE} values up to 99.9% are reached with 150 trains variable load scenario.

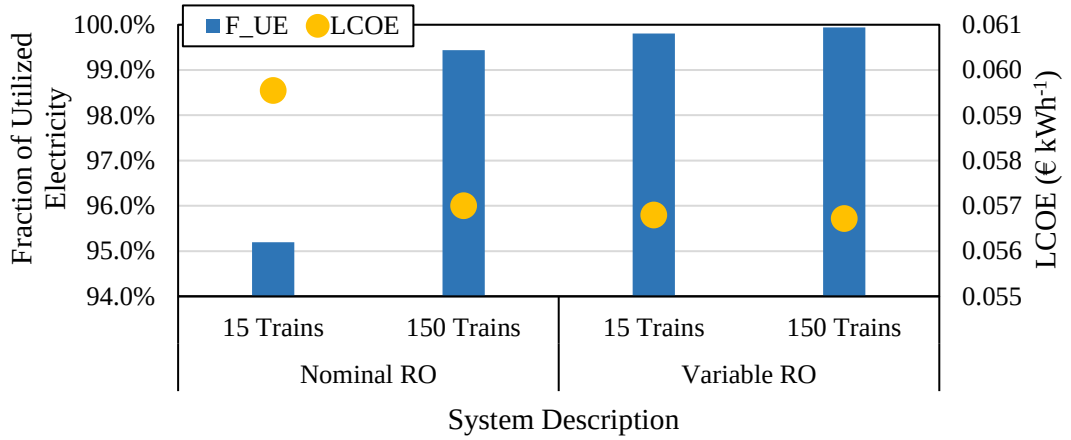

Figure 4.3. The F_{UE} and LCOE of the PV system to power the WWTP+RO system with 1 000 m^{-3} and 10 000 m^{-3} RO train capacities with nominal and variable RO operation.

Figure 4.4 presents the individual and overall CFs and LCOWs of PV powered WWTP and RO systems, and UF of RO for different RO operational strategies and configurations. The WWTP capacity is found to be 44.3% for all cases as the operation of WWTP is always prioritized over RO operation, and the PV generation is always the same as no operating strategy is employed for the PV system as there's no storage system. Considering the CF of individual systems together with their installed capacities, the water production of the PV powered WWTP constitutes 7.4% of the overall water production potential, which results in varying WWTP contributions between 27.9% and 25.2% to the actual water production depending on the overall water production where the installed capacity of WWTP is only 16.7% of the total water system capacity.

Concerning the economic performance of the WWTP plant, as the CF of the WWTP system is always the same, the LCOW of the WWTP plant changes only with LCOE. The variation of LCOE is found to be less than 5.0% as depicted in Fig. 4.3, and the reflection of this decrease in LCOE on the LCOW of WWTP is found to be even smaller with a maximum decrease of 1.5% and concluded to be almost negligible. Notably, Fig. 4.4 reveals that the LCOW of RO is significantly higher than the LCOW of WWTP regardless of the modularization and operating

strategy of RO. The huge gap between LCOW of RO and WWTP is caused by higher capital costs, lower CF, and the higher SEC of the RO plant compared to WWTP and reaches its maximum for the case where the CF of RO is lowest. For 15 trains RO configuration with nominal load operation, the maximum ratio of LCOW of RO to LCOW of WWTP is identified as 4.8.

As illustrated in Fig. 4.4, the higher modularization of the RO plant, i.e., increasing train number from 15 to 150, results in a 5.6% increase in the CF of RO with a 5.0% reduction in LCOW of RO which in turn reduces the overall LCOW by 3.7% for the nominal load operation. A significantly more remarkable performance improvement is observed when the operational strategy of RO is switched to variable load operation; a 14.5% increase is observed in CF with a 12.2% decrease in LCOW of RO, which leads to a 9.1% reduction in overall LCOW for 15 train RO configuration. The increase of the capacity factor by the variable load RO operation can be attributed to two main reasons, first, the better utilization of the produced PV electricity due to lowered start-up and operating energy requirement of RO trains, and the lower SEC values of the RO plant at partial loads where variable load operation aims to operate the maximum number of RO trains at partial loads instead of a limited number of trains at nominal load. Associatively, the decrease in LCOW of RO can be explained by lowered SEC and decreased effects of capital costs of RO on the unit cost of water as the produced volume is increased with the increased capacity factor of RO. Even though the impact of LCOE reduction on LCOW of WWTP is found to be insignificant, still, it should be noted that due to the RO system being more energy intensive, the effect of LCOE on LCOW should not be neglected where LCOE is also dependent on utilized electricity. Any increase observed in CF of the RO plant indicates an increase in the utilized energy which results in lower LCOE. Overall, the lowest LCOW is found to be 1.34 € m^{-3} where the CF of the RO is the maximum at 26.3% with 150 trains RO configuration and variable load strategy. The CF of 29.3% is achieved for overall water systems with the mentioned scheme. However, it is essential to note that higher RO modularization does not lead to a significant

improvement, either on CF or LCOW, in case of variable load RO operation, the increase of CFs and decrease of LCOWs are found to be less than 1.0%.

Finally, the UF stands as an indicator of the operated trains of the RO plant. For the nominal case scenario, the CF and UF are precisely the same as the trains are either operated in design load or shut down. However, at variable loads, the operated train number is increased as a result of the proposed variable load operating strategy of the RO plant. For the 15 train configuration, the UF increased by 42.0% with variable load operation compared to the nominal load strategy.

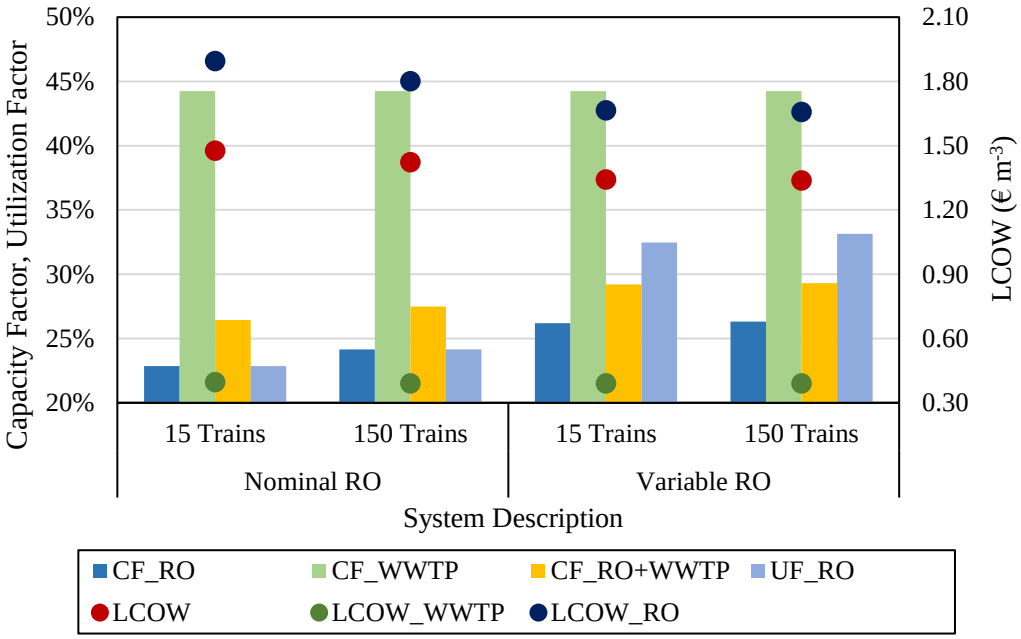

Figure 4.4. The individual and overall CFs and LCOWs of RO+WWTP, and UF of RO plant with 1 000 m^{-3} and 10 000 m^{-3} RO train capacities with nominal and variable RO operation powered by PV.

However, the increase in UF does not necessarily lead to a reduced number shutdown/start-up instances. Figure 4.5 shows the trends of hourly PV generation, operated RO train number and WWTP unit number for the first 72 hours of the year for 15 units WWTP and 15 trains RO configuration for the first 72 hours of the year with nominal and variable RO operation. Fig. 4.5 clearly illustrates that the

intermittent operation of the WWTP and RO plants is inevitable due to the fluctuations of the solar resources as there's no storage system coupled with the PV plant. As already presented in Fig. 4.4, the variable load operation increases the CF remarkably; however, Fig. 4.5 shows that it also causes an increase in the number of shut-down and start-up instances of the RO plant. When the hours with PV generation are examined, e.g. hours of 8-16, 32-40 and 56-64, it is observed from Fig. 4.5.b that the variable RO load operation results in a higher number of active RO trains; and consequently, an escalated number of start/stop instances compared to the nominal RO load operation presented in Fig. 4.5.a.

Hence, it is concluded that operating the RO at variable loads is advantageous for enhanced water production; however, the proposed variable load strategy should be re-considered for PV-only powered RO system depending on what is prioritized, better energetic performance or less number of shut-down/start-up instances. As another strategy of the variable load RO operation, instead of operating all possible trains at lower loads, the maximum number of trains can be operated at design load and the minimum number of trains can be operated at partial loads to reduce the turn-off and turn-on instances at the cost of higher SEC.

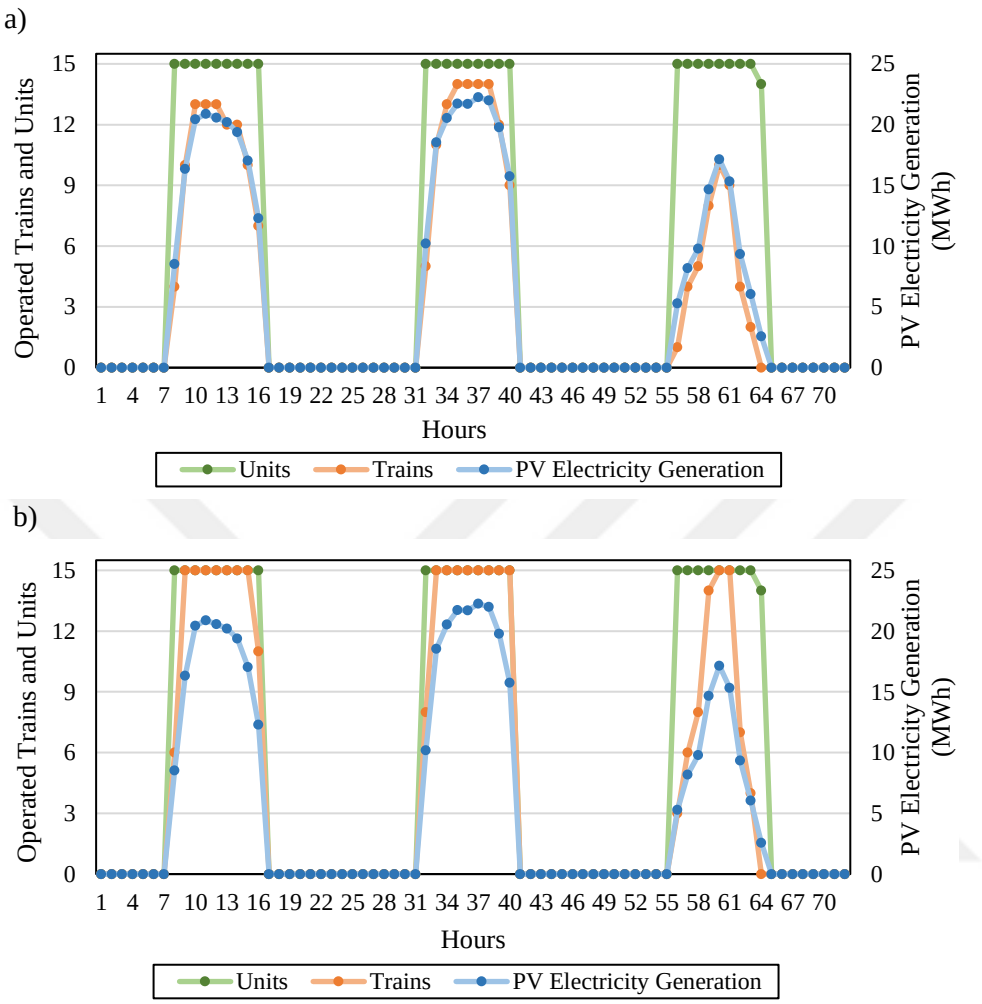

Figure 4.5. The trends of the PV electricity generation, operated trains of RO and operated units of WWTP with 15 units WWTP and 15 trains RO configuration with a) nominal load b) variable load strategy of the RO plant in the first 72 hours of the year for PV powered RO+WWTP.

4.4 RO+WWTP Powered by CSP

The single value outputs of the CSP system simulated in SAM and exported to MATLAB are provided in Table 4.2 for the RO+WWTP water supply scenario.

Table 4.2 The outputs of the central receiver CSP system with 22.9 MWe net turbine capacity and 12 hours of storage capacity to power a RO plant with 150 000 m^3 day^{-1} capacity and a WWTP with 30 000 m^3 day^{-1} capacity.

Parameter	Value	Unit
Total land	776.44	acres
Number of heliostats	2789	-
TES thermal capacity	741.90	MWh_{th}
Receiver height	12.23	m
Receiver outer diameter	10.12	m
Tower height	125.16	m
HTF volume	3440	m^3
Max flow rate to the receiver	518.33	kg s^{-1}

The fraction of the utilized energy over the produced energy is higher than 99% for all cases. Therefore, F_{UE} is concluded to have a negligible effect on the LCOE, and LCOE solely depends on the capacity factor. Figure 4.6 represents the CF and the LCOE of the CSP plant for two different operating strategies. Even though the available thermal energy to the heat transfer fluid is the same for all cases, as shown in Fig. 4.6, the CF of the CSP with the proposed strategy is 3.8% lower than the base case. This decrease in CF is associated with the higher inefficiencies of the turbine due to the decrease in the EF as the partial load operation of the turbine is promoted with the proposed CSP operational strategy. As any decrease in CF increases the effect of the capital costs on the unit cost of electricity, this 3.8% reduction in the CF of the CSP system leads to a 4.0% rise in the LCOE.

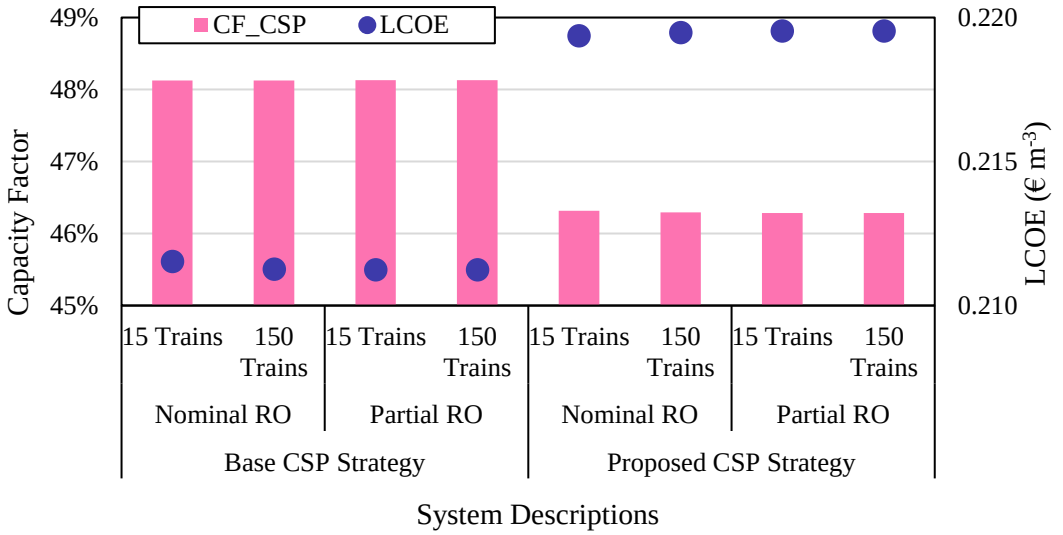

Figure 4.6. The CF and LCOE of the CSP system with the base and proposed CSP strategy to power the WWTP+RO system with 1 000 m^{-3} and 10 000 m^{-3} RO train capacities with nominal and variable RO operation.

The operational pattern of the WWTP units and RO trains is provided in Figure 4.7 for the base and proposed operating strategy of the CSP plant with 15 units WWTP and 15 trains RO configuration with the nominal and variable RO operating strategy for the first 72 hours of the year. The first 72 hours of the year are selected as the example to have the same initial condition for all cases as the state of charge of the TES is the same for the beginning of the year, but it changes differently throughout the year depending on the CSP operating strategy. As Fig. 4.7 suggests, the number of the operated trains mostly follows the same trend in both nominal and variable load operations with the base strategy as this strategy aims to provide the nominal turbine output. When the CSP turbine operates at the nominal load, all the RO trains operate at the design load. Therefore, the only difference occurs in the hours when the turbine operates at a partial load. In those hours, the variable load strategy enables more RO trains to operate as can be observed in Figure 4.7.a and 4.7.b for hour 52. On the other hand, Fig. 4.7.c and 4.7.d clearly demonstrate that the proposed CSP operation, which aims to distribute TES energy among the hours with Q_{HTF}=0, results better in terms of continuous operation of the units and

trains compared to the base strategy. Taking hours of 26-33 as the example, it is observed that proposed CSP strategy enables all WWTP units to operate and reduces the number the RO trains which are turned off. The same performance improvement is also achieved between hours of 53-60.

It is vital to emphasize that the continuous operation of WWTP units and RO trains is also the indicator of the continuous electricity production of the turbine, whose intermittent operation is not desirable as frequent start-ups/shut-downs and steep load gradients reduce the lifetime of the power block due to the high thermal stresses in the steam cycle components. Hence, it is proved that the proposed CSP strategy does not only improve the operation of the water systems, but also the operation of CSP power block. Considering both water and energy systems, the best strategy is concluded to be the variable load operation of RO with the proposed CSP plant operation among all combinations of CSP and RO operating strategies.

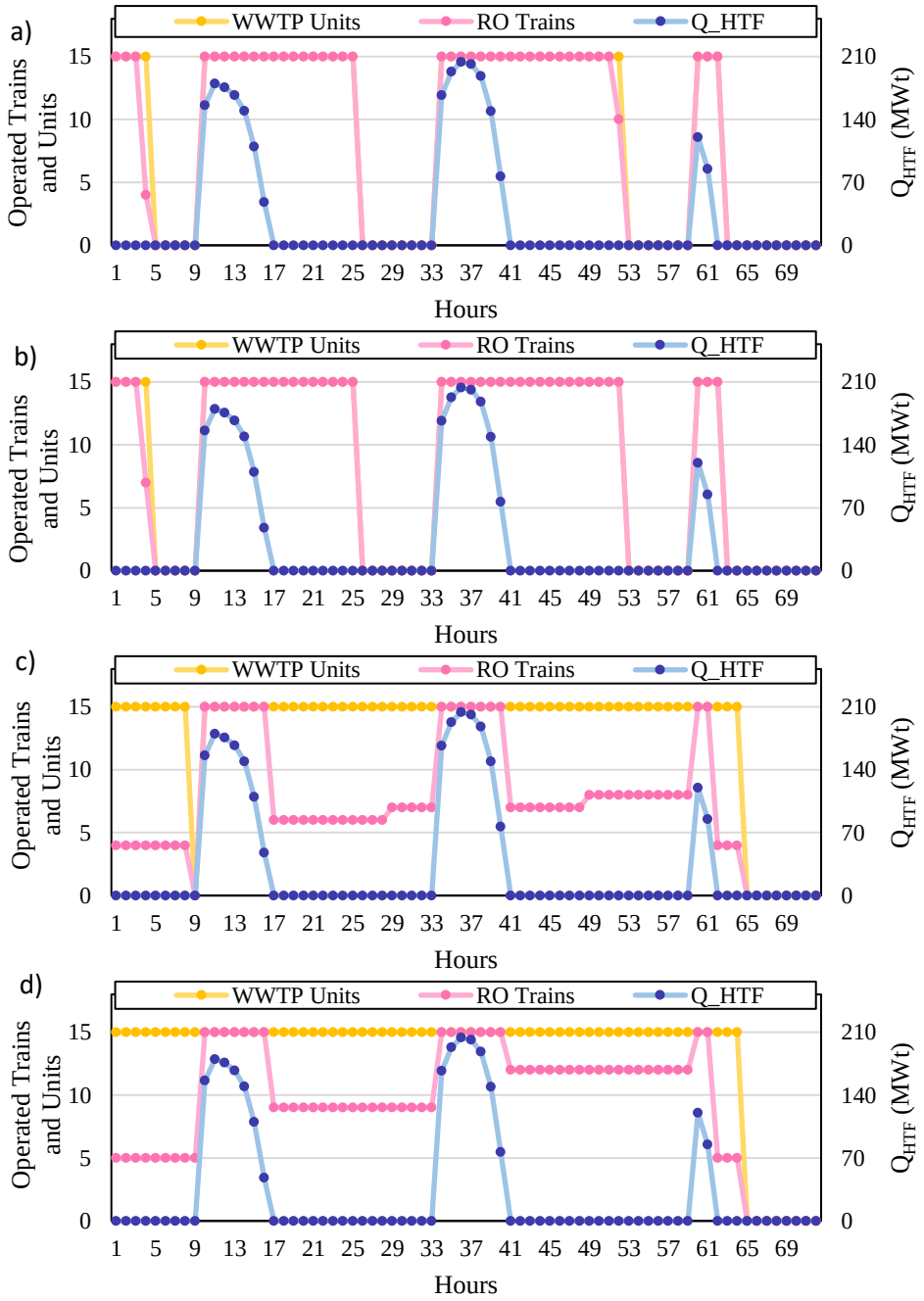

Figure 4.7. The trends of the Q_{HTF}, operated trains of RO and operated units of WWTP with 15 units WWTP and 15 trains RO configuration with a) base CSP and RO nominal load strategy, b) base CSP and RO variable load strategy, c) proposed CSP and RO nominal load strategy and d) proposed CSP and RO variable load strategy.

Also, it should be emphasized that any increase in the CF of the WWTP plant is appreciated not only because its SEC is lower than RO but also as it promotes the reuse of the already existing wastewater whose generation is inevitable due to urban activities, and which will be discharged to the sea if not treated by the quaternary treatment. The reuse of the WWTP is energetically, economically and environmentally more desirable than seawater desalination.

Figure 4.8 presents the individual and overall CFs and LCOWs of the RO and WWTP systems and UF of the RO plant for different CSP and RO operating strategies and train capacities. The advantage of the proposed CSP strategy, already demonstrated in Figure 4.7 for the 72 hours of the year, is also prominent when the capacity factor of the WWTP is compared for the base and proposed strategy. The increased operation hours of the CSP turbine at lower loads with the proposed CSP strategy lead to the higher capacity factors of the WWTP. Comparing the variable RO load with 15 trains for the base and proposed CSP strategy, a 38.2% increase is observed in CF of the WWTP with a 6.0% decrease in CF of RO while the overall CF of the water system is almost kept the same with a 1.4% increase.

Concerning the installed capacities and capacity factors of the water systems, the water production from WWTP has the share of 8.1% and 11.3% in the total water production potential, and 16.9% and 23.0% in the actually produced water for the variable RO operation with 15 trains for the base and proposed CSP operating strategies, respectively. The increase in the water volume provided by WWTP and its contribution to total water production results in a 5.6% decrease in LCOW of WWTP and a 3.4% increase in LCOW of RO, resulting in a 1.4% decrease in total LCOW. The lowest LCOW, 1.36 € m^{-3}, is observed with the proposed operating strategy of CSP and variable load RO operation as a direct implication of the increased share of WWTP in the water production where the LCOW of the WWTP is 58.0% lower than RO's. Nonetheless, taking a step back, it is worth highlighting that the overall LCOW does not show a significant improvement even when the increase in CF of WWTP is quite remarkable; however, as discussed previously, the main advantage of the proposed CSP strategy is mainly related to the increased

lifetime and decreased maintenance requirements of the energy and water systems, and enhanced utilization of the wastewater.

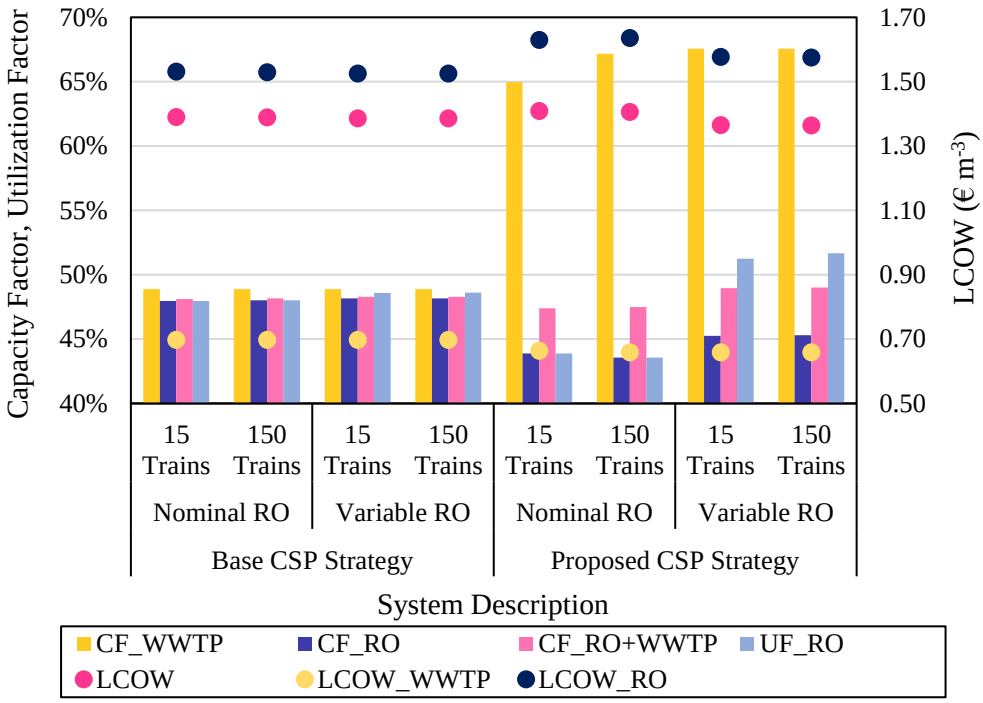

Figure 4.8. The individual and overall CFs and LCOWs of RO+WWTP, and UF of RO plant with 1 000 m^{-3} and 10 000 m^{-3} RO train capacities with nominal and variable RO operation powered by CSP with base and proposed operating strategy.

Overall, it is concluded that the best technical, economic, and operational performance of the water systems is obtained with the proposed CSP strategy coupled with the variable RO operation.

4.5 RO+WWTP Powered by PV CSP Hybridization

After discussing the individual performance characteristics of PV and CSP plants and the RO+WWTP plant operated by those, in this section, the hybridization of the PV and CSP is examined. The PV and CSP systems are hybridized using their stand-alone installed capacities as a first approach.

It has already been demonstrated and discussed that the proposed CSP operating strategy is more advantageous than the base strategy regarding higher capacity factors of the WWTP plant, which is the prioritized water resource, avoided excess electricity generation and reduced intermittent turbine and RO train operation. Therefore, for the conciseness of this study, the PV+CSP system will be analyzed only with the novel PV+CSP operating strategy proposed in this study.

Figure 4.9 represents the individual and overall CFs and the LCOEs of the PV and CSP plant with different RO train capacities and operating strategies. As discussed previously in Section 4.3, the water system operating strategies do not affect the CF of the PV since no operating strategies are adopted for PV due to the lack of storage system that allows dispatching of the electricity. Concerning the CSP and overall performance of the energy systems, no significant difference is observed between the cases neither for CF nor LCOE, the overall LCOE shows a 1.6% decrease at most. This is mainly because the hourly electricity production of the CSP plant in the proposed operating strategy is designed to adapt to any water system configuration; therefore, the different water system configurations do not have any remarkable impact on the LCOE.

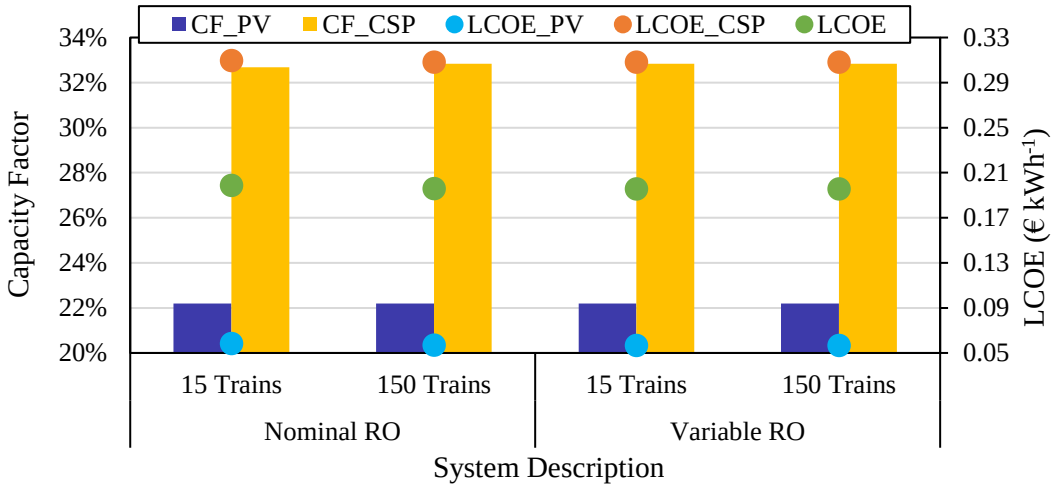

Figure 4.9. The individual CFs and individual and overall LCOEs of the PV+CSP with 1 000 m^{-3} and 10 000 m^{-3} RO train capacities with nominal and variable RO operation.

The operational pattern of the CSP turbine, WWTP units and RO trains is displayed in Figure 4.10 for 15 units WWTP and 15 trains RO configuration with nominal and variable RO operation for the first 72 hours of the year with PV+CSP scheme. At first glance, the fluctuations in the number of the operated trains of RO are remarkable with the nominal load RO operation. These fluctuations are entirely related to the nature of the solar resources and turbine operation limits. The 10th hour of the year can be taken as an example to understand the reason for these fluctuations better. As can be seen, even though Q_{HTF} is non-zero, the electricity production of the CSP plant is zero when PV generates 20.4 MW of electricity which is lower than the design energy requirement of the water system, 22.9 MWe. In this particular hour, the remaining electricity demand of the water system after the electricity supplied by PV is less than the minimum safe operating limit of the turbine load. Therefore, even though Q_{HTF} and TES are available for the power block of the CSP system to operate, the turbine is not operated due to the turbine safe operation limits. As a result of the available electricity to RO, 13 RO trains are operated when the nominal load operation is adopted for RO. The mentioned behavior is observed also at all other hours where PV electricity production decreases the unfulfilled electricity demand of the water system from the CSP system below the CSP turbine safe operational limits, and subsequently, the rapid fluctuations in operated RO train number occur in these hours. Therefore, it can be concluded that with the nominal load operation of RO, the operation of the RO system is still quite susceptible to solar resources. The variable load RO operation is able to dampen these fluctuations as it allows higher numbers of RO trains to operate at partial loads instead of a limited number of trains at design load. Considering the hours of 12-18, it is shown in Fig. 4.10.c that all RO trains are operated continuously with variable load RO operation without experiencing any shutdown due to the fluctuations in electricity supply. The same trends are observed in all other hours, eg. between 30-41 and 59-62, where nominal load RO operation causes tremendous swings in the operated train numbers.

Even though the stable operation of the water systems is achieved to a certain extent, the fluctuations in the CSP electricity output should also be discussed. It should be noted that the CSP electricity generation trend is also stabilized during the hours with no solar resources by the proposed CSP operating strategy by distributing the TES energy among those hours; however, the fluctuations in CSP turbine electricity generation are not eliminated for the periods when the PV electricity production and non-zero Q_{HTF} coincide. It is crucial to bear in mind that the energy system is isolated from the grid; and, the LCOE is calculated based on the utilized fraction of the produced electricity as presented in Section 3.3.1. In other words, any unused portion of the produced electricity increases the LCOE. Hence, excess electricity generation is undesirable, especially for the CSP system where LCOE is already remarkably high. As a result, the lowered CSP production during PV operation is inevitable to prevent the electricity production from exceeding the hourly electricity requirement of the water systems. Therefore, these fluctuations cannot be avoided unless the system is connected to the grid to sell the excess generation or additional systems are added to the overall system to exploit the excess electricity. Finally, it is worth noting that the operation of all WWTP units is maintained continuously for 65 hours without any shutdowns with the PV+CSP hybridization.

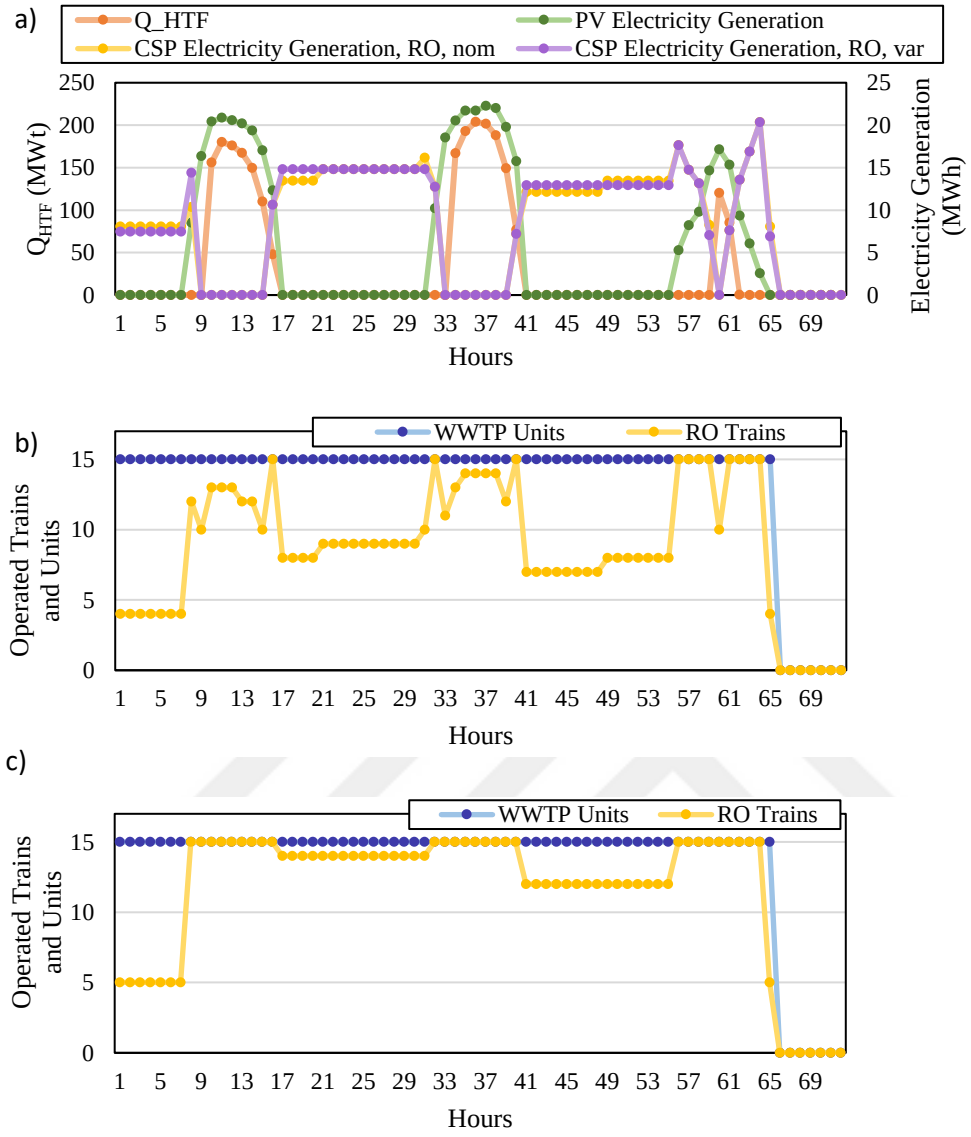

Figure 4.10. The trends of Q_{HTF}, the PV and CSP electricity generation, operated trains of RO and operated units of WWTP with 15 units WWTP and 15 trains RO configuration with a) nominal load b) variable load strategy of the RO plant in the first 72 hours of the year for PV+CSP powered RO+WWTP.

Figure 4.11 presents the individual and overall CFs and LCOWs of RO and WWTP, and UF of the RO powered by hybridized PV and CSP systems for different RO operating strategies and train capacities. As depicted in Fig. 4.11, the CF of the WWTP exceeds 80% for all cases regardless of the RO configuration or

operating strategy as a direct implication of the proposed PV+CSP operating strategy which prolongs the turbine operation. The energy requirement of whole WWTP plant is less than the minimum turbine load; therefore, the whole WWTP plant operates at all hours in which CSP turbine produces electricity.

On the other hand, the RO variable load operating strategy increases the CF factor of the RO by 6.9% resulting in a 5.0% decrease in LCOW compared to the nominal load strategy for 15 trains configuration. Also, the UF of the RO reaches 68.5% with the variable load operation for 15 train configuration, where the CF factor is 59.3%. Interpreting this 15.5% improvement in the number of operated trains reflected by UF and the stabilized trend of the number of operated trains shown in Fig. 4.10.c concurrently, it is concluded that variable load RO operation brings the RO system operation closer to the desired operational characteristics.

The higher modularization, i.e., a higher number of trains, does not significantly improve either the CF or the LCOW. The maximum improvement regarding the higher modularization is observed with nominal load RO operation with a 1.6% increase in CF and a 1.3% reduction in LCOW. Among all cases, the lowest LCOW, 1.142 € m^{-3}, is achieved with 150 trains RO configuration with the overall water system CF of 63.23% whereas the 15 trains configuration results in the CF of 63.17% with LCOW of 1.143 € m^{-3}. All in all, it is concluded that the higher modularization does not lead to any significant performance improvement either technically or economically. Also, it is worth addressing that higher modularization results in higher capital and operational costs theoretically; however, due to the lack of detailed economic data, these increases in the costs cannot be exhibited by the economic key performance indicators. Hence, considering the associated complexity with higher modularization, and additional RO costs remained unreflected on LCOW, there is no explicit benefit of higher modularization of RO plant especially for variable load operation in the scope of this work.

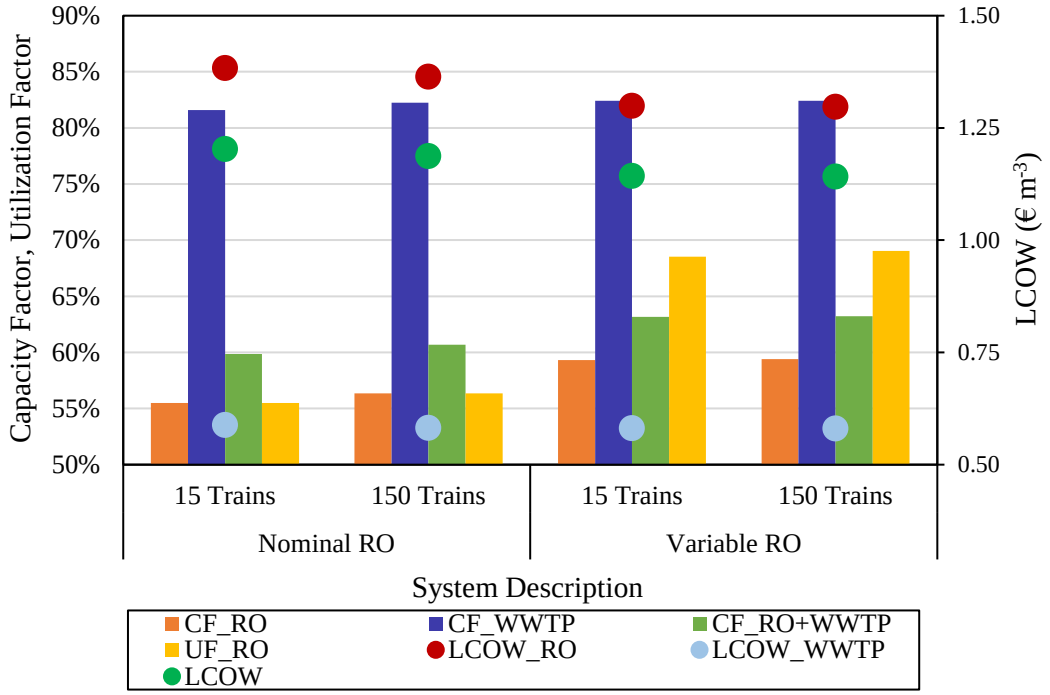

Figure 4.11. The individual and overall CFs and LCOWs of RO+WWTP, and UF of RO plant with 1 000 m^{-3} and 10 000 m^{-3} RO train capacities with nominal and variable RO operation powered by PV+CSP.

4.6 Comparison of Different Energy Scenarios for RO+WWTP

As the analysis of the individual energy systems is completed, it is concluded that

- the variable load RO operating strategy is favorable, mainly considering the ideal operation of turbine and RO trains for the energy systems including CSP. Also, slight improvements are observed in LCOW and CF compared to nominal load RO operation.
- the variable load RO operating strategy is favorable considering the CF and LCOW for the PV system; however, the start-up shut-down instances of RO membrane are increased by the proposed strategy of the variable load operation.

- the higher modularization does not significantly affect the CF and LCOW especially when the variable load RO operating strategy is adopted.

In this section, the different energy systems used to power RO+WWTP systems are compared with 15 train RO configuration. As the advantage of proposed CSP operating strategy is clearly demonstrated in Section 4.4, the base strategy of CSP is not included here.

Firstly, the CF and LCOE of different energy scenarios to power RO+WWTP plant with nominal and variable load operation of a 15 train RO plant are compared in Figure 4.12. The CF of PV does not change either based on energy scheme or RO operating strategy as the PV system has no operating strategy. As Figure 4.12 suggests, the lowest LCOE, 0.057 € kWh^{-1}, is observed when the PV-only scenario is used to power the water systems where RO is operated with the variable load RO strategy. On the other hand, the LCOE is increased by almost a factor of 4 when the stand-alone CSP is employed as the energy system of RO+WWTP. This huge LCOE discrepancy is mainly associated with the higher capital costs of the CSP plant compared to the PV plant. When PV and CSP systems are hybridized, the LCOE of the CSP system further increases by 40.5%, reaching 0.31 € kWh^{-1}. This remarkable increase in the LCOE of the CSP is a direct result of the 29.0% decrease in the capacity factor of the CSP with the hybridized scenario compared to the CSP-alone scenario. This reduction in CF is mainly associated with the inevitable coincidence of the hours with PV generation and non-zero Q_{HTF}. As previously explained in Section 4.5, when the remaining energy requirement of the water systems after the PV electricity supply is less than the minimum turbine load of the CSP system, the CSP system is not operated for the PV+CSP scenario. In those hours, the incident irradiation on the receiver is stored in TES if the storage system is not fully charged. However, due to the consecutive hours with the described pattern of the solar resources, the TES becomes full, and the heliostats are defocused more frequently compared to the CSP system. Hence, in addition to restrictions imposed by the minimum turbine load regarding electricity production,

the TES capacity also limits the utilization of solar resources through the CSP plant when the PV+CSP hybridization is considered. As a direct result of the reduced electricity production of the CSP plant, the effect of the investment costs of the CSP system becomes more prominent on the unit cost of electricity. However, despite the increased LCOE of the CSP plant, the overall LCOE of the hybridized solar systems is found to be 0.19 € kWh^{-1}, 9.4% less than the CSP-alone scenario thanks to the contribution of cheap PV electricity. However, as already demonstrated in the previous chapters of this thesis, the LCOE is not the conclusive indicator for the economical performance of water systems since CF of the water systems also has a considerable effect on the LCOW.

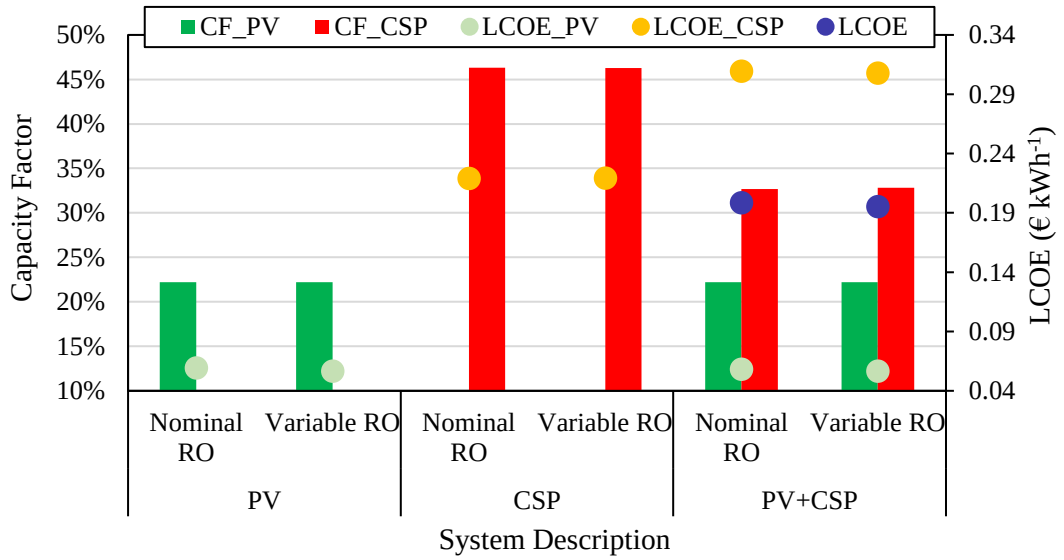

Figure 4.12. Comparison of CF and LCOE of PV, CSP, and PV+CSP systems to power WWTP+RO system with 10 000 m^{-3} RO train capacity with nominal and variable RO operation.

Figure 4.13 compares individual and overall CFs and LCOWs of RO+WWTP powered by different energy scenarios. As Figure 4.13 presents, the capacity factor of the WWTP plant shows a 52.6% and 86.2% increase when the water systems are powered by CSP and PV+CSP, respectively, compared to PV-only system for variable load operation of RO. This increase is achieved not only due to the storage system introduced by the CSP system but also due to the operating strategy of the

energy systems which include CSP. The WWTP electricity requirement in this study is less than the allowed minimum turbine output and WWTP operation is always prioritized than RO; therefore, all WWTP units are operated whenever the CSP turbine operates. As CSP turbine operation is prolonged by the proposed CSP strategy; as a direct result, the CF of the WWTP plant is also enhanced. Considering the larger picture, the highest CF of the combined water systems, 63.2%, is reached with the hybridization of PV and CSP as expected since the installed energy system capacity is increased with the hybridization.

When the LCOW is analyzed for different energy supply scenarios, it is observed that the PV-only system with nominal RO operation shows the highest LCOW with 1.48 € m^{-3}. If this unit cost of water is broken down, the second lowest LCOW of the WWTP and the highest LCOW of the RO plant are found to be associated with PV only scenario. It should be reminded that the lowest LCOE belongs to the PV-only plant as already shown in Fig. 4.12. Hence, the effect of the lowest LCOE is observed in the LCOW of WWTP as the capital costs of the WWTP plant are comparable with its operational costs; the low LCOE results in low electricity consumption, and consequently, the low LCOW of the WWTP plant. On the other hand, for the RO system, the associated capital costs are significantly higher, two orders of magnitude, compared to WWTP. Therefore, despite the lowest LCOE is obtained by the PV plant, the highest LCOW of RO is attained due to the dominant effects of the capital costs of the RO system on the unit cost of water caused by the lowest annual RO water production designated by CF of RO. The highest LCOW of the WWTP is observed with the CSP scenario. The correlation between LCOE and LCOW of WWTP explained for the PV case is also valid for the CSP scenario; therefore, the system with the highest LCOE resulted in the highest LCOW of WWTP. Finally, and most importantly, the lowest LCOW, 1.14 € m^{-3} is achieved with the PV+CSP hybridization. Further breaking down the LCOW, it is observed that the lowest LCOW of RO is also associated with the PV+CSP scenario. This is primarily attributed to the enhanced CF of RO system as the LCOE is 216.7% higher than PV-only scheme as shown in Figure 4.12.

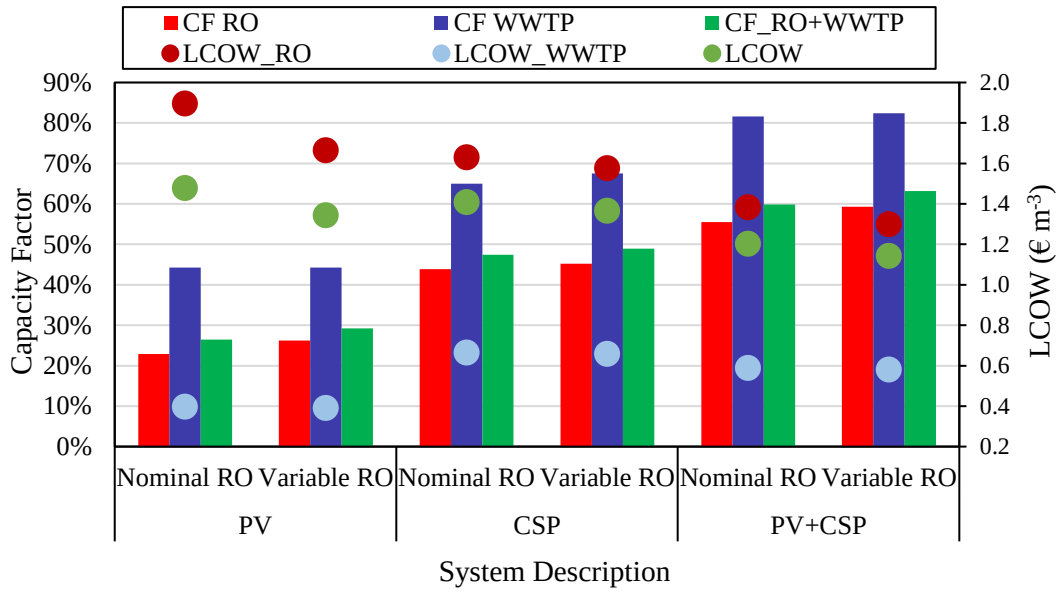

Figure 4.13. The comparison of individual and overall CFs and LCOWs of RO+WWTP, and UF of RO plant with 10 000 m^{-3} RO train capacity with nominal and variable RO operation powered by PV, CSP, and PV+CSP.

To assess the environmental impact of the different energy systems, the emission factor of the produced water is analyzed. The contribution of RO and WWTP to the total water production and the emission factor of the water are presented in Figure 4.14 for different energy systems. Before evaluating the results, it should be underlined that the emission factor of the produced water is a direct indicator of the average SEC of the water produced since the emission factors of PV and CSP systems are almost the same as presented in Table 3.12. At first glance, it is observed that the variable load RO operation results in lower emission factors than the nominal load RO operation regardless of the energy system. This is a direct result of the proposed variable load RO operating strategy in which a higher number of trains are operated at lower loads instead of operating fewer trains at nominal load. It should be recalled that SEC of RO reduces at partial loads compared to nominal load as demonstrated in Fig. 4.1; therefore, the variable load RO operation always results in lower emission factors. Specifically, the variable

load RO operation leads to a reduction in the emission factor by 5.1%, 3.3% and 3.8% for PV-only, CSP and PV+CSP schemes, respectively.

Even though the emission factors of PV and CSP are almost the same, 85.33 and 85.67 $gCO_{2eq}\,kWh^{-1}$, the emission factor of water is the lowest with PV with variable load RO operation as provided in Fig. 4.14. This is first explained by the lower emission factor of PV compared to CSP, and secondly, higher WWTP contribution to the total capacity factor of the water systems considering that the SEC of the WWTP is lower than RO. The highest shares of WWTP in actual water production are observed as 27.9% and 25.3% for PV case with nominal and variable RO operating strategies, resulting in the lowest emissions per m^3 of water produced. Even though CSP addition to PV system results in 2.2% and 3.5% increase in emission factor for nominal and variable load RO operation compared to PV-only scheme, these increases can be interpreted as acceptable considering 79.3% and 67.7% increase in CF, respectively. On the other hand, the highest emission factor is found with the CSP scenario and nominal load RO operation as 255.9 $gCO_{2eq}\,m^{-3}$. PV+CSP hybridization decreases the emission factor by 0.12% and 0.63% with a 26.3% and 29.0% improvement in CF for nominal and variable load RO operation compared to the counterparts of the CSP scenario.

Of particular significance, it is noteworthy that solar energy systems reduce the emission factor of water approximately by 88% compared to the grid regardless of the system details.

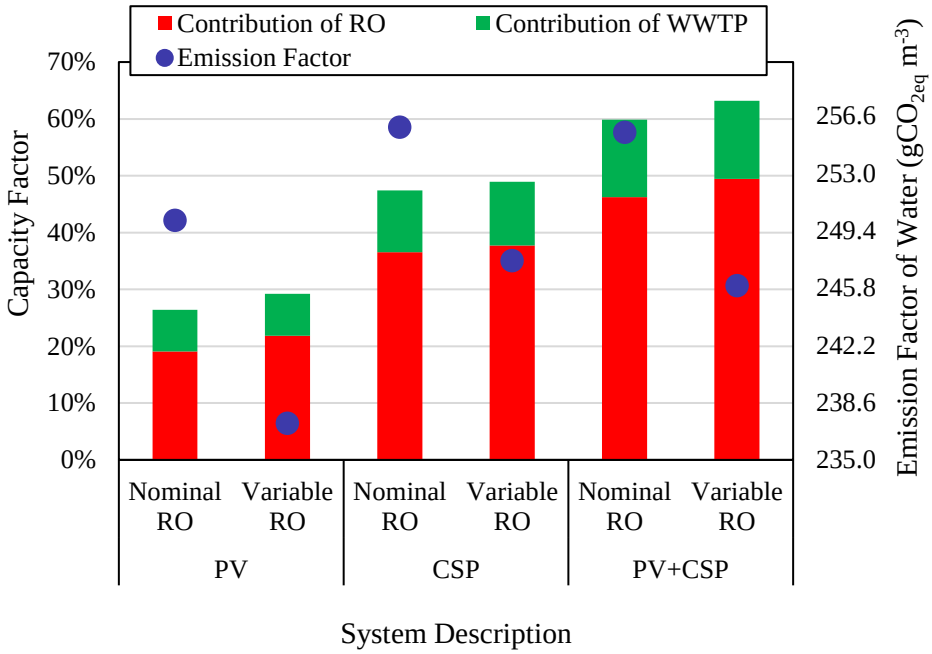

Figure 4.14. Comparison of the contribution of RO and WWTP to the total water production and emission factor of water with 10 000 m^{-3} RO train capacity with nominal and variable RO operation powered by PV, CSP, and PV+CSP.

4.7 Comparison of RO+WWTP System with RO-only System

In this section, the RO+WWTP system is compared with the RO-only system with the same overall water production capacity, 180 000 m^3 day^{-1}, to demonstrate the influence of the addition of WWTP to the water production systems. Even though it is already presented in Section 3.2.4.5, it is worth recalling that the nominal energy requirement of the system increases by 6.1% for the RO-only scenario which also results in a 6.2% and 7.6% increase in the land use of PV and CSP systems, respectively.

The systems are evaluated only for variable load RO operating strategy with 10 000 m^3 day^{-1} train capacity as the advantage of this scheme has already been demonstrated in previous sections.

Figure 4.15 presents the contributions of RO and WWTP to the CF of the overall water systems and the associated LCOWs. As the first observation, the overall capacity factor of the water systems is almost the same regardless of the energy system; the addition of WWTP increased the overall CF at most by 1.9% for the PV case. For almost the same overall CF, the WWTP has the share of 25.3%, 23.0%, and 21.7% in the actual water production of systems powered by PV-only, CSP and PV+CSP, respectively where the installed WWTP capacity only constitutes of 16.7% of the overall water production capacity. These contributions are achieved as a direct result of the prioritized WWTP operation and they are truly valuable since the reuse of the wastewater is augmented which would be discharged to sea otherwise, and desalination would use higher energy to produce fresh water from seawater.

Concerning the economic aspect, LCOW is decreased with the addition of WWTP regardless of the energy system. This LCOW decrease is primarily associated with the lower LCOW of WWTP induced by lower capital costs and operating costs compared to RO including lower SEC. As can be inferred from Fig. 4.15, the LCOW of WWTP is found to be 23.4%, 41.7%, and 44.7% of the LCOW of RO with WWTP+RO scheme powered by PV, CSP, and PV+CSP, respectively. Subsequently, the contribution of the WWTP water production reduces the overall LCOW by 12.9%, 10.0%, and 9.6% compared to RO-only scenario for PV, CSP and PV+CSP schemes, respectively.

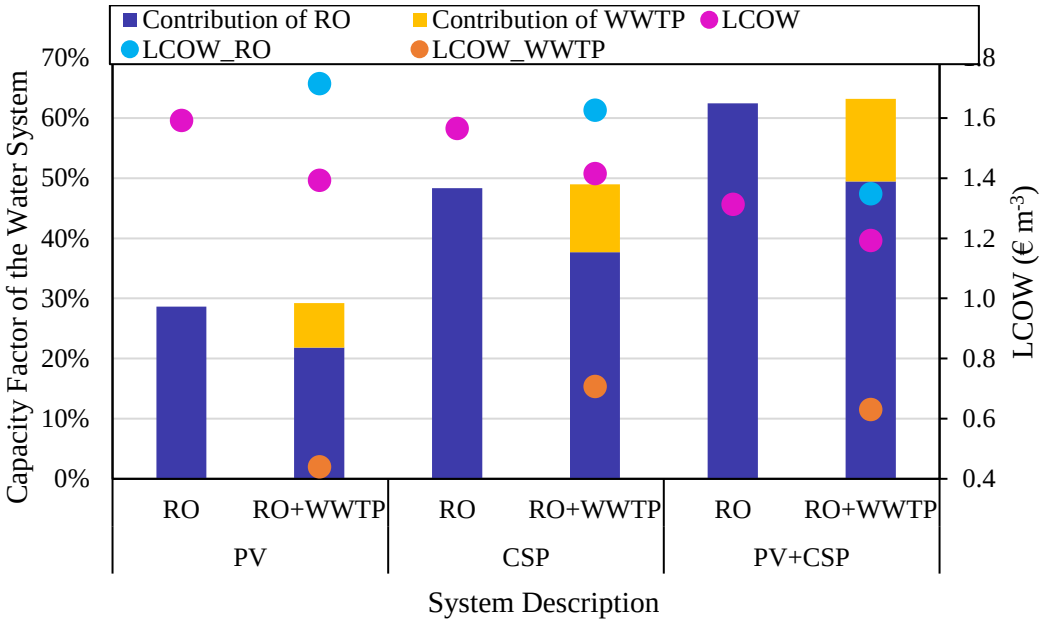

Figure 4.15. Comparison of the contribution of RO and WWTP to the total water production for RO-only and RO+WWTP scenarios and associated LCOWs with 10 000 m^{-3} RO train capacity and variable RO operation powered by PV, CSP, and PV+CSP.

Figure 4.16 presents the emission factor of the produced water by RO-only and RO+WWTP powered by different energy systems. It is previously explained that the emission factor of the water is a direct indicator of the average SEC of the produced water. Therefore, it is to be expected that the system of RO+WWTP results in lower emissions than RO-only plant regardless of the energy system as the SEC of the WWTP is lower than RO. Numerically, the addition of WWTP decreases the emission factor of water by 2.6%, 7.2% 6.9% for PV-only, CSP, and PV+CSP scenarios, respectively, compared to the RO-only scenario. These reductions in emission factors avoid 491.3, 509.2, and 636.1 tonnes of CO_2 emission per year for PV-only, CSP, and PV+CSP scenarios, respectively.

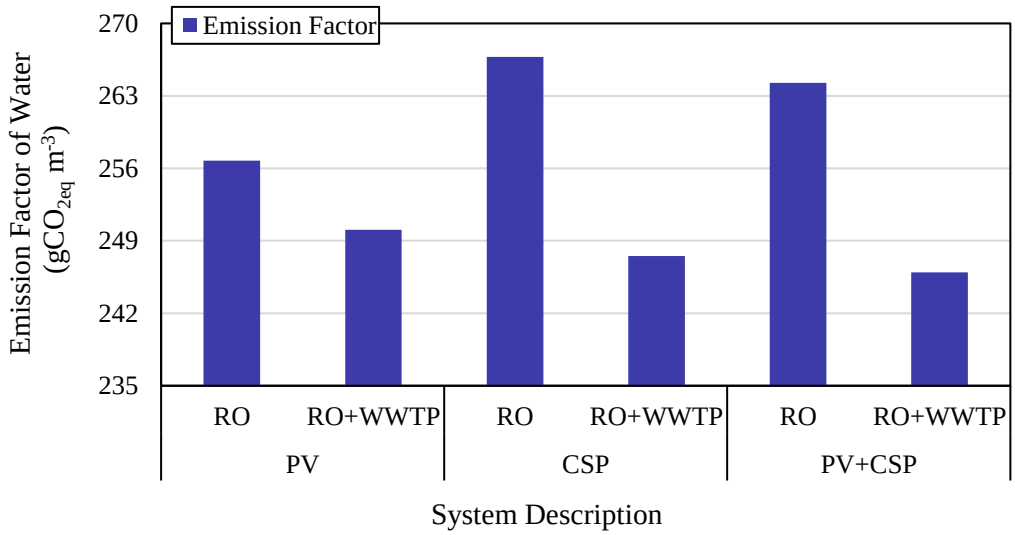

Figure 4.16. Comparison of emission factor of water for RO-only and RO+WWTP scenarios with 10 000 m^{-3} RO train capacity and variable RO operation powered by PV, CSP, and PV+CSP.

It is concluded that utilizing the WWTP in addition to RO by reducing RO capacity to have the same daily capacity to produce irrigation water is advantageous energetically, economically, and environmentally.

4.8 Parametric Study of RO+WWTP System Powered by PV CSP Hybridization

Going back to the water supply scheme proposed in this study; in this section, the results of the parametric study conducted for RO+WWTP system powered by PV+CSP are presented. During the parametric studies, solar multiple, TES system storage capacity and installed PV capacity are determined as the design variables and their values are varied. The LCOW and CF of the overall water system installations are assessed to analyze the effects of these variables on the system performance.

It is noteworthy that even though the studied installed PV capacities are kept as the same for all solar multiple values, the storage capacities are increased in parallel

with the increased values of solar multiple. As explained in Section 3.2.4.7, solar multiple is a measure of oversizing the heliostat field, resulting in higher incident irradiation on the receiver. Therefore, it is reasonable to enhance the storage capacity of the TES as solar multiple increases to take advantage of the increased incident irradiation.

Figure 4.17 presents the effect of the storage capacity and installed PV capacity on LCOW and CF of water systems for SM=2.5. As the first observation, the lowest LCOW, 1.035 € m^{-3}, and the highest CF of the water systems, 69.75%, are found with 16 hours of storage and 37.5 MW installed PV capacity for SM=2.5.

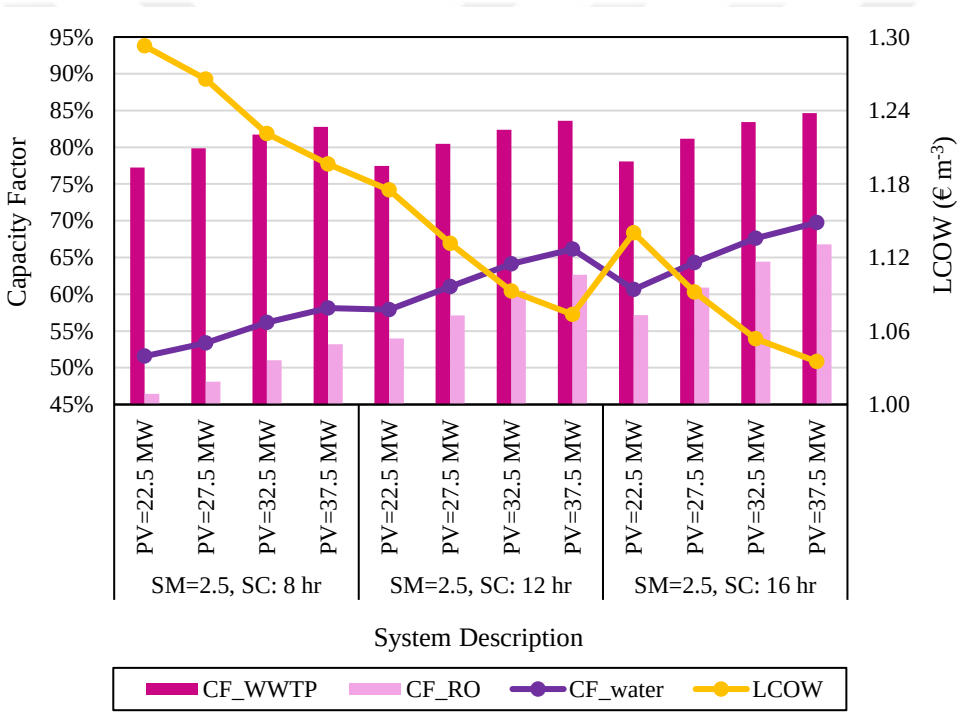

Figure 4.17. The parametric results of CF and LCOW of RO+WWTP with varying installed PV capacities and TES storage capacities for SM=2.5.

Figure 4.18 presents the effect of the storage capacity and installed PV capacity on LCOW and CF of water systems for SM=3. The lowest LCOW, 1.032 € m^{-3}, and the highest CF of the water systems, 74.03%, are observed with 20 hours of storage and 37.5 MW installed PV capacity for SM=3.

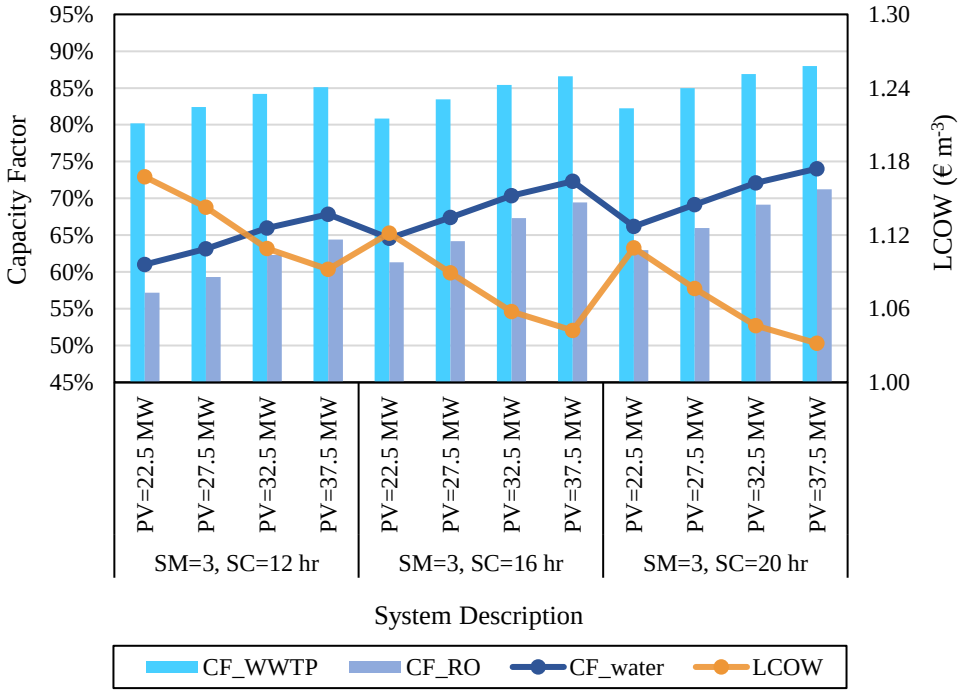

Figure 4.18. The parametric results of CF and LCOW of RO+WWTP with varying installed PV capacities and TES storage capacities for SM=3.

Figure 4.19 presents the effect of the storage capacity and installed PV capacity on LCOW and CF of water systems for SM=3.5. The lowest LCOW, 1.034 € m^{-3}, and the highest CF of the water systems, 77.59%, are observed with 20 hours of storage and 37.5 MW installed PV capacity for SM=3.5.

Evaluating all results together, it is found that increasing installed PV capacity, SC, and SM improves the individual and combined CF of the water systems. Therefore, the highest CF of overall water systems, 77.6%, is found for SM=3.5, SC=24 hr, and PV=37.5 MW. With this particular energy system, the CF of the RO and WWTP reaches 90.3% and 75.1%, respectively.

However, the same conclusions cannot be drawn for LCOW. Even though the increase in the PV capacity for the same storage capacity and the increase in storage capacity for the same SM decreases LCOW, the higher SM does not necessarily result in lower LCOW when the other variables are the same. This is

attributed to the dominant effect of heliostat field costs which rise as SM values are increased. When two systems with SM=3 and SM=3.5 are compared with SC=20 hr, and PV=37.5 MW, the lower LCOW is observed for SM=3 value, being 0.9% less than the LCOW found for SM=3.5 even though 2.8% improvement is observed in CF of water systems with higher SM.

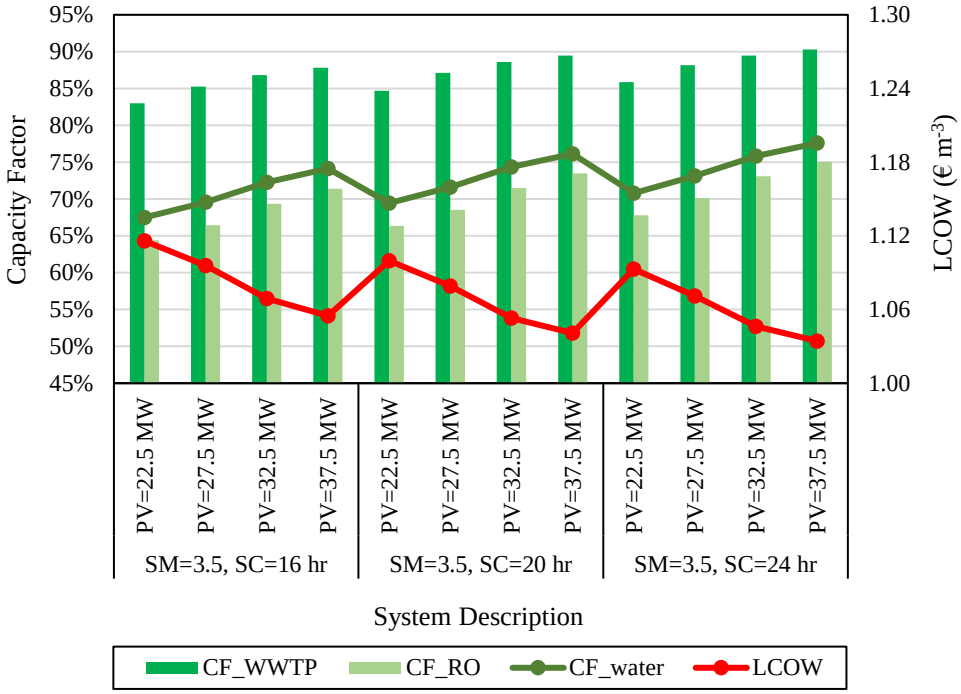

Figure 4.19. The parametric results of CF and LCOW of RO+WWTP with varying installed PV capacities and TES storage capacities for SM=3.5.

All in all, the lowest LCOW is found to be 1.03 € m^{-3} with SM=3, SC=20 hr, and PV=37.5 MW.

It is indispensable to mention that the achieved CF for WWTP, 90.3%, is quite promising, especially considering that the WWTP system is slightly oversized in this study. Based on the results presented, the continuous treatment of wastewater even for the whole year is concluded to be plausible.

Even though PV=37.5 MW results in the best technical and economic performance of the system among other PV installation capacities for any SM and SC, it should

be noted that it also results in excess electricity production or PV curtailment as the installed PV capacity is considerably higher than the nominal energy requirement of the water systems. The exemplary case is selected as SM=3.5, SC=24 hr case where the highest CF is reached with PV=37.5 MW to observe the effect of the PV excess electricity generation. The F_{UE} of the PV and overall solar systems, and the overall capacity factor of the water system are presented in Figure 4.20.a. whereas the LCOE of PV and LCOW are shown in Figure 4.20.b. As depicted from Figure 4.20.a, the excess energy generation of PV becomes evident for PV=37.5 MW case with 7.3% non-utilized electricity production of PV plant, leading to non-utilization of 3.4% of the total electricity production. As the fraction of non-utilized PV electricity increases, the LCOE of the PV also increases since the LCOE is calculated based on the electricity generation utilized by water systems. Specifically, it causes a 7.8% increase in the LCOE with PV=37.5 MW compared to PV=22.5 MW. However, at the same time, the CF of the water systems is improved by 9.6% with this 15 MW increase of the installed PV capacity. Assessing these results concurrently, despite the increase in LCOE of PV, the LCOW is found to decrease with increasing PV capacity due to the increased CF of the water system and reach its minimum with 1.03 € m^{-3} with 37.5 MW installed PV capacity. A milder scenario regarding the generation of excess electricity is the PV=32.5 MW; in this case, the non-utilized portion of produced electricity can be considered insignificant where F_{UE} and $F_{UE,PV}$ are 98.2% and 99.2%, respectively. Compared to PV=22.5 MW, the decrease of LCOW is 4.3% despite the 1.8% increase in the LCOE of the PV system. Considering the 7.1% increase in CF of the water systems and the 4.3% reduction of overall LCOW, it is reasonable to compromise the excess energy corresponding to 0.8% of the total electricity generation. Therefore, considering the improvements in water system performance, PV systems with higher capacities than the nominal electricity requirement of the water system are viable to be installed by the cost of excess electricity generation or PV curtailment.

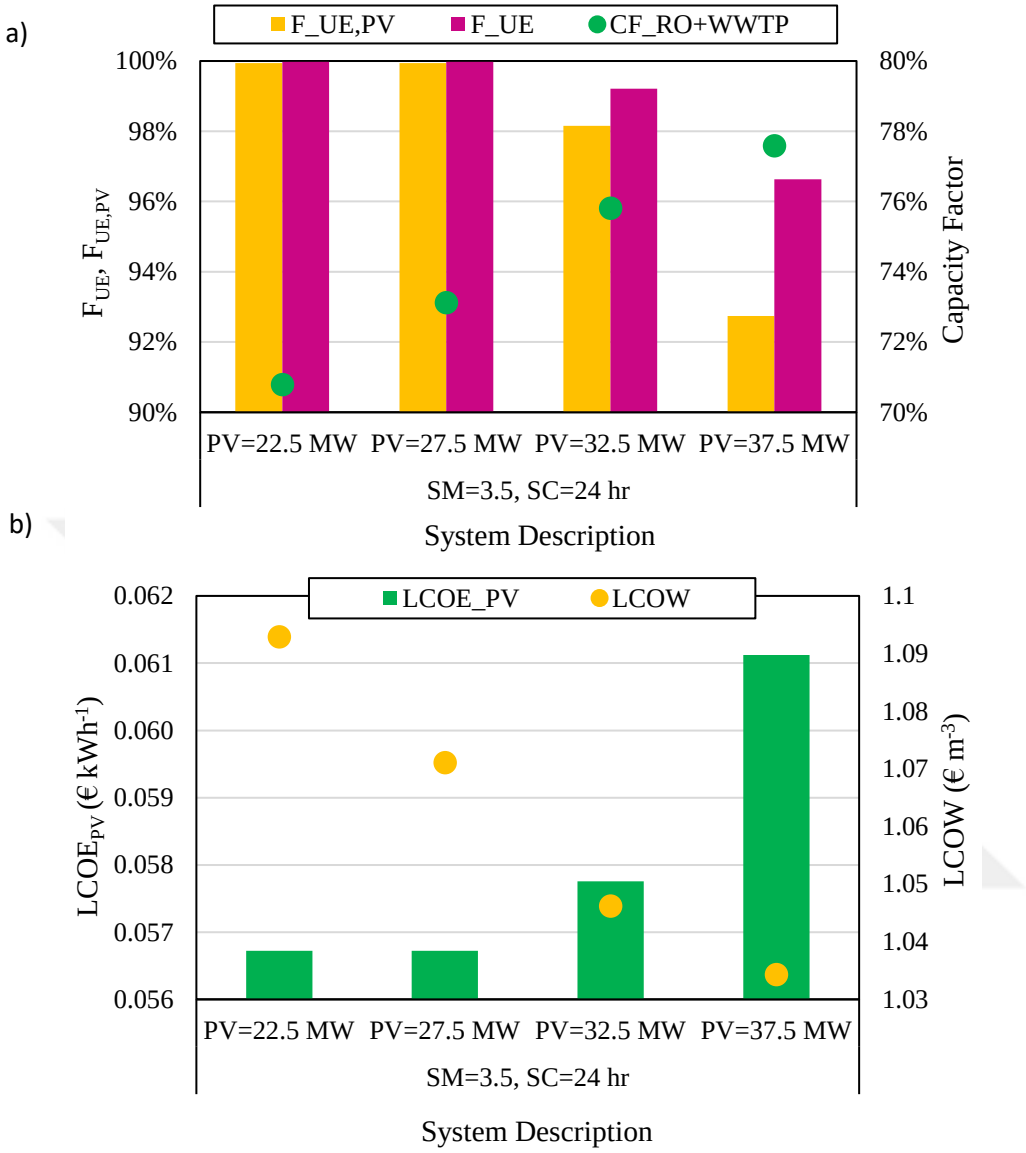

Figure 4.20. a) The F_{UE} of the PV and overall solar systems, and the overall CF of the water system, and b) LCOE of PV and overall LCOW with varying installed PV capacities for SM=3.5 and SC=24 hr.

As a final word, even though mostly minimizing the LCOW or maximizing the CF of the water systems are studied as the objective in the literature and taken here as the main design consideration, the land use of the energy systems should be a severe concern, especially considering the fertile land occupation when these systems are installed in the agricultural regions.

CHAPTER 5

CONCLUSIONS AND FUTURE WORK

5.1 Conclusions

The reuse of urban wastewater and seawater reverse osmosis desalination can be potential solutions to meet the world's increasing need for agricultural irrigation water. Solar systems hold huge potential to power these water systems for fertile but arid regions with good solar and seawater resources, but there are also several technical and economic challenges of solar powered water treatment systems that needs to be addressed.

In that sense, PV CSP hybridization is investigated as a promising solution to power water treatment systems in this thesis. Three solar systems are considered to power the quaternary stage of an urban WWTP and seawater RO plant to produce agricultural irrigation water: 1) PV-only, 2) CSP with thermal energy storage, and 3) PV and CSP hybridization with thermal energy storage. Novel operating strategies for CSP and PV+CSP plants are proposed according to the water system requirements. Also, two different operating strategies of RO are analyzed to improve RO performance: 1) nominal load operation and 2) variable load operation. The models are run for Erdemli, Mersin, Türkiye.

It is demonstrated that the proposed operating strategies of CSP and PV+CSP systems coupled with the variable load RO operating strategy improve the continuous operation of turbine and RO trains and dampen the effects of variable nature of solar resources on water systems.

It is proven that PV and CSP hybridization with variable load operation of RO results in the highest CF of water systems with the lowest LCOW when the systems are hybridized with their stand-alone capacities. With the PV and CSP

hybridization, the LCOW is found to be decreased by 14.9% and 16.3%, with 116.3% and 29.0% increase in CF of water systems compared to PV-only and CSP scenarios, respectively.

The WWTP+RO plant is compared with the RO-only plant for the same daily water production capacity. The addition of WWTP is found to result in 12.9%, 10.0%, and 9.6% lower LCOW compared to the RO-only scenario for PV, CSP, and PV+CSP schemes, respectively. Also, the emission factor of water decreases by 2.6%, 7.2%, and 6.9% for PV-only, CSP, and PV+CSP scenarios, respectively with the introduction of WWTP.

Finally, the hybridization of PV and CSP is studied parametrically for WWTP+RO. The overall water system CF of 77.6% is reached with 90.3% CF of the WWTP plant resulting in LCOW of 1.03 € m^{-3}.

5.2 Further Opportunities and Future Work

Even though the TES integration into other renewables, specifically PV, has gained attention in recent years, the low efficiencies and energy losses during electricity-heat-electricity conversion hinder its practical application, and more studies are needed to confirm its economic benefits before its commercialization [43]. As the LCOW is found to decrease with increased PV capacity in this study, and it is shown that PV occupies less land compared to the CSP heliostat field, the TES can be analyzed as the storage system of PV to utilize excess PV production to explore its technical, economic, and environmental viability.

The water systems should also be analyzed with grid connected energy systems in addition to the off-grid scenario considered here. A smart grid is a network which combines and integrates electrical information using advanced control and information technologies to balance the demand and supply [161]. Considering the increasing penetration of renewables to the grid globally and application targeted renewable energy installations, water systems in this study, smart grids and grid

connected RE systems can offer several advantages with more advanced state of art technologies and improved operating strategies of both water systems.

The accelerated transition to sustainable energy resources is expected to raise the global competition for land [162]. Therefore, the land use of energy systems deserves particular attention, especially if they are land intensive. To retain their position in the global market and gain competitive advantage, the land use of solar systems also needs to be studied extensively. Hence, this study, in which the solar systems are required to be installed in agricultural regions, can be enriched with future studies to optimize their land use.

Even though it is not examined in this study, brine disposal is a challenging and controversial topic in desalination considering its environmental impacts. The brine salinity reaches up to 200% of the seawater, resulting in reduced oxygen solubility and the formation of convective currents due to variations in density. In addition to increased salinity, chemical additives such as antiscalants, coagulants, etc., and particles of heavy metals caused by corrosion increase the turbidity and discoloration of the water and affect the light penetration. The mentioned issues subsequently result in changes in photosynthesis, metabolic and growth rates of the organism in the seawater, and even mortality of those [163]. Hence, the aspect of brine management also needs to be studied as a part of desalination studies to achieve a holistic approach.

Circularity has gained a growing emphasis lately concerning the rapid depletion of resources and associated vulnerability of linear paradigms. The linear water economy is encouraged to evolve into a circular one, where the reuse of water is promoted and associated byproducts is proposed to be used as the feedstocks of other processes with economical values [164]. Brine mining [165] and energy harnessing from salinity gradients [166] are two examples of valorization of the brine as a resource. Similarly, the sludge of the urban wastewater treatment plants holds huge potential regarding sustainable resource management. The sludge of water treatment can be reused as pollutant adsorbent, soil conditioner, or even

construction material [167]. In conclusion, the opportunities associated with water system byproducts need to be explored to contribute to the promoted circularity practices.

Also, the emission analysis of this study only includes the emissions of energy systems, excluding the CO_2 emissions of the life cycles of the WWTP and RO plants. A detailed LCA of the solar powered water treatment systems could provide valuable insights regarding the environmental impacts of the proposed system here.

Direct sunlight can be used for some photo-driven AOPs instead of UV lamps [120], [168], [169] and it is commented in [170] that it can be an attractive solution for small WWTP plants. Even though, the UV/H_2O_2 studied in this thesis cannot be considered as a small WWTP, opportunities related to the use of direct sunlight could be investigated to advocate the utilization of solar energy as the primary energy source and to eliminate the high costs associated with UV lamp electricity consumption.

Most importantly, as these systems are oriented to meet urgent needs detected globally and have practical purposes, their applicability and acceptance should also be investigated. According to the recent findings of [171] and [172], the use of desalinated water and treated wastewater in agricultural irrigation are still penalized by stakeholders due to the lack of knowledge, awareness, or experience. Considering Türkiye's immature market in utility-scale CSP technologies, and lack of experience in desalination plants, and insufficient practices regarding the reuse of treated wastewater, the social acceptance of these technologies, the attitude of the stakeholders, public perception, and policy aspects require special attention and investigation.

REFERENCES

[1] I. A. Shiklomanov, "Appraisal and Assessment of World Water Resources," *Water Int*, vol. 25, no. 1, pp. 11–32, Mar. 2000, doi: 10.1080/02508060008686794.

[2] WWAP (UNESCO World Water Assessment Programme), "The United Nations World Water Development Report 2021: Valuing Water," Paris, 2021.

[3] Z. Çelik, Ş. Özçelik, Z. Albayram Doğan, and B. Aydın, "Üreticilerin Damla Sulama Hibelerinden Yararlanma Durumu ve Davranışları: İzmir, Manisa, Denizli Örneği," *Tarım Ekonomisi Dergisi*, Jun. 2022, doi: 10.24181/tarekoder.1030950.

[4] WWAP (UNESCO World Water Assessment Programme), "The United Nations World Water Development Report 2015: Water for a Sustainable World," Paris, 2015.

[5] "THE 17 GOALS | Sustainable Development." https://sdgs.un.org/goals (accessed Jun. 09, 2022).

[6] UNFCCC (United Nations Framework Convention on Climate Change), "The Paris Agreement," United Nations, 2016. Accessed: Oct. 25, 2021. [Online]. Available: https://www.un.org/en/climatechange/paris-agreement

[7] M. Çeçen, C. Yavuz, C. A. Tırmıkçı, S. Sarıkaya, and E. Yanıkoğlu, "Analysis and evaluation of distributed photovoltaic generation in electrical energy production and related regulations of Turkey," *Clean Technol Environ Policy*, vol. 24, no. 5, pp. 1321–1336, Jul. 2022, doi: 10.1007/s10098-021-02247-0.

[8] "Turkey - Agriculture." https://www.trade.gov/country-commercial-guides/turkey-agriculture (accessed Apr. 21, 2023).

[9] “Türkiye’s Policy on Water Issues / Republic of Türkiye Ministry of Foreign Affairs.” https://www.mfa.gov.tr/turkiye_s-policy-on-water-issues.en.mfa (accessed Apr. 21, 2023).

[10] A. J. Englande, P. Krenkel, and J. Shamas, “Wastewater Treatment &Water Reclamation☆,” in *Reference Module in Earth Systems and Environmental Sciences*, Elsevier, 2015. doi: 10.1016/B978-0-12-409548-9.09508-7.

[11] Metcalf & Eddy Inc., “Introduction to Wastewater Treatment and Process Analysis,” in *Wastewater engineering: Treatment and resource recovery*, 5th ed.New York, NY: McGraw-Hill Education, 2014.

[12] WWAP (United Nations World Water Assessment Programme), “The United Nations World Water Development Report 2017. Wastewater: The Untapped Resource,” Paris, 2017.

[13] M. Zamparas, “The role of resource recovery technologies in reducing the demand of fossil fuels and conventional fossil-based mineral fertilizers,” *Low Carbon Energy Technologies in Sustainable Energy Systems*, pp. 3–24, Jan. 2021, doi: 10.1016/B978-0-12-822897-5.00001-8.

[14] Council of the European Union, “Council Directive 91/271/EEC of 21 May 1991 concerning urban waste-water treatment.” Directorate-General for Environment, DG11/B/03, 1991.

[15] “Proposal for a revised Urban Wastewater Treatment Directive.” https://environment.ec.europa.eu/publications/proposal-revised-urban-wastewater-treatment-directive_en (accessed May 21, 2023).

[16] European Commision Directorate-General for Environment, “Proposal for a revised Urban Wastewater Treatment Directive.” Brussels, 2022.

[17] J. (European I. B. Bofill, “Microplastics and micropollutants in water: Contaminants of emerging concern,” 2023.

[18] P. Krzeminski *et al.*, “Performance of secondary wastewater treatment methods for the removal of contaminants of emerging concern implicated in crop uptake and antibiotic resistance spread: A review,” *Science of The Total Environment*, vol. 648, pp. 1052–1081, Jan. 2019, doi: 10.1016/j.scitotenv.2018.08.130.

[19] P. Falås, A. Wick, S. Castronovo, J. Habermacher, T. A. Ternes, and A. Joss, “Tracing the limits of organic micropollutant removal in biological wastewater treatment,” *Water Res*, vol. 95, pp. 240–249, May 2016, doi: 10.1016/j.watres.2016.03.009.

[20] L. Rizzo *et al.*, “Best available technologies and treatment trains to address current challenges in urban wastewater reuse for irrigation of crops in EU countries,” *Science of The Total Environment*, vol. 710, p. 136312, Mar. 2020, doi: 10.1016/j.scitotenv.2019.136312.

[21] L. Rizzo, “Bioassays as a tool for evaluating advanced oxidation processes in water and wastewater treatment,” *Water Res*, vol. 45, no. 15, pp. 4311–4340, Oct. 2011, doi: 10.1016/j.watres.2011.05.035.

[22] M. Muruganandham *et al.*, “Recent Developments in Homogeneous Advanced Oxidation Processes for Water and Wastewater Treatment,” *International Journal of Photoenergy*, vol. 2014, pp. 1–21, 2014, doi: 10.1155/2014/821674.

[23] S. F. Anis, R. Hashaikeh, and N. Hilal, “Functional materials in desalination: A review,” *Desalination*, vol. 468, p. 114077, Oct. 2019, doi: 10.1016/j.desal.2019.114077.

[24] M. A. Abdelkareem, M. El Haj Assad, E. T. Sayed, and B. Soudan, “Recent progress in the use of renewable energy sources to power water desalination plants,” *Desalination*, vol. 435, pp. 97–113, Jun. 2018, doi: 10.1016/j.desal.2017.11.018.

[25] N. Voutchkov, “Energy use for membrane seawater desalination – current status and trends,” *Desalination*, vol. 431, pp. 2–14, Apr. 2018, doi: 10.1016/j.desal.2017.10.033.

[26] D. Zarzo and D. Prats, “Desalination and energy consumption. What can we expect in the near future?,” *Desalination*, vol. 427, pp. 1–9, Feb. 2018, doi: 10.1016/j.desal.2017.10.046.

[27] M. Qasim, M. Badrelzaman, N. N. Darwish, N. A. Darwish, and N. Hilal, “Reverse osmosis desalination: A state-of-the-art review,” *Desalination*, vol. 459, pp. 59–104, Jun. 2019, doi: 10.1016/j.desal.2019.02.008.

[28] Y. Ghalavand, M. S. Hatamipour, and A. Rahimi, “A review on energy consumption of desalination processes,” *Desalination Water Treat*, pp. 1–16, Mar. 2014, doi: 10.1080/19443994.2014.892837.

[29] A. A. Bayod-Rújula, “Solar photovoltaics (PV),” *Solar Hydrogen Production: Processes, Systems and Technologies*, pp. 237–295, Jan. 2019, doi: 10.1016/B978-0-12-814853-2.00008-4.

[30] N. M. Pearsall, “Introduction to photovoltaic system performance,” *The Performance of Photovoltaic (PV) Systems: Modelling, Measurement and Assessment*, pp. 1–19, Jan. 2017, doi: 10.1016/B978-1-78242-336-2.00001-X.

[31] A. Allouhi, S. Rehman, M. S. Buker, and Z. Said, “Up-to-date literature review on Solar PV systems: Technology progress, market status and R&D,” *J Clean Prod*, vol. 362, p. 132339, Aug. 2022, doi: 10.1016/j.jclepro.2022.132339.

[32] D. Zhang and A. Allagui, “Fundamentals and performance of solar photovoltaic systems,” *Design and Performance Optimization of Renewable Energy Systems*, pp. 117–129, Jan. 2021, doi: 10.1016/B978-0-12-821602-6.00009-2.

[33] H. A. Mohamed, H. A. Khattab, A. Mobarka, and G. A. Morsy, “Design, control and performance analysis of DC-DC boost converter for stand-alone PV system,” in *2016 Eighteenth International Middle East Power Systems Conference (MEPCON)*, IEEE, Dec. 2016, pp. 101–106. doi: 10.1109/MEPCON.2016.7836878.

[34] C. M. Whitaker, T. U. Townsend, A. Razon, R. M. Hudson, and X. Vallvé, “PV Systems,” in *Handbook of Photovoltaic Science and Engineering*, Chichester, UK: John Wiley & Sons, Ltd, 2011, pp. 841–895. doi: 10.1002/9780470974704.ch19.

[35] M. B. Elbeh and A. K. Sleiti, “Analysis and optimization of concentrated solar power plant for application in arid climate,” *Energy Sci Eng*, vol. 9, no. 6, pp. 784–797, Jun. 2021, doi: 10.1002/ESE3.742.

[36] R. Pitz-Paal, “Concentrating Solar Power,” in *Future Energy*, Elsevier, 2020, pp. 413–430. doi: 10.1016/B978-0-08-102886-5.00019-0.

[37] M. T. Islam, N. Huda, A. B. Abdullah, and R. Saidur, “A comprehensive review of state-of-the-art concentrating solar power (CSP) technologies: Current status and research trends,” *Renewable and Sustainable Energy Reviews*, vol. 91, pp. 987–1018, Aug. 2018, doi: 10.1016/j.rser.2018.04.097.

[38] A. Peinado Gonzalo, A. Pliego Marugán, and F. P. García Márquez, “A review of the application performances of concentrated solar power systems,” *Appl Energy*, vol. 255, p. 113893, Dec. 2019, doi: 10.1016/j.apenergy.2019.113893.

[39] K. Lovegrove and W. S. Csiro, “Introduction to concentrating solar power (CSP) technology,” in *Concentrating Solar Power Technology*, Elsevier, 2012, pp. 3–15. doi: 10.1533/9780857096173.1.3.

[40] A. Caraballo, S. Galán-Casado, Á. Caballero, and S. Serena, “Molten Salts for Sensible Thermal Energy Storage: A Review and an Energy Performance

Analysis," *Energies (Basel)*, vol. 14, no. 4, p. 1197, Feb. 2021, doi: 10.3390/en14041197.

[41] V. Kronhardt *et al.*, "High-temperature Thermal Storage System for Solar Tower Power Plants with Open-volumetric Air Receiver Simulation and Energy Balancing of a Discretized Model," *Energy Procedia*, vol. 49, pp. 870–877, 2014, doi: 10.1016/j.egypro.2014.03.094.

[42] N. Siegel, M. Gross, C. Ho, T. Phan, and J. Yuan, "Physical Properties of Solid Particle Thermal Energy Storage Media for Concentrating Solar Power Applications," *Energy Procedia*, vol. 49, pp. 1015–1023, 2014, doi: 10.1016/j.egypro.2014.03.109.

[43] A. Vossier and J. Zeitouny, "Hybrid PV–CSP Systems," in *Concentrating Solar Thermal Energy*, Wiley, 2022, pp. 259–282. doi: 10.1002/9781394169702.ch9.

[44] W. T. Hamilton, M. A. Husted, A. M. Newman, R. J. Braun, and M. J. Wagner, "Dispatch optimization of concentrating solar power with utility-scale photovoltaics," *Optimization and Engineering*, vol. 21, no. 1, pp. 335–369, Mar. 2020, doi: 10.1007/s11081-019-09449-y.

[45] "Atacama I / Cerro Dominador 110MW CSP + 100 MW PV | Concentrating Solar Power Projects | NREL." https://solarpaces.nrel.gov/project/atacama-i-cerro-dominador-110mw-csp-100-mw-pv (accessed Apr. 26, 2023).

[46] "About – Noor Energy." http://noorenergy.ae/a-about/ (accessed Apr. 26, 2023).

[47] "China now has 30 CSP projects with thermal energy storage underway - SolarPACES." https://www.solarpaces.org/china-now-has-30-csp-projects-with-thermal-energy-storage-underway/ (accessed Apr. 26, 2023).

[48] A. Green, C. Diep, R. Dunn, and J. Dent, “High Capacity Factor CSP-PV Hybrid Systems,” *Energy Procedia*, vol. 69, pp. 2049–2059, May 2015, doi: 10.1016/j.egypro.2015.03.218.

[49] A. R. Starke, J. M. Cardemil, R. A. Escobar, and S. Colle, “Assessing the performance of hybrid CSP+PV plants in northern Chile,” *Solar Energy*, vol. 138, pp. 88–97, Nov. 2016, doi: 10.1016/j.solener.2016.09.006.

[50] C. A. Pan and F. Dinter, “Combination of PV and central receiver CSP plants for base load power generation in South Africa,” *Solar Energy*, vol. 146, pp. 379–388, Apr. 2017, doi: 10.1016/j.solener.2017.02.052.

[51] R. Zhai, H. Liu, Y. Chen, H. Wu, and Y. Yang, “The daily and annual technical-economic analysis of the thermal storage PV-CSP system in two dispatch strategies,” *Energy Convers Manag*, vol. 154, pp. 56–67, Dec. 2017, doi: 10.1016/j.enconman.2017.10.040.

[52] M. Moser, F. Trieb, T. Fichter, and J. Kern, “Integrated techno-economic assessment of hybrid CSP-PV plants,” 2018, p. 180008. doi: 10.1063/1.5067180.

[53] A. Giaconia and R. Grena, “A model of integration between PV and thermal CSP technologies,” *Solar Energy*, vol. 224, pp. 149–159, Aug. 2021, doi: 10.1016/j.solener.2021.05.043.

[54] M. Petrollese and D. Cocco, “Optimal design of a hybrid CSP-PV plant for achieving the full dispatchability of solar energy power plants,” *Solar Energy*, vol. 137, pp. 477–489, Nov. 2016, doi: 10.1016/j.solener.2016.08.027.

[55] A. R. Starke, J. M. Cardemil, R. Escobar, and S. Colle, “Multi-objective optimization of hybrid CSP+PV system using genetic algorithm,” *Energy*, vol. 147, pp. 490–503, Mar. 2018, doi: 10.1016/j.energy.2017.12.116.

[56] R. Bravo and D. Friedrich, “Two-stage optimisation of hybrid solar power plants,” *Solar Energy*, vol. 164, pp. 187–199, Apr. 2018, doi: 10.1016/j.solener.2018.01.078.

[57] F. Giudici, A. Castelletti, E. Garofalo, M. Giuliani, and H. R. Maier, “Dynamic, multi-objective optimal design and operation of water-energy systems for small, off-grid islands,” *Appl Energy*, vol. 250, pp. 605–616, Sep. 2019, doi: 10.1016/j.apenergy.2019.05.084.

[58] R. Fornarelli, F. Shahnia, M. Anda, P. A. Bahri, and G. Ho, “Selecting an economically suitable and sustainable solution for a renewable energy-powered water desalination system: A rural Australian case study,” *Desalination*, vol. 435, pp. 128–139, Jun. 2018, doi: 10.1016/j.desal.2017.11.008.

[59] B. Rahimi, H. Shirvani, A. A. Alamolhoda, F. Farhadi, and M. Karimi, “A feasibility study of solar-powered reverse osmosis processes,” *Desalination*, vol. 500, p. 114885, Mar. 2021, doi: 10.1016/J.DESAL.2020.114885.

[60] Z. Wang, X. Lin, N. Tong, Z. Li, S. Sun, and C. Liu, “Optimal planning of a 100% renewable energy island supply system based on the integration of a concentrating solar power plant and desalination units,” *International Journal of Electrical Power & Energy Systems*, vol. 117, p. 105707, May 2020, doi: 10.1016/j.ijepes.2019.105707.

[61] S. Casimiro, M. K. A. Ahmed, J. P. Cardoso, and J. Farinha Mendes, “Reverse osmosis powered by concentrating solar power (CSP): A case study for Trapani, Sicily,” *Desalination Water Treat*, vol. 61, pp. 183–195, Jan. 2017, doi: 10.5004/dwt.2016.11105.

[62] M. Laissaoui, P. Palenzuela, M. A. Sharaf Eldean, D. Nehari, and D. C. Alarcón-Padilla, “Techno-economic analysis of a stand-alone solar desalination plant at variable load conditions,” *Appl Therm Eng*, vol. 133, pp. 659–670, Mar. 2018, doi: 10.1016/j.applthermaleng.2018.01.074.

[63] C. Valenzuela, C. Mata-Torres, J. M. Cardemil, and R. A. Escobar, “CSP + PV hybrid solar plants for power and water cogeneration in northern Chile,” *Solar Energy*, vol. 157, pp. 713–726, 2017, doi: 10.1016/j.solener.2017.08.081.

[64] C. Mata-Torres, P. Palenzuela, A. Zurita, J. M. Cardemil, D. C. Alarcón-Padilla, and R. A. Escobar, “Annual thermoeconomic analysis of a Concentrating Solar Power + Photovoltaic + Multi-Effect Distillation plant in northern Chile,” *Energy Convers Manag*, vol. 213, no. January, p. 112852, 2020, doi: 10.1016/j.enconman.2020.112852.

[65] Álvaro Marín Silvestre, “Modelado y análisis tecno económico de plantas termosolares de receptor central hibridadas con fotovoltaica para aplicaciones de cogeneración de electricidad y agua desalada,” Almeria University, 2020.

[66] P. Feron, “The use of wind power in autonomous reverse osmosis seawater desalination,” *Wind Engineering*, vol. 9, no. 3, pp. 180–199, 1985.

[67] R. Pohl, M. Kaltschmitt, and R. Holländer, “Investigation of different operational strategies for the variable operation of a simple reverse osmosis unit,” *Desalination*, vol. 249, no. 3, pp. 1280–1287, Dec. 2009, doi: 10.1016/j.desal.2009.06.029.

[68] B. S. Richards, G. L. Park, T. Pietzsch, and A. I. Schäfer, “Renewable energy powered membrane technology: Safe operating window of a brackish water desalination system,” *J Memb Sci*, vol. 468, pp. 400–409, Oct. 2014, doi: 10.1016/j.memsci.2014.05.053.

[69] A. Ruiz-García and I. Nuez, “Performance evaluation and boron rejection in a SWRO system under variable operating conditions,” *Comput Chem Eng*, vol. 153, p. 107441, Oct. 2021, doi: 10.1016/j.compchemeng.2021.107441.

[70] R. W. (Richard W. Baker, “5. Reverse Osmosis,” in *Membrane technology and applications*, John Wiley & Sons, 2012, pp. 179–206.

[71] B. S. Richards, D. P. S. Capão, W. G. Früh, and A. I. Schäfer, “Renewable energy powered membrane technology: Impact of solar irradiance fluctuations on performance of a brackish water reverse osmosis system,” *Sep Purif Technol*, vol. 156, pp. 379–390, Dec. 2015, doi: 10.1016/j.seppur.2015.10.025.

[72] M. Freire-Gormaly and A. M. Bilton, “Experimental quantification of the effect of intermittent operation on membrane performance of solar powered reverse osmosis desalination systems,” *Desalination*, vol. 435, pp. 188–197, Jun. 2018, doi: 10.1016/j.desal.2017.09.013.

[73] M. Freire-Gormaly and A. M. Bilton, “Impact of intermittent operation on reverse osmosis membrane fouling for brackish groundwater desalination systems,” *J Memb Sci*, vol. 583, pp. 220–230, Aug. 2019, doi: 10.1016/j.memsci.2019.04.010.

[74] A. Ruiz-García and I. Nuez, “Long-term intermittent operation of a full-scale BWRO desalination plant,” *Desalination*, vol. 489, p. 114526, Sep. 2020, doi: 10.1016/j.desal.2020.114526.

[75] S. L. Roback, K. P. Ishida, Y.-H. Chuang, Z. Zhang, W. A. Mitch, and M. H. Plumlee, “Pilot UV-AOP Comparison of UV/Hydrogen Peroxide, UV/Free Chlorine, and UV/Monochloramine for the Removal of *N* -Nitrosodimethylamine (NDMA) and NDMA Precursors,” *ACS ES&T Water*, vol. 1, no. 2, pp. 396–406, Feb. 2021, doi: 10.1021/acsestwater.0c00155.

[76] J. Scaria and P. V. Nidheesh, “Comparison of hydroxyl-radical-based advanced oxidation processes with sulfate radical-based advanced oxidation processes,” *Curr Opin Chem Eng*, vol. 36, p. 100830, Jun. 2022, doi: 10.1016/j.coche.2022.100830.

[77] J. A. Andrades, M. Lojo-López, A. Egea-Corbacho, and J. M. Quiroga, “Comparative Effect of UV, UV/H2O2 and UV/H2O2/Fe on Terbuthylazine

Degradation in Natural and Ultrapure Water," *Molecules*, vol. 27, no. 14, p. 4507, Jul. 2022, doi: 10.3390/molecules27144507.

[78] L. Haroune, S. Saibi, C. Thiec, H. Cabana, R. Leduc, and J.-P. Bellenger, "Evaluation of oxidation processes for pharmaceutical compounds removal," *Catal Commun*, vol. 172, p. 106533, Dec. 2022, doi: 10.1016/j.catcom.2022.106533.

[79] L. Prieto-Rodríguez, I. Oller, N. Klamerth, A. Agüera, E. M. Rodríguez, and S. Malato, "Application of solar AOPs and ozonation for elimination of micropollutants in municipal wastewater treatment plant effluents," *Water Res*, vol. 47, no. 4, pp. 1521–1528, Mar. 2013, doi: 10.1016/J.WATRES.2012.11.002.

[80] M. T. Sturm, E. Myers, D. Schober, C. Thege, A. Korzin, and K. Schuhen, "Adaptable Process Design as a Key for Sustainability Upgrades in Wastewater Treatment: Comparative Study on the Removal of Micropollutants by Advanced Oxidation and Granular Activated Carbon Processing at a German Municipal Wastewater Treatment Plant," *Sustainability*, vol. 14, no. 18, p. 11605, Sep. 2022, doi: 10.3390/su141811605.

[81] "TORAY Design System 2." Toray Industries, Inc.

[82] "Design Tool | Knowledge Base | Toray Membrane | TORAY." https://www.water.toray/knowledge/tool/ (accessed Jun. 25, 2023).

[83] D. Zarzo and D. Prats, "Desalination and energy consumption. What can we expect in the near future?," *Desalination*, vol. 427, pp. 1–9, Feb. 2018, doi: 10.1016/j.desal.2017.10.046.

[84] "System Advisor Model Version 2021.12.2 (SAM 2021.12.2)." National Renewable Energy Laboratory, Golden, CO.

[85] The MathWorks Inc., "MATLAB." Natick, Massachusetts, 2021.

[86] “Home - System Advisor Model - SAM.” https://sam.nrel.gov/ (accessed Jun. 20, 2023).

[87] “Quenching the world’s thirst with off-grid water desalination | Research and Innovation.” https://ec.europa.eu/research-and-innovation/en/horizon-magazine/quenching-worlds-thirst-grid-water-desalination (accessed Jun. 26, 2023).

[88] A. A. Monjezi *et al.*, “Development of an off-grid solar energy powered reverse osmosis desalination system for continuous production of freshwater with integrated photovoltaic thermal (PVT) cooling,” *Desalination*, vol. 495, p. 114679, Dec. 2020, doi: 10.1016/j.desal.2020.114679.

[89] L. Karimi, L. Abkar, M. Aghajani, and A. Ghassemi, “Technical feasibility comparison of off-grid PV-EDR and PV-RO desalination systems via their energy consumption,” *Sep Purif Technol*, vol. 151, pp. 82–94, 2015, doi: https://doi.org/10.1016/j.seppur.2015.07.023.

[90] I. Padrón, D. Avila, G. N. Marichal, and J. A. Rodríguez, “Assessment of Hybrid Renewable Energy Systems to supplied energy to Autonomous Desalination Systems in two islands of the Canary Archipelago,” *Renewable and Sustainable Energy Reviews*, vol. 101, pp. 221–230, Mar. 2019, doi: 10.1016/j.rser.2018.11.009.

[91] A. Mostafaeipour, M. Qolipour, M. Rezaei, and E. Babaee-Tirkolaee, “Investigation of off-grid photovoltaic systems for a reverse osmosis desalination system: A case study,” *Desalination*, vol. 454, pp. 91–103, Mar. 2019, doi: 10.1016/j.desal.2018.03.007.

[92] A. M. Delgado-Torres and L. García-Rodríguez, “Off-grid SeaWater Reverse Osmosis (SWRO) desalination driven by hybrid tidal range/solar PV systems: Sensitivity analysis and criteria for preliminary design,” *Sustainable Energy Technologies and Assessments*, vol. 53, p. 102425, Oct. 2022, doi: 10.1016/j.seta.2022.102425.

[93] M. Z. Jacobson, M. A. Delucchi, M. A. Cameron, and B. A. Frew, “Low-cost solution to the grid reliability problem with 100% penetration of intermittent wind, water, and solar for all purposes,” *Proceedings of the National Academy of Sciences*, vol. 112, no. 49, pp. 15060–15065, Dec. 2015, doi: 10.1073/pnas.1510028112.

[94] D. Eltigani and S. Masri, “Challenges of integrating renewable energy sources to smart grids: A review,” *Renewable and Sustainable Energy Reviews*, vol. 52, pp. 770–780, Dec. 2015, doi: 10.1016/j.rser.2015.07.140.

[95] P. Gilman, “SAM Photovoltaic Model Technical Reference,” 2015, Accessed: Apr. 21, 2023. [Online]. Available: www.nrel.gov/publications.

[96] “Available Solar Radiation,” in *Solar Engineering of Thermal Processes, Photovoltaics and Wind*, Wiley, 2020, pp. 45–140. doi: 10.1002/9781119540328.ch2.

[97] M. Sodhi, L. Banaszek, C. Magee, and M. Rivero-Hudec, “Economic Lifetimes of Solar Panels,” *Procedia CIRP*, vol. 105, pp. 782–787, 2022, doi: 10.1016/j.procir.2022.02.130.

[98] J. Kim, M. Rabelo, S. P. Padi, H. Yousuf, E.-C. Cho, and J. Yi, “A Review of the Degradation of Photovoltaic Modules for Life Expectancy,” *Energies (Basel)*, vol. 14, no. 14, p. 4278, Jul. 2021, doi: 10.3390/en14144278.

[99] J. Wohlgemuth, D. Cunningham, P. Monus, J. Miller, and A. Nguyen, “Long Term Reliability of Photovoltaic Modules,” in *2006 IEEE 4th World Conference on Photovoltaic Energy Conference*, IEEE, 2006, pp. 2050–2053. doi: 10.1109/WCPEC.2006.279905.

[100] D. C. Jordan and S. R. Kurtz, “Photovoltaic Degradation Rates -- An Analytical Review: Preprint,” 2012, Accessed: Apr. 21, 2023. [Online]. Available: http://www.osti.gov/bridge

[101] A. R. Starke, J. M. Cardemil, R. A. Escobar, and S. Colle, “Assessing the performance of hybrid CSP+PV plants in northern Chile,” *Solar Energy*, vol. 138, pp. 88–97, Nov. 2016, doi: 10.1016/j.solener.2016.09.006.

[102] R. Zhai, H. Liu, Y. Chen, H. Wu, and Y. Yang, “The daily and annual technical-economic analysis of the thermal storage PV-CSP system in two dispatch strategies,” *Energy Convers Manag*, vol. 154, pp. 56–67, Dec. 2017, doi: 10.1016/j.enconman.2017.10.040.

[103] B. Ehrhart and D. Gill, “Evaluation of annual efficiencies of high temperature central receiver concentrated solar power plants with thermal energy storage,” *Energy Procedia*, vol. 49, pp. 752–761, 2014, doi: 10.1016/J.EGYPRO.2014.03.081.

[104] P. Łuczyński, D. Toebben, L. Pehle, M. Wirsum, W. F. D. Mohr, and K. Helbig, “Thermostructural Analysis of Steam Turbine in Prewarming Operation With Hot Air,” *J Eng Gas Turbine Power*, vol. 141, no. 11, Nov. 2019, doi: 10.1115/1.4044311.

[105] P. Łuczyński, L. Pehle, M. Wirsum, W. F. D. Mohr, J. Vogt, and K. Helbig, “Thermo-Structural Analysis of Steam Turbine Startup With and Without Integrated Prewarming System Using Hot Air,” *J Eng Gas Turbine Power*, vol. 143, no. 3, Mar. 2021, doi: 10.1115/1.4049502.

[106] I. V. Muralikrishna and V. Manickam, “Life Cycle Assessment,” in *Environmental Management*, Elsevier, 2017, pp. 57–75. doi: 10.1016/B978-0-12-811989-1.00005-1.

[107] “Solar Resource Map Direct Normal Irradiation Turkey.” The World Bank, Source: Global Solar Atlas 2.0, Solar resource data: Solargis, 2020. [Online]. Available: https://solargis.com/maps-and-gis-data/download/turkey

[108] T.C. Mersin Valiliği İl Tarım Müdürlüğü, “Mersin Tarım Master Planı,” Mersin, 2011. [Online]. Available:

http://www.mersin.gov.tr/kurumlar/mersin.gov.tr/Genel/depo/TARIM%20MASTER%20PLAN-01.11.2011.pdf

[109] M. Serin and S. Horuz, "Mersin ili Silifke ilçesi domates seralarında görülen bakteriyel hastalıkların surveyi ve yaygınlıklarının belirlenmesi," *Mustafa Kemal Üniversitesi Tarım Bilimleri Dergisi*, vol. 27, no. 1, pp. 79–87, Apr. 2022, doi: 10.37908/mkutbd.1026011.

[110] "Meteonorm 7.2." [Online]. Available: https://meteonorm.com/en/

[111] "DSİ 2022 Yılı Faaliyet Raporu," 2022. Accessed: Apr. 25, 2023. [Online]. Available: www.dsi.gov.tr

[112] B. Çakmak, M. Yıldırım, and T. Aküzüm, "Türkiye'de Tarımda Su Yönetimi, Sorunlar Ve Çözüm Önerileri," in *TMMOB 2. Su Politikaları Kongresi*, 2008.

[113] Erdemli Belediyesi Strateji Geliştirme Müdürlüğü, "Erdemli Belediyesi 2020-2024 Stratejik Plan," 2019. Accessed: Apr. 21, 2023. [Online]. Available: http://www.sp.gov.tr/upload/xSPStratejikPlan/files/lZYo4+ERDEMLI_BELEDIYESI-SP-2019-2023.pdf

[114] D. Zarzo, E. Campos, and P. Terrero, "Spanish experience in desalination for agriculture," *Desalination Water Treat*, vol. 51, no. 1–3, pp. 53–66, 2013, doi: 10.1080/19443994.2012.708155.

[115] "TÜİK - Coğrafi İstatistik Portalı." https://cip.tuik.gov.tr/ (accessed Apr. 21, 2023).

[116] H. Kumbur, V. Yamaçlı, and A. Küçükbahar, "Mersin province water projections and water information and management system: Erdemli district model," *International Advanced Researches and Engineering Journal*, vol. 2, no. 3, pp. 261–266, 2018.

[117] “TURKSTAT Corporate.” https://data.tuik.gov.tr/Bulten/Index?p=Water-and-Wastewater-Statistics-2020-37197&dil=2 (accessed Apr. 21, 2023).

[118] R. López-Timoner *et al.*, “UVC-Assisted Tertiary Treatments for the Removal of Pollutants of Emerging Concern in Real WWTP Matrices,” *Water (Basel)*, vol. 15, no. 5, p. 882, Feb. 2023, doi: 10.3390/w15050882.

[119] P. B. Moser, B. C. Ricci, C. B. Alvim, A. C. F. Cerqueira, and M. C. S. Amaral, “Removal of organic matter of electrodialysis reversal brine from a petroleum refinery wastewater reclamation plant by UV and UV/H $_2$ 0 $_2$ process,” *Journal of Environmental Science and Health, Part A*, vol. 53, no. 5, pp. 430–435, Apr. 2018, doi: 10.1080/10934529.2017.1409580.

[120] S. Miralles-Cuevas, D. Darowna, A. Wanag, S. Mozia, S. Malato, and I. Oller, “Comparison of UV/H 2 O 2 , UV/S 2 O 8 2− , solar/Fe(II)/H 2 O 2 and solar/Fe(II)/S 2 O 8 2− at pilot plant scale for the elimination of micro-contaminants in natural water: An economic assessment,” *Chemical Engineering Journal*, vol. 310, pp. 514–524, Feb. 2017, doi: 10.1016/j.cej.2016.06.121.

[121] N. De la Cruz *et al.*, “Degradation of emergent contaminants by UV, UV/H2O2 and neutral photo-Fenton at pilot scale in a domestic wastewater treatment plant,” *Water Res*, vol. 47, no. 15, pp. 5836–5845, Oct. 2013, doi: 10.1016/j.watres.2013.07.005.

[122] B. S. Souza *et al.*, “Evaluation of UV/H $_2$ O $_2$ for the disinfection and treatment of municipal secondary effluents for water reuse,” *Journal of Chemical Technology & Biotechnology*, vol. 88, no. 9, pp. 1697–1706, Sep. 2013, doi: 10.1002/jctb.4021.

[123] C. Baresel, M. Harding, and C. Junestedt, “Removal of pharmaceutical residues from municipal wastewater using UV/H2O2,” Stockholm, 2019.

[124] “FilmTec^{TM} Reverse Osmosis Membranes Technical Manual,” 2023.

[125] LANXESS Deutschland GmbH, “Principles of Reverse Osmosis Membrane Separation,” 2013. [Online]. Available: https://water.ma/media/documentation-en/Principles%20of%20Reverse%20Osmosis%20Membrane%20Separation.pdf

[126] R. W. Baker, “4. Concentration Polarization,” in *Membrane Technology and Applications*, Wiley, 2012, pp. 179–206. doi: 10.1002/9781118359686.

[127] D. Akgul, M. Çakmakcı, N. Kayaalp, and I. Koyuncu, “Cost analysis of seawater desalination with reverse osmosis in Turkey,” *Desalination*, vol. 220, no. 1–3, pp. 123–131, Mar. 2008, doi: 10.1016/j.desal.2007.01.027.

[128] A. Nashed and B. Van Dang, “Solar and water: high-technology readiness technologies,” in *Solar-Driven Water Treatment*, Elsevier, 2022, pp. 67–117. doi: 10.1016/B978-0-323-90991-4.00007-4.

[129] B. Huang, K. Pu, P. Wu, D. Wu, and J. Leng, “Design, Selection and Application of Energy Recovery Device in Seawater Desalination: A Review,” *Energies (Basel)*, vol. 13, no. 16, p. 4150, Aug. 2020, doi: 10.3390/en13164150.

[130] R. L. Stover, “Seawater reverse osmosis with isobaric energy recovery devices,” *Desalination*, vol. 203, no. 1–3, pp. 168–175, Feb. 2007, doi: 10.1016/J.DESAL.2006.03.528.

[131] A. Zein, S. Karaki, and M. Al-Hindi, “Analysis of variable reverse osmosis operation powered by solar energy,” *Renew Energy*, vol. 208, pp. 385–398, May 2023, doi: 10.1016/J.RENENE.2023.03.001.

[132] B. Huang, K. Pu, P. Wu, D. Wu, and J. Leng, “Design, Selection and Application of Energy Recovery Device in Seawater Desalination: A Review,” *Energies 2020, Vol. 13, Page 4150*, vol. 13, no. 16, p. 4150, Aug. 2020, doi: 10.3390/EN13164150.

[133] M. Á. Aumesquet-Carreto, B. Ortega-Delgado, and L. García-Rodríguez, "Opportunities of Reducing the Energy Consumption of Seawater Reverse Osmosis Desalination by Exploiting Salinity Gradients," *Membranes 2022, Vol. 12, Page 1045*, vol. 12, no. 11, p. 1045, Oct. 2022, doi: 10.3390/MEMBRANES12111045.

[134] B. Rahimi, M. Afzali, F. Farhadi, and A. A. Alamolhoda, "Reverse osmosis desalination for irrigation in a pistachio orchard," *Desalination*, vol. 516, p. 115236, Nov. 2021, doi: 10.1016/j.desal.2021.115236.

[135] J. A. Duffie (Deceased), W. A. Beckman, and N. Blair, *Solar Engineering of Thermal Processes, Photovoltaics and Wind*. Wiley, 2020. doi: 10.1002/9781119540328.

[136] N. B. Desai, S. B. Kedare, and S. Bandyopadhyay, "Optimization of design radiation for concentrating solar thermal power plants without storage," *Solar Energy*, vol. 107, pp. 98–112, Sep. 2014, doi: 10.1016/j.solener.2014.05.046.

[137] M. J. Montes, A. Abánades, J. M. Martínez-Val, and M. Valdés, "Solar multiple optimization for a solar-only thermal power plant, using oil as heat transfer fluid in the parabolic trough collectors," *Solar Energy*, vol. 83, no. 12, pp. 2165–2176, Dec. 2009, doi: 10.1016/j.solener.2009.08.010.

[138] "Gemasolar Thermosolar Plant / Solar TRES | Concentrating Solar Power Projects | NREL." https://solarpaces.nrel.gov/project/gemasolar-thermosolar-plant-solar-tres (accessed May 06, 2023).

[139] Ç. ve İ. D. B. EVÇED, "Türkiye Ulusal Elektrik Şebekesi Emisyon Faktörü Bilgi Formu," 2022. [Online]. Available: https://enerji.gov.tr/Media/Dizin/EVCED/tr/%C3%87evreVe%C4%B0klim/%C4%B0klimDe%C4%9Fi%C5%9Fikli%C4%9Fi/TUESEmisyonFktr/Belgeler/Bform2020.pdf

[140] R. Turconi, A. Boldrin, and T. Astrup, “Life cycle assessment (LCA) of electricity generation technologies: Overview, comparability and limitations,” *Renewable and Sustainable Energy Reviews*, vol. 28, pp. 555–565, Dec. 2013, doi: 10.1016/j.rser.2013.08.013.

[141] “Republic of Turkey Ministry of Energy and Natural Resources - Electricity.” https://enerji.gov.tr/infobank-energy-electricity (accessed May 20, 2023).

[142] R. Kommalapati, A. Kadiyala, Md. Shahriar, and Z. Huque, “Review of the Life Cycle Greenhouse Gas Emissions from Different Photovoltaic and Concentrating Solar Power Electricity Generation Systems,” *Energies (Basel)*, vol. 10, no. 3, p. 350, Mar. 2017, doi: 10.3390/en10030350.

[143] S. Raikar and S. Adamson, “Renewable energy finance in the international context,” in *Renewable Energy Finance*, Elsevier, 2020, pp. 185–220. doi: 10.1016/B978-0-12-816441-9.00013-1.

[144] N. M. Eshoul, B. Agnew, A. Anderson, and M. S. Atab, “Exergetic and economic analysis of two-pass RO desalination proposed plant for domestic water and irrigation,” *Energy*, vol. 122, pp. 319–328, Mar. 2017, doi: 10.1016/J.ENERGY.2017.01.095.

[145] I. S. Mesquita, C. P. Borges, and F. V. da Fonseca, “Membrane biorreactor, reverse osmosis and UV/H2O2 process integration for ethinylestradiol removal: A cost-benefit analysis,” *J Environ Manage*, vol. 310, p. 114760, May 2022, doi: 10.1016/J.JENVMAN.2022.114760.

[146] S. Loutatidou and H. A. Arafat, “Techno-economic analysis of MED and RO desalination powered by low-enthalpy geothermal energy,” *Desalination*, vol. 365, pp. 277–292, Jun. 2015, doi: 10.1016/J.DESAL.2015.03.010.

[147] E. J. Okampo and N. Nwulu, “Techno-economic evaluation of reverse osmosis desalination system considering emission cost and demand

response," *Sustainable Energy Technologies and Assessments*, vol. 46, p. 101252, Aug. 2021, doi: 10.1016/J.SETA.2021.101252.

[148] OECD, "Carbon Pricing in Times of COVID-19: What Has Changed in G20 Economies?," Paris, 2021.

[149] "Carbon pricing in Turkey", Accessed: Apr. 21, 2023. [Online]. Available: www.oecd.org/tax/tax-policy/carbon-pricing-background-notes.pdf.

[150] "TCMB." https://www.tcmb.gov.tr/wps/wcm/connect/en/tcmb+en (accessed May 20, 2023).

[151] D. Feldman, V. Ramasamy, R. Fu, A. Ramdas, J. Desai, and R. Margolis, "U.S. Solar Photovoltaic System and Energy Storage Cost Benchmark: Q1 2020," 2020, Accessed: Aug. 11, 2022. [Online]. Available: www.nrel.gov/publications.

[152] J. Hoffmann and A. S. Pidaparthi, "Heliostat Cost Reduction for Power Tower Plants," 2017, Accessed: May 06, 2023. [Online]. Available: https://scholar.sun.ac.za

[153] C. S. Turchi *et al.*, "CSP Systems Analysis - Final Project Report," 2016. [Online]. Available: www.nrel.gov/publications.

[154] "DesalData." https://www.desaldata.com/ (accessed Aug. 11, 2022).

[155] N. N. Mahamuni and Y. G. Adewuyi, "Advanced oxidation processes (AOPs) involving ultrasound for waste water treatment: A review with emphasis on cost estimation," *Ultrason Sonochem*, vol. 17, no. 6, pp. 990–1003, Aug. 2010, doi: 10.1016/j.ultsonch.2009.09.005.

[156] M. H. Plumlee, B. D. Stanford, J.-F. Debroux, D. C. Hopkins, and S. A. Snyder, "Costs of Advanced Treatment in Water Reclamation," *Ozone Sci Eng*, vol. 36, no. 5, pp. 485–495, Sep. 2014, doi: 10.1080/01919512.2014.921565.

[157] P. B. Moser, B. C. Ricci, C. B. Alvim, A. C. F. Cerqueira, and M. C. S. Amaral, “Removal of organic matter of electrodialysis reversal brine from a petroleum refinery wastewater reclamation plant by UV and UV/H $_2$ 0 $_2$ process,” *Journal of Environmental Science and Health, Part A*, vol. 53, no. 5, pp. 430–435, Apr. 2018, doi: 10.1080/10934529.2017.1409580.

[158] Y. Başaran, “Sulama Sularının Kalitesi ve Kullanılmış Suların Yeniden Kullanılması Hakkında Yönetmelik,” 2015. [Online]. Available: https://www.tarimorman.gov.tr/SYGM/Belgeler/su%20kalitesi%20sunum/No.1%20Sulama%20Sular%C4%B1%20Hizmet%20%C4%B0%C3%A7i%20E%C4%9Fitimi.pptx

[159] “SolarTwins’ Deliverable D3.1: Synthesis: Mid-term Summary & Assessment of METU-GÜNAM & PSA-CIEMAT Joint ESR Mentoring & Research Programs ,” 2021.

[160] E. Gedik, D.-C. Alarcón-Padilla, and D. Baker, “Techno-Economic Analysis of Reverse Osmosis Desalination Plant Powered by Hybridized PV and CSP Systems for Irrigation Water,” in *28th International Conference on Concentrating Solar Power and Chemical Energy Systems, SolarPACES 2022*, Albuquerque, 2022.

[161] S. Kakran and S. Chanana, “Smart operations of smart grids integrated with distributed generation: A review,” *Renewable and Sustainable Energy Reviews*, vol. 81, pp. 524–535, Jan. 2018, doi: 10.1016/j.rser.2017.07.045.

[162] D. J. van de Ven *et al.*, “The potential land requirements and related land use change emissions of solar energy,” *Scientific Reports 2021 11:1*, vol. 11, no. 1, pp. 1–12, Feb. 2021, doi: 10.1038/s41598-021-82042-5.

[163] K. Elsaid, M. Kamil, E. T. Sayed, M. A. Abdelkareem, T. Wilberforce, and A. Olabi, “Environmental impact of desalination technologies: A review,” *Science of the Total Environment*, vol. 748, Dec. 2020, doi: 10.1016/j.scitotenv.2020.141528.

[164] M. S. Mauter and P. S. Fiske, “Desalination for a circular water economy,” *Energy Environ Sci*, vol. 13, no. 10, pp. 3180–3184, 2020, doi: 10.1039/D0EE01653E.

[165] M. O. Mavukkandy, C. M. Chabib, I. Mustafa, A. Al Ghaferi, and F. AlMarzooqi, “Brine management in desalination industry: From waste to resources generation,” *Desalination*, vol. 472, p. 114187, Dec. 2019, doi: 10.1016/J.DESAL.2019.114187.

[166] N. Y. Yip, D. Brogioli, H. V. M. Hamelers, and K. Nijmeijer, “Salinity Gradients for Sustainable Energy: Primer, Progress, and Prospects,” *Environ Sci Technol*, vol. 50, no. 22, pp. 12072–12094, Nov. 2016, doi: 10.1021/acs.est.6b03448.

[167] M. D. Nguyen, M. Thomas, A. Surapaneni, E. M. Moon, and N. A. Milne, “Beneficial reuse of water treatment sludge in the context of circular economy,” *Environ Technol Innov*, vol. 28, p. 102651, Nov. 2022, doi: 10.1016/J.ETI.2022.102651.

[168] I. Muñoz, J. Rieradevall, F. Torrades, J. Peral, and X. Domènech, “Environmental assessment of different solar driven advanced oxidation processes,” *Solar Energy*, vol. 79, no. 4, pp. 369–375, Oct. 2005, doi: 10.1016/J.SOLENER.2005.02.014.

[169] G. Ferro, M. I. Polo-López, A. B. Martínez-Piernas, P. Fernández-Ibáñez, A. Agüera, and L. Rizzo, “Cross-Contamination of Residual Emerging Contaminants and Antibiotic Resistant Bacteria in Lettuce Crops and Soil Irrigated with Wastewater Treated by Sunlight/H_2O_2,” *Environ Sci Technol*, vol. 49, no. 18, pp. 11096–11104, Sep. 2015, doi: 10.1021/acs.est.5b02613.

[170] L. Rizzo *et al.*, “Best available technologies and treatment trains to address current challenges in urban wastewater reuse for irrigation of crops in EU

countries," *Science of The Total Environment*, vol. 710, p. 136312, Mar. 2020, doi: 10.1016/j.scitotenv.2019.136312.

[171] J. A. Aznar-Sánchez, L. J. Belmonte-Ureña, J. F. Velasco-Muñoz, and D. L. Valera, "Farmers' profiles and behaviours toward desalinated seawater for irrigation: Insights from South-east Spain," *J Clean Prod*, vol. 296, p. 126568, May 2021, doi: 10.1016/J.JCLEPRO.2021.126568.

[172] R. Saliba, R. Callieris, D. D'Agostino, R. Roma, and A. Scardigno, "Stakeholders' attitude towards the reuse of treated wastewater for irrigation in Mediterranean agriculture," *Agric Water Manag*, vol. 204, pp. 60–68, May 2018, doi: 10.1016/J.AGWAT.2018.03.036.

[173] A. A. Merrouni, A. Amrani, and A. Mezrhab, "Electricity production from large scale PV plants: Benchmarking the potential of Morocco against California, US," *Energy Procedia*, vol. 119, pp. 346–355, Jul. 2017, doi: 10.1016/j.egypro.2017.07.118.

[174] P. Kokkinos, D. Venieri, and D. Mantzavinos, "Advanced Oxidation Processes for Water and Wastewater Viral Disinfection. A Systematic Review," *Food Environ Virol*, vol. 13, no. 3, pp. 283–302, Sep. 2021, doi: 10.1007/s12560-021-09481-1.

[175] A. Al-Karaghouli and L. L. Kazmerski, "Energy consumption and water production cost of conventional and renewable-energy-powered desalination processes," *Renewable and Sustainable Energy Reviews*, vol. 24. Elsevier Ltd, pp. 343–356, 2013. doi: 10.1016/j.rser.2012.12.064.

[176] "Reverse osmosis demineralization." https://www.lenntech.com/processes/reverse-osmosis-demineralization.htm (accessed Jun. 26, 2023).

APPENDICES

A. The Energy Systems for RO-only Plant

Table A.1 The technical inputs of the PV system for RO plant with 180 000 m^3 day^{-1} capacity.

Parameter	Value	Unit
Module type	SunPower SPR-E20-440-COM	-
Inverter type	SunPower: SPR-24000m-3-H	-
DC to AC Ratio	1.1	-
Capacity (MW)	29.2	MWdc
Tracking	1 Axis (tilted N-S axis)	-
Tilt angle	Latitude	°
Surface azimuth angle	180	°

Table A.2 The technical inputs of the central receiver CSP system for RO plant with 180 000 m^3 day^{-1} capacity.

Parameter	Value	Unit
DNI design point	800	W m^{-2}
Solar multiple	3	-
Design turbine gross output	27.03	MWe
Turbine gross to net efficiency	90%	-
Turbine operating range	30%-100%	-
HTF fluid	60% $NaNO_3$, 40% KNO_3	-
Hot tank fluid temperature	575	℃
Cold tank fluid temperature	290	℃
Storage size	12	h
Initially charged volume of hot tank	30%	-

Table A.3 The single value outputs of the central receiver CSP system with 24.3 MWe net turbine capacity and 12 hours of storage capacity to power a RO plant with 180 000 m^3 day^{-1} capacity.

Parameter	Value	Unit
Total land	835.1	acres
Number of heliostats	2978	-
TES thermal capacity	787.3	MWh_{th}
Receiver height	12.18	m
Receiver outer diameter	10.56	m
Tower height	126.022	m
HTF volume	3650	m^3
Max flow rate to the receiver	550.04	kg s^{-1}